NTNU – Trondheim
Norwegian University of
Science and Technology

Design of Roof PV Installation in Oslo

Siv Helene Nordahl

Master of Energy and Environmental Engineering
Submission date: June 2012
Supervisor: Lars Einar Norum, ELKRAFT

Norwegian University of Science and Technology
Department of Electric Power Engineering

Problem Description

The international photovoltaic industry has experienced a powerful growth, and has had a yearly growth between $30 - 135$ % the last three years. During this growth the module and inverter prices have been reduced to a level where it is competitive with conventional power production in several countries. With this tendency in mind it is increasingly interesting to evaluate photovoltaic installations in Norway.

The objective of this thesis is to design a suiting photovoltaic system for a flat roof in Oslo, Norway. The production of the photovoltaic system is found with the use of the simulation software PVsyst. Input to the simulation software such as meteorological data has been evaluated. The energy production of the final two or three alternative systems is evaluated with respect to the energy consumption within the building where the installation is to be located. The regulations when connecting a photovoltaic system to the grid are also studied.

Assignment given:	Trondheim, 23.01.2012
Supervisor:	Lars Norum,
	Department of Electrical Power Engineering

Summary

This thesis is centered around the design of a grid-connected photovoltaic (PV) roof installation at a specific location in Oslo, Norway. The motivating factor in this study has been the growth of the solar industry globally, while there has been little to none larger PV investments in Norway. The objective is to investigate how much renewable PV energy that can be produced from the designed system, with an electrical focus.

Factors such as the suns position during each day of the year, the shadings on modules, the electrical effect of shading and bypass diodes, and other factors influence the production of a PV installation. Due to the complexity of power production in a PV system, the simulation software PVsyst was used as support. A 3D representation of the building and shading elements was constructed in the simulation program for shading calculation purposes. Meteorological data from local weather stations in Lier, Ås and Blindern was compared with meteorological data provided by interpolation and satellite images. The distance between modular rows was dimensioned after a shading criterion so that there would be no shading from other modular rows during spring equinox (March 21st). The modular tilt was adjusted (from the optimal tilt angle of 40°) in order to reduce shading loss and improve the performance ratio of the system. The number of module and inverter types and manufacturers was limited to three different module types, and four different inverter series. The simulated production from the three best alternatives, based on performance ratio and production were compared with the energy consumption in the building. Simple economical evaluations of the three best alternatives have been performed using the simple payback method and life cycle costing.

As a result of the limited area on the roof, the shading objects and the dimensioning criteria (maximize performance ratio and production of the system) it was found that the module tilt was 20°. The modules in the system are directed towards geographical south, and there is a pitch distance of 2 meters between the module rows. The resulting three final alternatives were two polycrystalline alternatives and one monocrystalline alternative. The polycrystalline alternatives used the same REC modules and different inverters, one from Eltek and the other from SMA. The monocrystalline alternative was simulated with SunPower

modules and SMA inverters. The installations have a simulated energy production of 22.4, 22.9 and 31.0 MWh/year, which would cover the average energy consumption of a household in Norway (20.4 MWh/year). However, the installation will only contribute to reduce the energy consumption in the six storey commercial building by approximately 1 % per year. Comparing the simulated productions and the consumption in 2011, it is found that the installation will not result in a surplus of energy which could have been injected into the grid. The installation will, therefore, not change the buildings customer status to a surplus customer (plusskunde). With the simplified economical evaluation it is found that the energy from the PV installation will cost more than the energy agreement of today and it is triple the yearly average market price of electricity the last three years. The polycrystalline alternative with SMA inverters was the least expensive alternative of the three and the polycrystalline alternative with highest production. The monocrystalline alternative gave best simulated production and performance ratio of the three alternatives, but was the most expensive alternative.

Sammendrag

Denne oppgavens hovedfokus er å designe et solcelleanlegg tilknyttet nettet på et spesifikt tak i Oslo. Motivasjonen i denne studien har vært den kraftige veksten av solindustrien i verden, mens det har vært lite og nesten ingen større utbygging av solcelleanlegg i Norge. Hensikten har vært å undersøke hvor mye fornybar solenergi som kan produseres ut fra det designede anlegget med hovedfokus på det elektriske aspektet.

Solens varierende posisjon i løpet av hver time, hver dag i løpet av et år, skyggene på modulene, den elektriske effekten av skygge på modulene og bypassdioder er blant flere faktorer som påvirker produksjonen i et solcelleanlegg. Simuleringsprogrammet PVsyst ble brukt som en støtte grunnet kompleksiteten i et solcelleanlegg og for å beregne produsert energi. I simuleringsprogrammet ble det laget en 3D-representasjon av bygningen og skyggeelementene for at skyggeberegninger skulle utføres i programmet. Meteorologiske data til programmet ble samlet fra de lokale værstasjonene på Blindern, Lier og Ås, samt databaser som benytter interpolering blant værstasjoner i sin database og databaser som baserer seg på satellittbilder. Dataen ble deretter analysert for å lage et nytt meteorologisk datasett til simulerings programmet. Dimensjoneringskriteriet for å finne avstanden mellom modulradene var at det ikke skulle oppstå skygge fra andre modulrader ved vårjevndøgn (21. mars). Helningen til modulene ble justert fra den optimale 40° helningen, for å redusere skyggetapene og oppnå en høyere effektivitet i anlegget. Den simulerte produksjonen fra de tre beste alternativene ble sammenlignet med energiforbruket til bygget anlegget er tenkt plassert på. Til slutt ble det gjort en forenklet økonomisk vurdering av de tre beste alternativene.

Som et resultat av begrenset areal, skyggeelementene på taket, samt dimensjoneringskriteriet (maksimering av effektiviteten og produksjonen til anlegget) ble helningsvinkelen på modulene 20°. Modulene i systemet er vendt mot geografisk sør og avstanden mellom radene er modellert til 2 meter. To av de tre beste alternativene var polykrystallinske REC moduler med ulike vekselrettere. Det ene alternativet var simulert med vekselrettere fra Eltek mens det andre var simulert med vekselrettere fra SMA. Det tredje alternativet var simulert med monokrystallinske SunPower moduler og en type vekselretter fra SMA. De tre

alternativene resulterte i en årlig energiproduksjon på henholdsvis 22,4, 22,9 og 31,0 MWh. Denne produksjonen ville ha dekt forbruket til en gjennomsnittlig bolig i Norge (som er på 20,4 MWh/år). Sammenlignet med energiforbruket i bygget solcelleanlegget er tenkt å stå på, dekker det bare ca. 1 % av forbruket til bygget i 2011. Dette er på grunn av størrelsen til bygget, som er syv etasjer. Den simulerte produksjonen sammenlignet med forbruket i 2011 i bygget viste at det ikke ville forekomme tilfeller hvor produksjonen oversteg forbruket med tanke på effekt. Bygget vil derfor ikke endre kundestatus til plusskunde med et slikt solcelleanlegg plassert på taket. Ut i fra de forenklede økonomiske beregningene er det vist at energien fra solcelleanlegget er dyrere enn den nåværende energiavtalen og dyrere enn den gjennomsnittlige årlige markedsprisen på energi levert til Oslo over de tre siste årene. Av de tre alternativene er alternativet med polycrystallinske moduler og vekselrettere fra SMA billigst og det som produserer mest av de to polykrystallinske alternativene. Det monokrystallinske alternativet er dyrest, men er alternativet med høyest effektivitet og produksjon.

Preface

This thesis is the result of the work done this final semester and marks the end of a five year masters programme (MSc) in Energy and Environmental Engineering at the Norwegian University of Science and Technology. I have learned much this past semester and I would like to thank those who have helped me during this semester with my thesis.

First of all, I would like to thank my supervisor Dr.Ing Lars Norum. He has asked important questions which I did not know that I also had. He has discussed with me and helped me progress. Secondly, I would like to thank my co-supervisor Dr.Ing Bjørn Thorud at Multiconsult who suggested the problem which was the start of this thesis. His enthusiasm has been an inspiration during this semester. I would also like to thank him and Multiconsult who gave me a flying start with this thesis with introductory presentations to the PV system and a trip to Glava Energy Center to see a PV plant in Sweden. I would also express my gratitude to PhD student Georgi Yordanow at the University of Agder, who has informed me of his work, answered my questions and helped analysing strange irradiation measurements from Lier and Ås' weather stations. In addition I would like to thank Linn Dalaker at Multiconsult and Elvedin Grudic at Hafslund, who have provided me with information concerning the building and answered my questions regarding connection to the grid.

In addition, I want to thank my fellow students, friends and family for the support they have given me through these five years. Thanks to my mother for all the love and support she has always provided. I would especially like to thank those who have helped me with the finishing touches in this thesis, Camilla Sun Kilnes, Morten Smedsrud, and Adam Gray. Finally I would like to thank Ingve Løkken for his support, endurance and love during these final semesters of my masters degree.

Siv Helene Nordahl
Trondheim, 20.06.2012

Contents

List of Figures

List of Tables

Acronyms and Abbreviations

AC	Alternating current
AM	Air mass
BIPV	Building Integrated Photovoltaic
BoS	Balance of System
CCC	Current Carrying Capacity
CSA	Cross Sectional Area
DC	Direct current
EF	Electrical Effect
GW	Gigawatt
I-V	Current and Voltage
IAM	Incidence Angle Modifier
ITS	Innotech Solar
MET	The Norwegian Institute of Meteorology
MPP	Maximum Power Point
MPPT	Maximum Power Point Tracker
NASA	National Aeronautics and Space Administration
NOCT	Nominal Operating Cell Temperature
NVE	Norwegian Water Resources and Energy Directorate
PV	Photovoltaic
PR	Performance Ratio

REC	Renewable Energy Corporation
SSE	Surface meteorology and Solar Energy
STC	Standard Test Conditions
TF	Transposition Factor
TSO	Transmission System Operator
USNO	U.S. Naval Observatory
Vp	Voltage peak
Wp	Watt peak

Nomenclature

α	Solar altitude (°)
β_{opt}	Optimum tilt angle (°)
ΔT	Temperature difference between the STC temperature (25° C) and the highest/lowest cell temperature
δ	Declination (°)
η_m	Module efficiency (-)
$\gamma_{I_{SC}}$	Short circuit current temperature coefficient of the module (A/° C)
γ_{V_OC}	Open circuit voltage temperature coefficient (V/°C)
$\gamma_{V_{MPP}}$	Voltage temperature coefficient (V/° C)
ω	Hour angle (°)
ϕ	Latitude (°)
ψ	Solar azimuth (°)
ρ	Resistivity (Ω/m/mm^2)
θ_z	Zenith angle (°)
A	Absorption coefficient (-)
C	Initial investment cost
G	Irradiation (W/m^2)
G_{eff}	Effective irradiance (W/m^2)
$k_{t,a}$	Annual average clearness index (-)
L	Length (m)
$L_{DC\ cable}$	Route length of DC cable (m)
S	Annual cost savings

T	The payback period (years)
T_a	Ambient temperature (° C)
T_m	Module temperature (° C)
U_c	Constant component of the thermal loss factor (W/m^2·k)
U_v	Factor proportional of the wind velocity (W· s/m^3·k)
v	Wind velocity (m/s)
w	latitude minus optimum tilt angle (°)
Y_f	Final PV system yield (kWh/kWp/day)
Y_r	Reference yield (kWh/m^2/day)

Chapter 1

Introduction

1.1 Motivation

The energy demand in the world is increasing. From 1976 to 2009 there has been a 40 % increase in the final energy consumption in Norway [1]. Generally, there is found a link between increasing economic growth and an increased consumption of energy. In the analysis and reference case of the International Energy Outlook 2011, an energy consumption in countries outside the Organization for Economic Cooperation and Development (non-OECD) increased by 85 %, compared to an increase of 18 % for the OECD economies [2]. The reference case considered does not incorporate prospective legislation or policies that might affect energy markets. Two major global energy problems that have become more accepted during the last 12 years are that the oil reserves is a limited resource and that climate change needs urgent international action in order to mitigate its effects resulting from the worlds consumption of fossil fuels. The Intergovernmental Panel on Climate Change (IPCC) provides with regular interval assessment reports of the state of knowledge on climate change, the last report being produced in 2007. Renewable power production is playing, and will continue to play, a large role in solving these issues.

Over the past seven years, the Photovoltaic (PV) sector has transformed from a small industry centered in Germany to become an industry with global reach. PV prices have fallen due to growth on account of government subsidies, capacity additions from both existing and new entrants and continual innovation. The global installed capacity exceeded 65 gigawatt (GW) in 2011 [3]. A new world record was set Friday, May 25th, this year (2012) when the German PV installations produced an accumulated power of 22 GW. During that Friday and Saturday the PV installations covered respectively one third and one half of Germany's power demand [4]. One other target from the German government which most likely

includes the PV industry is that all its new buildings should be climate neutral from 2012, which means they will run entirely on renewable energy [5].

A common assumption is that PV systems are not suited for latitudes as far north as Norway, since the amount of sunny days are not as many as for countries located further south. However, small scale PV installations have been used for some time in Norway as stand-alone PV systems installed at cottages around the country. Currently there is planned a commercial building in Trondheim with a PV façade, a sea water heat pump and a heat exchanger. This building should produce more than it consumes during its life time [6]. Construction start is planned next year, 2013. Becoming a producer of energy can be a comprehensive process. In order to simplify the process of becoming a surplus customer there has been given a dispensation from entering into a balancing agreement with the national Transmission System Operator (TSO) from the Norwegian Water Resources and Energy Directorate (NVE) in 2010. The surplus customers are customers which do not normally exceed their own consumption during a year, but has some surplus energy which could be sold to the grid. In counties Oslo, Akershus and Østfold there is at this time only one surplus customer.

1.2 Objectives and Limitations

The objective of this thesis is to design a grid-connected PV system for a specific roof on a commercial building in Oslo, Norway. The system should be optimized with respect to the performance ratio of the system and the production. When a few final system alternatives (with different components) are finalized, a comparison of the production of the PV systems should be done with respect to the energy demand in the building where the system is to be placed. An investigation should be performed concerning the regulations and compliances which should be met when connecting to the grid.

A PV system as a whole is complicated as there are many variables and several different disciplines that have to work together in order to achieve a good PV system. However, this thesis has been limited to consider the electrical behaviour of a PV system and the elements related to the electrical behaviour of the system. PVsyst, the simulation program that was used in this thesis, was used as a support tool. It is considered a comprehensive PV simulation program. However, all simulation programs have their limitations, whether considering the accuracy of the methods used or whether or not elements are considered at all. The choice of module and inverter manufacturers was limited to three each. Furthermore, the number of possible inverters and modules were limited to one series each.

1.3 Outline of the Thesis

Chapter 2 gives a basic introduction to a grid-connected PV system and the electrical characteristics of the solar cell and the inverter. This chapter could be disregarded by readers with this knowledge. Chapter 3 is first structured in chronological order of the steps that are necessary in order to perform a simulation of a grid-connected PV system in the simulation software PVsyst:

1. Project
2. Orientation
3. Shade
4. System
5. Module layout

In order to perform the simulation, all of these steps has to have defined parameters. In order to define the parameters some background information will be provided. The final two sections of Chapter 3 are sections regarding the connection to the grid and economic models used.

Chapter 4 presents the results from simulations where some of the parameters are varied. The simulations are compared with a base case of a PV system in order to evaluate the change in the results when varying parameters. Chapter 4 is, therefore, documenting the process in reaching the final three alternative PV systems which then will be examined further in Chapter 5. The production of the final three alternatives is more thoroughly examined in Chapter 5 and is compared with the energy consumption within the building where the PV system is placed. Simple economical calculations are also performed in chapter 5. Finally there are some recommendations for further work in Chapter 6, and conclusions are drawn in Chapter 7.

Chapter 2

Photovoltaic systems

2.1 PV Systems in General

PV systems can in general be divided into two different systems, stand-alone systems and grid-connected systems (see Figure 2.1.1). Stand-alone systems would have PV modules, a energy storage medium and a load. The storage and a backup generator is drawn into Figure 2.1.1 with dotted lines, since this is optional. Stand-alone systems can for example be found in cottages in Norway. In this study a grid-connected PV system is to be dimensioned. As the dimensioning methods for these two systems differ, only the grid-connected PV system will be discussed from this point on.

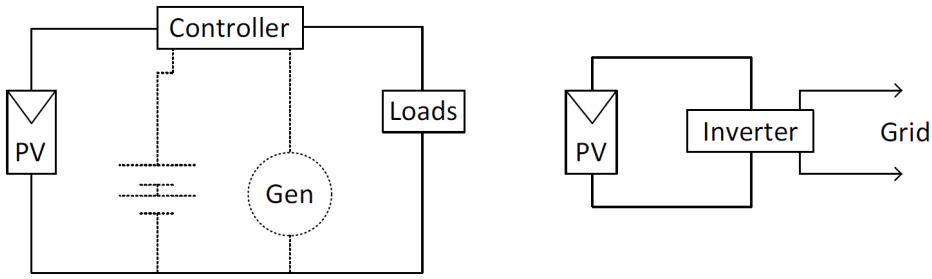

Figure 2.1.1: Schematic of a stand-alone PV system to the left and a grid-connected PV system to the right

A grid-connected PV system comprises of PV modules and Balance of System (BoS) components. The BoS components include the inverters, mounting systems, array cabling to a possible junction box, possible cables from the junction box to the inverter, protection and disconnection switches, lightning pro-

tection, the Alternating current (AC) cabling from the inverter, metering and system monitoring [7, p.131]. The main components of a grid-connected PV system which will be explained in more detail are the modules and the inverters. The modules produce electricity from solar irradiation and the inverters convert the Direct current (DC) current produced by the modules into AC current which can be injected into the electricity grid.

2.2 The Electrical Characteristics of a PV Cell, PV Module, PV String and a PV Array

Figure 2.2.1 illustrates the configuration in the generating part of the PV system, from the cell to an array. Each cell produces energy, and each module consists of several cells in series. It is a 36 cell module illustrated in the figure. If each cell in the module produces 0.5 V peak (Vp), the module would be rated approximately with 18 Vp, 12 V nominal [7, p.50] Modules coupled in series are called strings, while strings coupled in parallel are called an array.

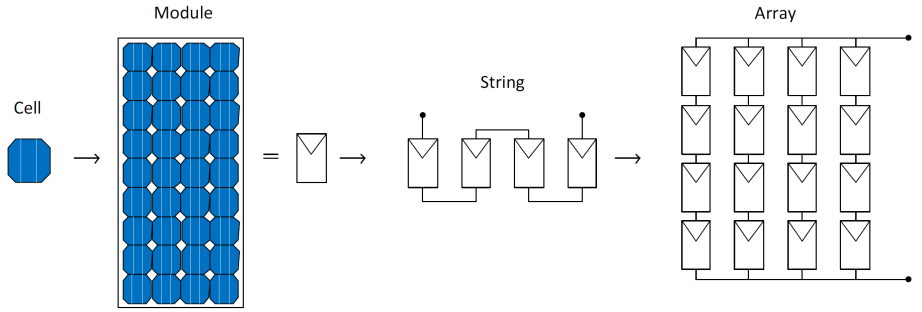

Figure 2.2.1: PV cell, PV module, PV string, PV array

Returning to the cell, its electrical properties can be described as a large diode (see Figure 2.2.2). When the current flows through the diode as shown in the figure, the characteristic curve in the first quadrant applies. At a particular voltage the currents starts to flow, in the figure at a threshold voltage of 0.7 V. If the current flows in the opposite direction (the reverse direction) the current flow is prevented until the breakdown voltage of the diode is exceeded (in this case 150 V). Reaching the breakdown voltage could destroy the diode.

An illuminated solar cell can be explained with a diode in parallel with a current source. As the cell is illuminated, the current source will produce a photoelectric current (I_{ph}). The diode characteristic curve is then shifted by the magnitude of the photoelectric current downwards in quadrant three and four, seen as the dotted line in Figure 2.2.2 [8]. The standard model used to represent a PV

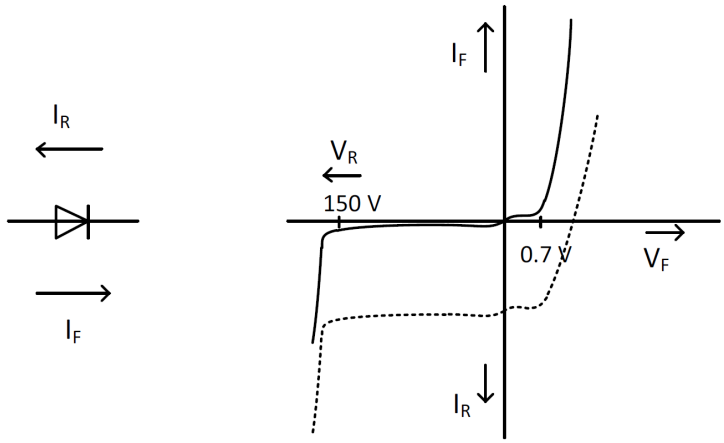

Figure 2.2.2: I-V characteristics of a diode. F = forward, R = reversed

cell is an extended equivalent circuit called the single-diode model (illustrated in Figure 2.2.3). A parallel resistance (R_P) is added to represent the voltage drop which occurs as the charge carriers migrate from the semiconductor to the electrical contacts. In addition a series (R_S) resistance is added in order to represent leakage currents.

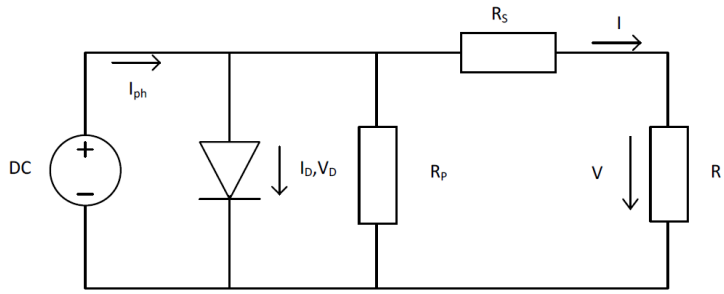

Figure 2.2.3: The single diode model

Figure 2.2.4 illustrates the current and voltage (I-V) characteristics and the power characteristics of a PV cell in the same figure. The Maximum Power Point (MPP) marked in this figure illustrates the operating point of the cell, with regards to current and voltage, in order to maximize production.

Figure 2.2.5 illustrates the I-V characteristic of an array when it consists of both series and parallel connected modules. When the modules are connected in series the voltage increases along the abscissa axis. When the modules are connected

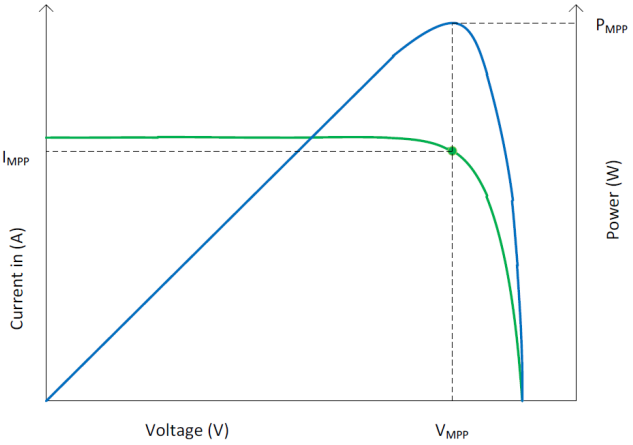

Figure 2.2.4: I-V and power characteristics of a PV cell

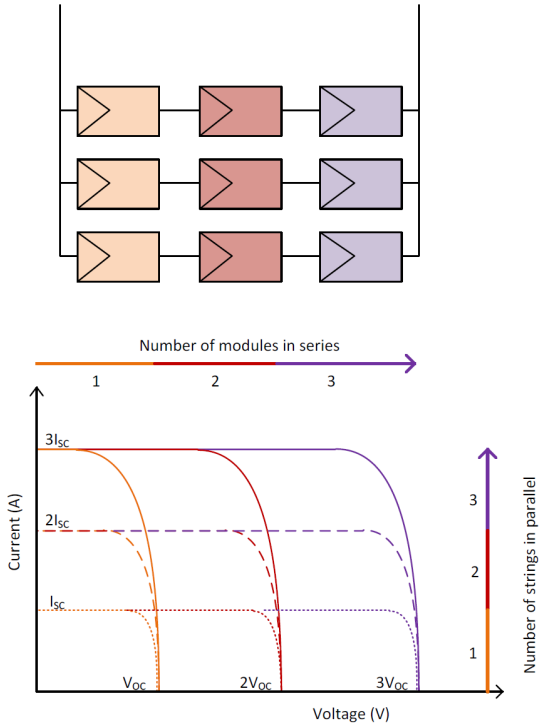

Figure 2.2.5: Interconnection of PV modules in series and parallel

in parallel the current increases as seen in the figure.

There are several cell technologies available on the market. Mocrystalline silicon, polycrystalline silicon, ribbon silicon, crystalline thin-film silicon, amorphous silicon, micromorphous silicon, hybrid HIT solar cell, cadmium telluride, high-efficiency III-V multijunction cells and dye-sensitised cells are some of the technologies that can be named [9]. The mono- and polycrystalline silicon cells have a commercially high efficiency which is of importance when there is limited amount of space for a PV field. The single-diode model of a cell si well suited for the silicon crystalline cells, however, other adaptions are required when reproducing the thin film technology [10]. Based on this, it is these two cell types which will be considered in this study.

2.3 The Inverter

As mentioned, the inverter transforms DC current from the PV installation to AC current. The transformed AC current produced by the inverters matches the voltage and phase of the electricity grid. In order to produce AC current, semiconductor switches are used to produce pulses of voltage where the width of these pulses are modified in order to achieve an accurate approximation of a sine wave [7, p.103]. These are so called switch-mode inverters, and there are several inverter switching schemes which can be used.

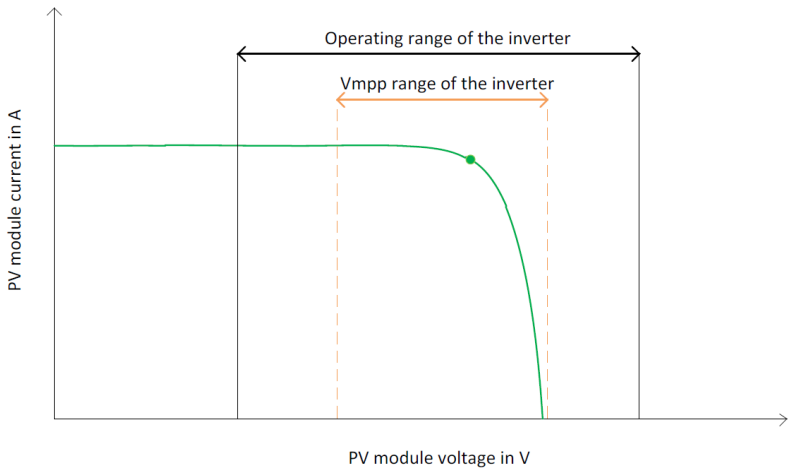

Figure 2.3.1: A PV module characteristic curve and the operating and MMP range of an inverter

Figure 2.3.1 illustrates a PV module I-V characteristic with the operating and

MPP range of an inverter. Within the MPP range of the inverter, it has a tracker, a Maximum Power Point Tracker (MPPT). The purpose of the MPPT is to locate the MPP, marked with a circle in the figure, in order to obtain as much power as possible from the system. There are several MPPT schemes which each have their advantages and limitations with regards to efficiency [11]. The subject of MPPT schemes will, not be discussed in this study. The PV array voltage has to match the operating range of the inverter in order for the inverter to function. Inverters can or can not be equipped with a transformer. Inverters without transformers offer improved efficiency, while inverters with provide galvanic (electric) isolation between the DC input side and the AC output side. Without the galvanic isolation between the DC and AC side, DC currents might be injected into the grid. The improved efficiency without a transformer is due to the losses which occur in a transformer. Transformer-less inverters are often lighter and could cost less than inverters with transformers, due to a smaller amount of metal [7].

Chapter 3

PVsyst

There are several PV system simulation programs. Some are:

- SOLDIM
- PVS
- PV*SOL
- DASTPVPS (Design and Simulation Tool for PV Pumping Systems)
- Greenius
- PV Design Pro (Solar Studio Suite)
- PVsyst

These are known as so called time-step simulation programs. All of the mentioned simulation programs except DASTPVPS apply for grid-connected systems. SOLDIM, PVS, PV*SOL, Greenius, PV Design Pro and PVsyst all apply for stand-alone systems, hybrid systems, PV pumping systems and some apply for other technologies such as wind, fuel cells, solar thermal plants etc. All provide an economical overview of viability. PVS, PV*SOL, PVsyst, PV Design Pro and SOLDIM provide shading calculations down to intervals of one hour. In addition PVS, PVsyst, PV Design Pro and SOLDIM provide a solar radiation generator [8, p.199].

PVsyst is considered one of the most comprehensive programs of the ones listed, and also one of the most complicated to use. PVsyst has a higher accuracy of shading calculations than PVS and PV*SOL, and is the only program which provides a 3D representation of the PV field. Greenius provides an extensive economical calculation, while the other programs are fairly similar with varying degrees of functionality. Tests of various programs in Europe showed that shading came in top for causing reduced yields and was responsible for considerable

reductions of as much as 30 % and more. The yield reductions generally turn out to be greater than one would suspect based on the shaded surface area. Thus, the shading analysis is known to be a sensitive point in PV system simulations [8, p.193]. Examples of other PV simulation systems are PVSIM, PVFORM, PVNet and SimPhoSys [12].

The simulation software PVsyst was used in this study in order to calculate the production of the PV installation. PVsyst is developed at the University of Geneva by André Mermoud [13]. PVsyst has the option of simulating a preliminary design or a project design. In addition PVsyst has a tool option, where background data management and didactic tools are located. The preliminary design option of PVsyst has not been used in this study, since this is a rougher simulation which is assumed to not contribute with significant information compared to the project design simulation option. The five first sections of this chapter (Section 3.1 to 3.5) follows the structure of a grid-connected project simulation in PVsyst. Section 3.6 describes the process of obtaining a grid-connected system in Norway. The last section, section 3.7 describes the economic methods used in this study.

3.1 Project: Geographical Location and Meteorology

The geographical location of the project and the local weather conditions influence the optimal tilt of the PV modules and is, therefore, of great importance. The building in this study is located in Skøyen, Oslo, Norway at a latitude of approximately 60°N.

3.1.1 Solar Radiation and Meteorology

The amount of effect produced by a PV module relies on how much radiation it receives at its precise location. The energy produced by the sun at a temperature close to 5800 K (5526.85°C) is emitted primarily as radiation. When the radiation enters the atmosphere it can collide with clouds and air molecules and the radiation can then scatter or be absorbed (illustrated in Figure 3.1.1). The beam or direct radiation is the radiation which is not reflected or absorbed and reaches the surface of e.g. a PV module in a direct line from the sun. The radiation after a scattering can either be re-emitted into the atmosphere or reach the surface of the module, this is called diffuse radiation. Albedo radiation is the radiation reaching the module surface after being reflected by the ground. Global radiation consists of all three components: beam, diffuse and albedo radiation [14].

On account of the absorption and scattering, the amount of solar radiation that reaches the Earth's surface decreases. The radiation passes through gases when

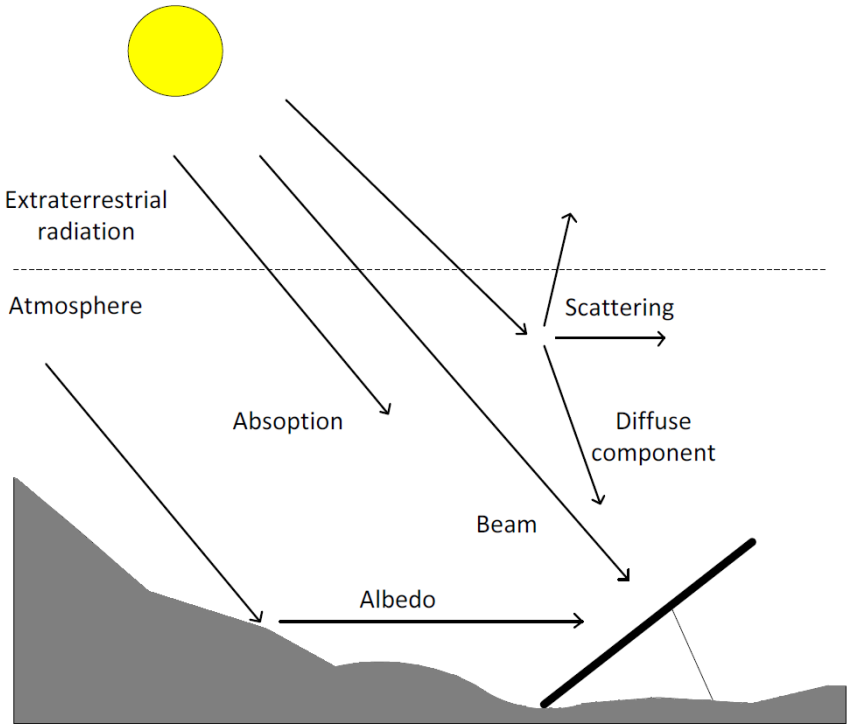

Figure 3.1.1: Solar radiation in the atmosphere

entering the atmosphere, as a result the radiation at Earth's surface has a different spectral composition than the radiation which has not passed through the atmosphere. Air mass (AM) characterises the relative length of the direct beam path through the atmosphere, and is defined as:

$$AM = \frac{1}{cos\,\theta_z} \tag{3.1.1}$$

Where θ_z is the zenith angle, between the sun and the line to a point directly overhead, see Figure 3.1.3.

The PV modules are rated at Standard Test Conditions (STC), which are:

- AM = 1.5
- Solar radiation = 1000 W/m^2

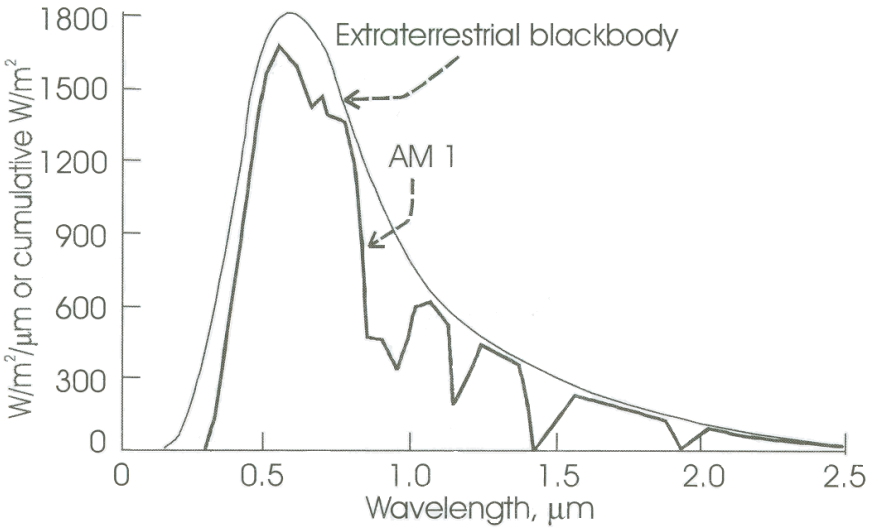

Figure 3.1.2: AM 1 solar spectrum after atmospheric absorption effects [15]

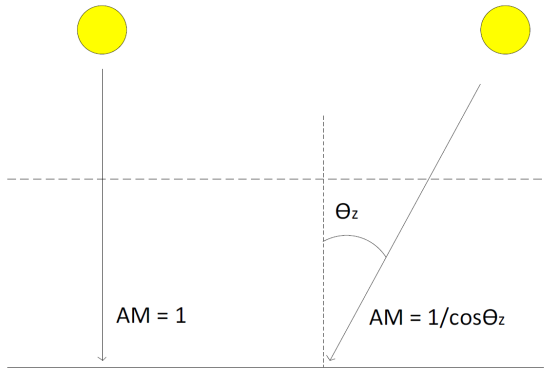

Figure 3.1.3: Air mass

- Cell temperature = 25° C

The characterisation of the PV module is further done by measuring the Nominal Operating Cell Temperature (NOCT), defined under the following conditions at open circuit [7]:

- AM = 1.5

- Solar radiation = 800 W/m^2
- Ambient temperature = 20° C
- Wind speed = > 1 m/s

An AM of 1.5 is a typical solar spectrum on the Earth's surface on a clear day. Although the global irradiance can be as high as 1000 W/m^2 and even somewhat higher, the available irradiance is usually considerably less because of the rotation of the Earth and adverse weather conditions [14]. There has, however, been measured over-irradiance or cloud enhancement events even in southern Norway peaking above 1400 W/m^2 for several minutes [16]. Naturally much stronger over-irradiances may be expected for the lower latitudes near the Equator, with magnitudes exceeding 1800 W/m^2. However, the contribution of over-irradiance events to the annual irradiation is very small. Figure 3.1.4 illustrates the solar irradiation in Norway in January and July while Figure 3.1.5 shows the yearly global irradiation of optimally inclined PV modules in Europe.

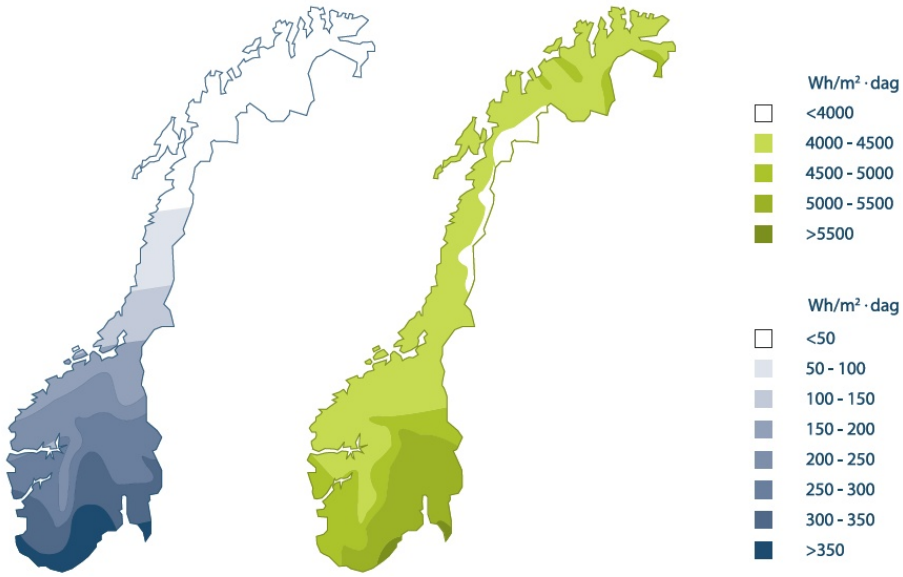

Figure 3.1.4: Solar irradiation map of Norway on a horizontal in January and July, measured in Wh/m^{2}day [17]

As seen in these two figures the solar irradiation increases when the latitude decreases. The mean annual irradiance is highest near the latitudes of the tropics of Cancer (23.5°N) and Capricorn (23.5°S). The mean annual irradiance is, however, lower in equatorial regions as a result of the cloud cover. At the tropics of Cancer and Capricorn, approximately at June 21st and December 21st, the sun is located with a zenith angle of 0°, which would be directly situated over a

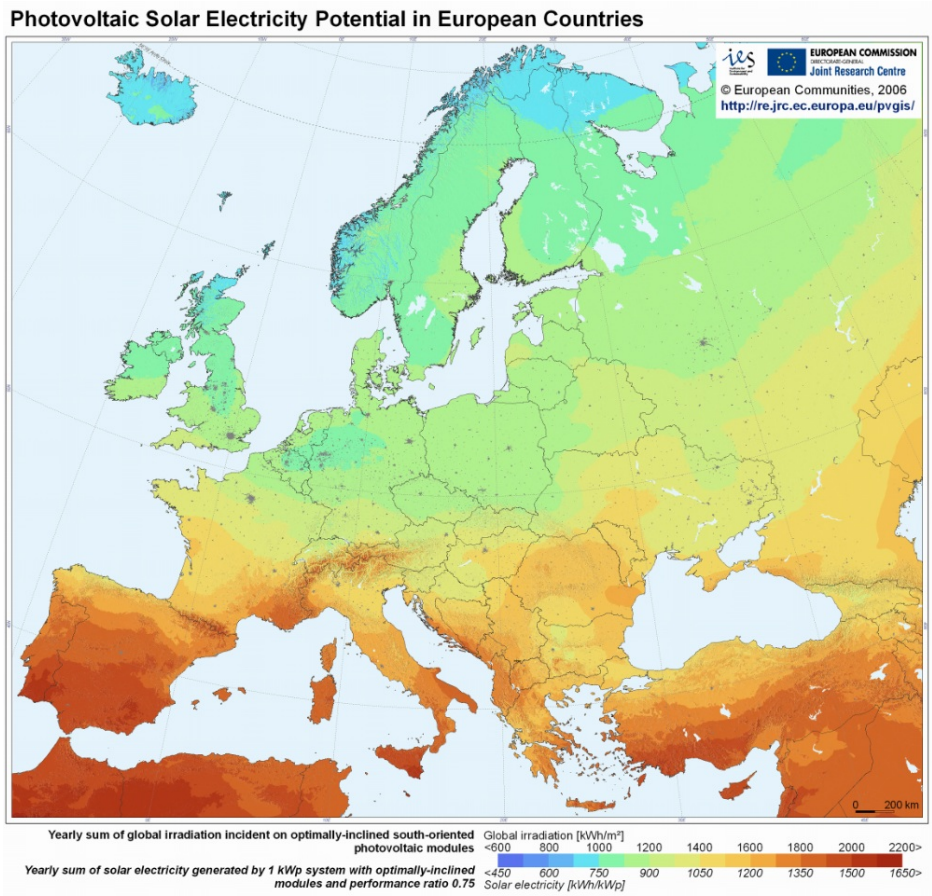

Figure 3.1.5: Yearly global irradiation on optimally inclined south oriented PV modules, Europe [18]

possible PV module. It is known as solstice when the sun is over either of the tropics. The reason why this does not occur at the equator is due to the axial tilt of the Earth. Approximately at March 21st and September 23rd the sun crosses the equator, at the equinoxes (vår- og høstjevndøgn). The equinoxes mark the day when the day and night is equally long.

Position of the sun

The location of the sun is defined by two angles:

- Altitude (α)
- Azimuth (ψ)

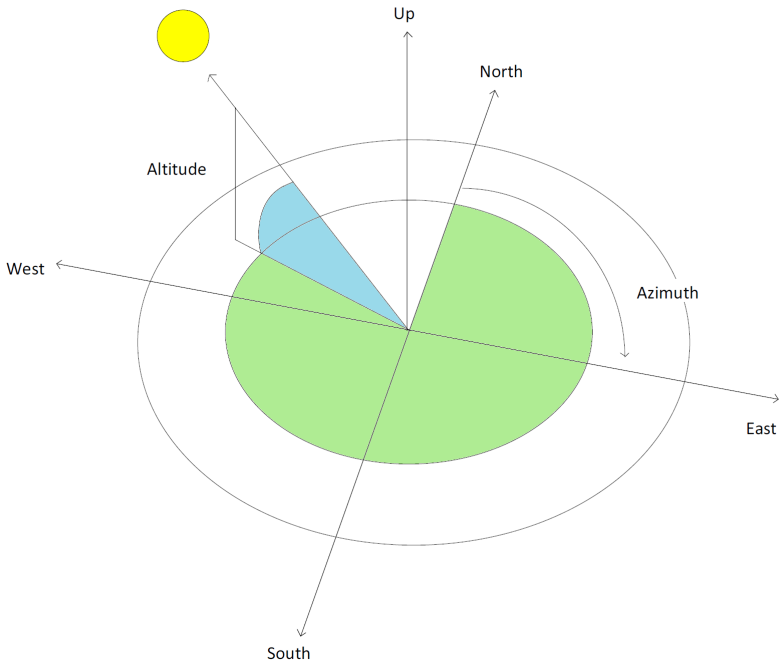

Figure 3.1.6: Altitude (blue angle) and azimuth angle (green angle)

As seen in Figure 3.1.6, the altitude of the sun is the angle between the sun and the ground. This angle is always between 0° and 90°. The sun rises in the east and sets in the west. Azimuth is the angle between north and the point where the sun is positioned. Altitude and azimuth can be determined from [15, p.30] the following equations:

$$sin\,\alpha = sin\,\delta\,sin\,\phi + cos\,\delta\,cos\,\phi\,cos\,\omega \tag{3.1.2}$$

$$cos\,\psi = \frac{sin\,\alpha\,sin\,\phi - sin\,\delta}{cos\,\alpha\,cos\,\phi} \tag{3.1.3}$$

where δ is the declination and ω is the hour angle. The declination is the angle of deviation of the sun from directly above the equator. The hour angle is the difference between noon and the desired time of day in terms of a 360° rotation in 24 hours. The equation describing the declination is often given as an approximation since a year is not exactly 365 days. The hour angle can also be described using an equation. However, there are different equations describing the hour angle depending on how many variables that are taken into account.

For example, one could take only the hour of the day into account [15, p.29] or take into account the local official time, the local longitude, a reference longitude and time difference with respect to time zones [9, p.989].

National Aeronautics and Space Administration (NASA) and the astronomical applications department under the U.S. Naval Observatory (USNO) both provide information concerning the azimuth and altitude angles of a given location described with coordinates. The USNO site takes as an additional input the time zone of the specific site. NASA gives monthly averaged hourly altitude angles and azimuth angles. The azimuth and altitude numbers provided by USNO and NASA are, therefore, not exactly the same.

Temperature and irradiance influence on the PV cell

The nominal operation of PV systems is at STC conditions, however, the PV systems rarely operate in nominal conditions. The modules usually operate in partial load due to its high dependence on temperature and irradiance.

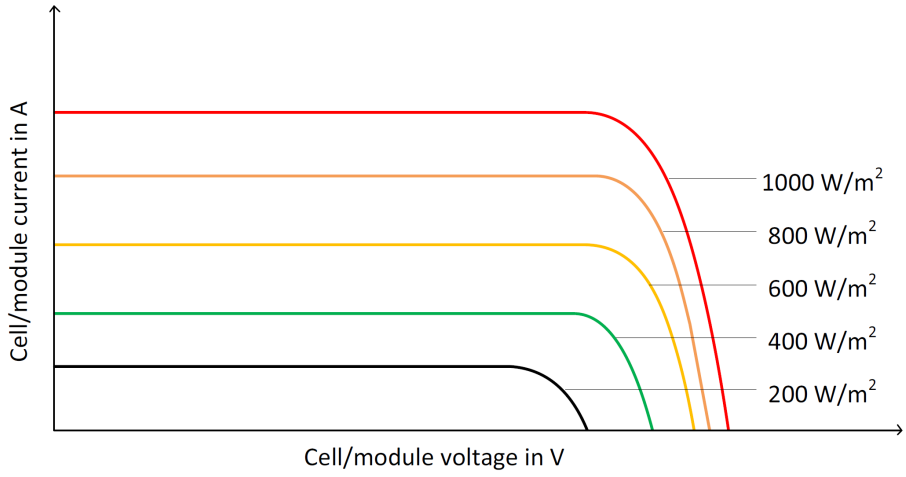

Figure 3.1.7: Cell/module I-V curves with varying irradiance and constant temperature

As explained in Section 2.2 the cell can be illustrated with an diode, and the photoelectric current produced by the cell is a result of illumination on the cell. The short circuit current of the cell is roughly directly proportional to the irradiance as seen in Figure 3.1.7. The figure illustrates how the current in the cell or the module decreases with decreasing irradiance. As seen it is the current that is mostly affected, however, the voltage is slightly affected as well. The cell has a negative temperature coefficient. A temperature coefficient of 2.3 mV/C°

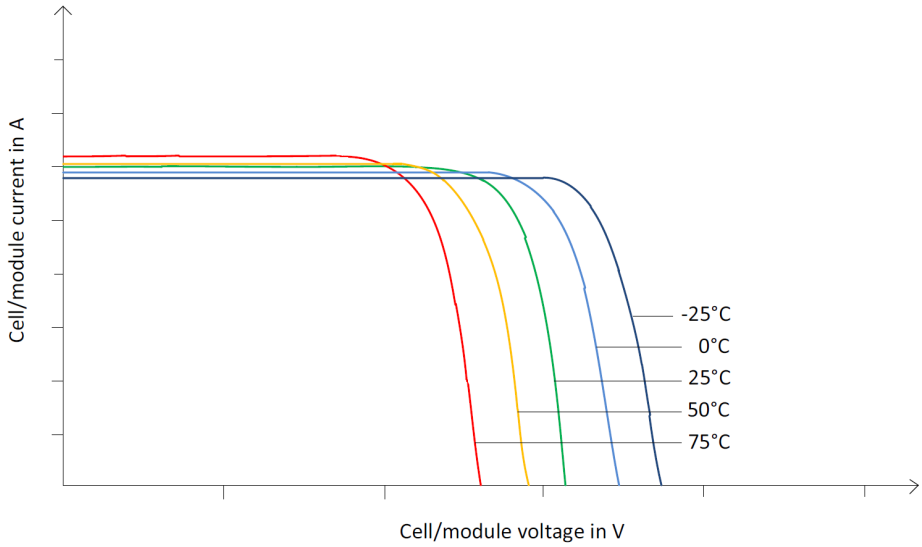

Figure 3.1.8: Cell/module I-V curves with different temperatures and constant irradiance

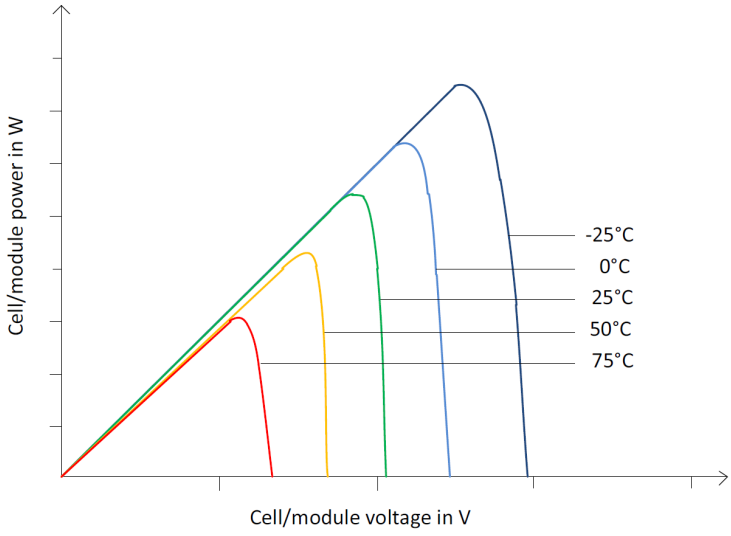

Figure 3.1.9: Cell/module power with different temperature and constant irradiance

describes the decrease of the open circuit voltage with increasing temperature. The short circuit current on the other hand remains nearly constant. The cell

power, therefore, decreases as well. Figure 3.1.8 illustrates how the voltage and current change under different temperatures under constant irradiance. As seen the voltage is mostly affected, however, there are small changes in the current as well. Figure 3.1.9 illustrates how the cell or module power decreases as the temperature decreases.

3.1.2 PVsysts Geographical and Meteorological Considerations

The project location is the first which is defined when performing a project design simulation in PVsyst. Country and site are chosen, and if there are multiple meteorological files, one can be chosen. When opening the meteorological file the latitude and longitude of the location is defined in decimals as well as in degrees and minutes. The altitude above sea level and time zone are also displayed. The monthly meteorological values are displayed along with the data source. The monthly meteorological values which are required are the horizontal global irradiation and the ambient temperature. Extra data which could be provided are data for the horizontal diffuse irradiation and the wind velocity. The sun path for the location is then constructed, as illustrated in Figure 3.1.10.

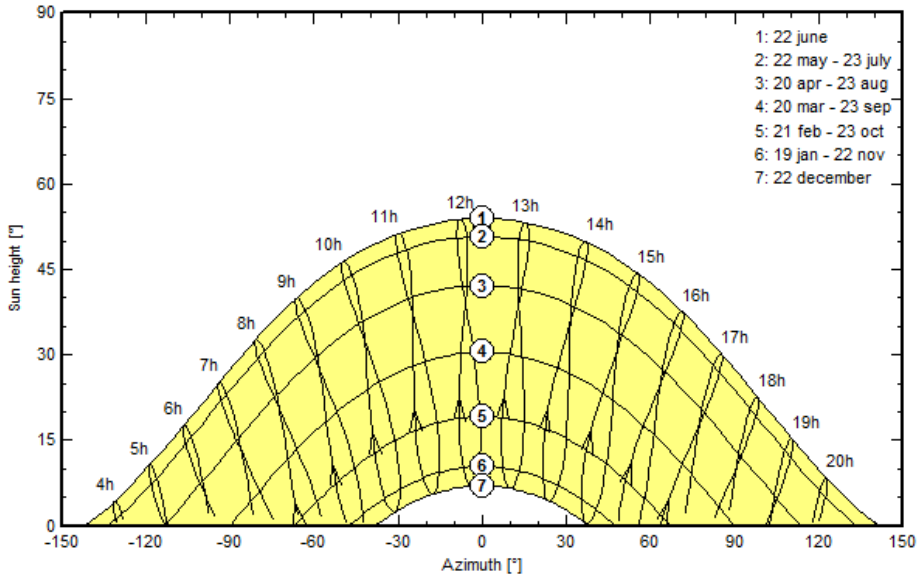

Figure 3.1.10: Solar paths at Oslo, (Lat 59.5°N, long. 10.4°E, alt. 5m)

The solar path seen in Figure 3.1.10 is constructed from the default meteorological file for Norway. The location for this meteorological file is approximately 44 km

from the location of the building. The meteorological file is constructed for a smaller location in Norway called Hurum. For the site it is further possible to define monthly albedo values. The common value equal for all months is default 0.2. Within PVsyst an overview of which albedo values represent certain surroundings is represented in Table 3.1.1. As seen, snow and aluminium has high albedo values due to a larger part of the light is reflected compared to e.g. asphalt. As the building is situated in an urban situation it has been assumed an albedo value equal to the default value 0.2 all year. It was considered to increase the albedo value from December through February, due to snow. In 2011 there was recorded a snow coating from January 1st until April 4th, with some snowfall during a few days in December [19]. However, the default value of 0.2 is chosen for all months since it is considered giving a more conservative result.

Table 3.1.1: Overview of usual albedo values given in PVsyst

Surroundings	Usual albedo values
Urban situation	0.14 - 0.22
Grass	0.15 - 0.25
Fresh grass	0.26
Fresh snow	0.82
Wet snow	0.55 - 0.75
Dry asphalt	0.09 - 0.15
Wet asphalt	0.18
Concrete	0.25 - 0.35
Red tiles	0.33
Aluminium	0.85
New galvanised steel	0.35
Very dirty galvanised steel	0.08

Site-dependent design parameters which are connected to the sizing of the array design with respect to the inverter input voltages, are defined in PVsyst under site and meteorological. The *lower temperature for VmaxAbs limit* has -10° C as default value. This represents the absolute lower cell temperature. However, for this limit the cell temperature is considered equal to the ambient temperature [10]. The reason for this is that during morning at first light the sun has not had time to heat the modules. The temperature of -10° C is the default value since it applies to most European countries. The minimum ambient temperature in Oslo from 2000 to 2011 was, however, found to be a few decimals lower than -20° C (for details see Appendix B). This value was, therefore, altered from -10° C to -20° C. The *lower temperature for VmaxAbs limit* parameter is used when determining the maximum possible voltage of the array. The absolute maximum voltage, the open circuit voltage at the lowest temperature, has to stay below the

absolute maximum inverter input voltage. Furthermore it should not overcome the maximum system voltage specified for the PV module. The *usual operating temperature under 1000 W/m* has 20° C as default value. This parameter is not used for sizing constraints in PVsyst and is, therefore, not changed. The *winter operating temperature for VmppMax design* parameter, describes the minimum cell temperature during operating conditions in winter. The maximum array operating voltage has to stay below the maximum inverter voltage (Vmax of the MPPT range of the inverter explained in Section 2.3). This is set with a default value of 20° C. The *summer operating temperature for VmppMin design* parameter describes the maximum cell temperature in operating conditions and is used to determine the array minimum operating voltage. The minimum array operating voltage should be above the minimum inverters operating range (Vmin of MPPT range). The *summer operating temperature for VmppMin design* parameter has a default value of 60° C. As explained in Section 3.1.1 higher temperature results in lower cell and module voltage.

The module and cell temperature is affected by several factors, such as irradiance and the mounting system. If there is free air convection on both sides of the module it could reduce the module temperature, which would not be the case with Building Integrated Photovoltaic (BIPV). An additional way in order to reduce the temperature of the modules even further, is by e.g. water cooling [20]. This will, however, not be taken into consideration in this study. The temperature of the module is roughly proportional to the incident irradiance and can be described with the following equation [14, p.88]

$$T_m = T_a + C_t \cdot G_{eff} \tag{3.1.4}$$

where C_t is described as follows

$$C_t = \frac{NOCT(^\circ C) - 20}{800\ W/m^2} \tag{3.1.5}$$

where T_m and T_a is the module and the ambient temperatures respectively, G_{eff} is the effective solar irradiance and where $NOCT(^\circ C)$ is the module type dependent test temperature at an irradiance of 800 W/m^2.

The NOCT is normally in the range between $42 - 46^\circ$ C [9][14]. Checking eight module series (four from Innotech Solar, three from REC and one from SunPower) four had a NOCT of 45° C, while the other four had NOCT of 47.9° C with an uncertainty of $\pm$ 2° C. When determining the module temperature in summer and winter the highest and lowest ambient temperature is applied (33° C and -20° C). As previously mentioned in Section 3.1.1 there occurs over-irradiance events in the southern parts of Norway which has been measured up till 1400 W/m^2 [16]. However, due to the short time periods when this occurs this is considered not applicable as G_{eff}. By assuming a G_{eff} of 1000 W/m^2, disregarding a difference

between summer and winter, 42° C, 45° C and 49.7° C (47.9+2) as NOCT coefficients, results in a range of module temperatures as shown in Table 3.1.2.

Table 3.1.2: Module temperatures during summer and winter

NOCT (°C)	Summer T_m (°C)	Winter T_m (°C)
42.0	60.500	7.500
45.0	64.250	11.250
49.9	70.375	17.375

As seen in Table 3.1.2 the default value of the summer operating temperature is in the lowest calculated temperature range with 60° C. The default value for the winter operating temperature of 20° C is above the range of calculated module temperatures. Modules on a roof could heat up to 70° C while with well ventilated systems a maximum temperature of 60° C could be assumed [8, p.142]. The results in Table 3.1.2 is assumed to be consistent with a well ventilated system due to the fact that the NOCT coefficient is the temperature attained by the PV modules with free air circulation all around the module. The summer operating temperature is chosen to be fixed at a temperature of 70° C and the winter operating temperature at 17° C in accordance to Table 3.1.2 with an NOCT of 49.9° C. It was chosen as a precaution if a module with a NOCT of 47.9° C is chosen, and if a module with a lower NOCT is chosen the system would not be operating outside the minimum operation range of the inverter.

Table 3.1.3: The site-dependent design parameters which will be used in the simulations

Parameters	Values
Lower temperature for VmaxAbs limit	-20°C
Winter operating temperature for VmppMax design	17°C
Usual operating temperature under 1000 W/m	50°C
Summer operating temperature for VmppMin design	70°C

Meteorological data sources

Within PVsyst there are possibilities to define new monthly meteorological values and redefine the location of the project as well as import both monthly and hourly meteorological data from a number of other databases, seen in Table 3.1.4. A comparison of the free web based databases was done alongside with local meteorological data where possible. A custom-made second meteorological

set was assembled, with a focus on monthly irradiance and temperature values, since these are the ones compulsory in order to run a PVsyst simulation.

Table 3.1.4: A summary of the meteorological databases with importing tool in PVsyst. Gh = global horizontal irradiation, Dh = diffuse horizontal irradiation, Ta = ambient temperature, WindVel = wind velocity [21].

Database	**Region**	**Values**	**Variables**	**Availability**
Meteonorm	Worldwide	Monthly	Gh, Ta, WindVel	Software
Meteonorm	Worldwide	Hourly	Gh, Dh, Ta, WindVel	Software
Satellight	Europe	Hourly	Gh, NO Ta	Web free
US TMY2	USA	Hourly	Gh, Dh, Ta, WindVel	Web free
ISM-EMPA	Switzerland	Hourly	Gh, Dh, Ta, WindVel	Included in PVsyst
Helioclim (SoDa)	Europe Africa	Hourly Hourly	Gh, NO Ta	Web restricted
NASA-SSE	Worldwide	Monthly	Gh, Ta	Web free
WRDC	Worldwide	Hourly Daily Monthly	Gh, NO Ta	Web free
PVGIS-ESRA	Europe Africa	Monthly	Gh, Ta, Light turbidity	Web free
Helioclim -1 (SoDa)	Europe Africa	Monthly	Gh, NO Ta	Web restricted
RETScreen	Worldwide	Monthly	Gh, Ta, WindVel	Software, free
SolarGIS	Europe Africa Asia, Brazil, West Australia	Hourly	Gh, Dh, Ta	Web, paid access

As seen from Table 3.1.4 there are four databases which do not provide ambient temperatures: Satellight, Helioclim, Helioclim -1 and WRDC. The ambient temperature would have to be supplemented in case these databases were to be utilized. Further it is seen from the table that two of the databases are valid only for USA and Switzerland. The default meteorological data embedded in PVsyst

for Oslo is a monthly data set from Meteonorm. Meteonorm is a database containing climatological data for solar engineering and could also be used to calculate solar radiation on arbitrarily oriented surfaces [22]. PVsyst uses the Meteonorm software in order to import a synthetic hourly meteorological file [10]. A comparison between Meteonorm values and values from the sources in Table 3.1.4 has been performed by the PVsyst team in [23]. The comparison was done of twelve locations in Europe, and there was made no comparison with respect to real measured values. It was, therefore, not concluded which source that could be most representative of real weather conditions. What was observed was that Meteonorm often gave lower values than the average. Meteonorm is, therefore, considered conservative and would give prudent results for the final yield of the simulated systems.

Figure 3.1.11 shows a comparison between four different meteorological databases which were made for Skøyen (the location of the PV installation) alongside two local weather stations in Lier and Ås. Further information and the tabular values for the different meteorological databases are found in Appendix B. There are two values for Meteonorm, one is the default value for Oslo, 44 km south of Skøyen (marked with a D), while the other is the value extracted from the program with the Skøyen coordinates. Meteonorm is, therefore, represented with two values. The weather stations at Lier and Ås are located approximately 27 km south west and south east of Skøyen. These local weather stations have since 2007 measured one hour averages of global horizontal irradiance. The irradiation form the local weather stations in Figure 3.1.11, is the average measurements of each month from $2007 - 2011$. The reliability of the measured data could be questioned since it is only a five years data series. Each year there are natural fluctuations which could differ as much as $10 - 15$ % to the average over a 20 year period. This data is considered to be important and is, therefore, included.

As seen in Figure 3.1.11 the default meteorological file used in PVsyst has a higher annual global horizontal irradiance than the two local weather stations with approximately 30 kWh/m^2. The NASA numbers, which are the highest, are based on satellite measurements from 1983 to 1993 and are valid within the boundaries of 60 and 59° N, and between 10 and 11° E. The values from Meteonorm are based on interpolation between the nearest weather stations between $1981 - 2000$. For Skøyen there were three stations available: the first in Karlstad (169 km away), the second in Borlaenge (273 km away) and the third in Bergen (301 km away).

Figure 3.1.12 illustrates the two different datasets from Meteonorm which are the closest in annual irradiation to the two local weather stations. It is seen that both in May and July the irradiance in the default set is about 13 % and 7 % higher than the local measurements. However, the other set from Meteonorm is between 8 and 15 % lower than the local weather sets. Since there is no reason to exclude any of the three sources of information (four data sets) an average of them are made. With the local stations being further south than Skøyen it could

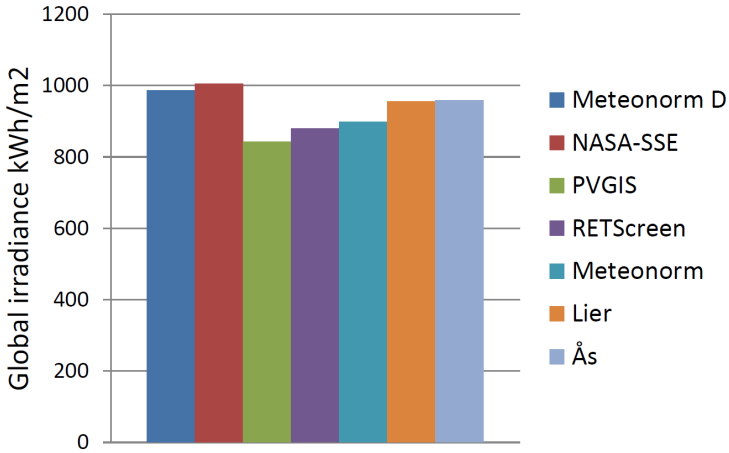

Figure 3.1.11: Yearly global horizontal irradiation (kWh/m^2/year) comparison between Meteonorm, NASA, PVGIS, RETScreen and two Bioforsk weather stations in Lier and Ås.

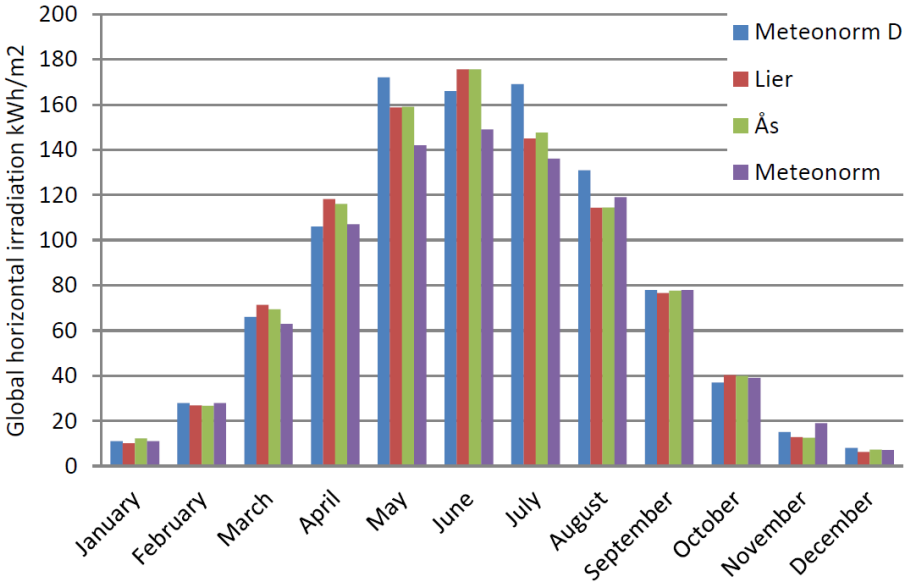

Figure 3.1.12: Global horizontal irradition, Meteonorm, Lier and Ås

be assumed that the irradiation at Skøyen would be somewhat lower than the local weather station measurements in Lier and Ås. This is also the result of the average of the four different data sets.

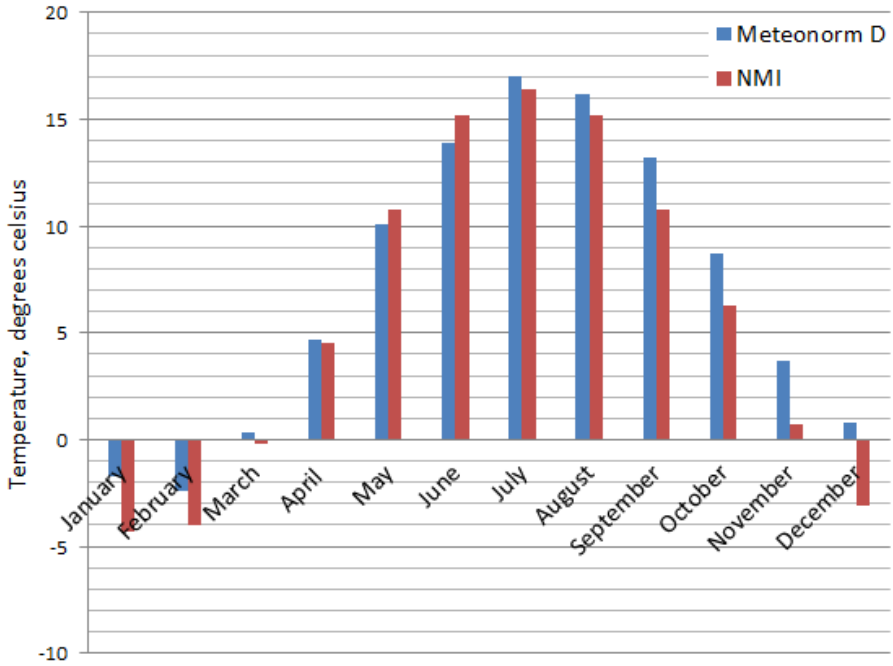

Figure 3.1.13: Comparison of temperature MET and Meteonorm default meteorological set

Figure 3.1.13 illustrates the difference between the Meteonorm default meteorological set for Oslo and the normalised temperature values from The Norwegian Institute of Meteorology (MET). The normalised temperatures from MET are based on daily normalised temperature values from 1961−1990, measured at Blindern in Oslo. Blindern is approximately 3 km from Skøyen. As seen in Figure 3.1.13 there are some deviations of two to three degrees between the Meteonorm default values and the values from MET, especially in the months November to February. Due to the length of time the series of temperature values are measured, and the short distance between Blindern and Skøyen, the temperature values from MET are used in the second meteorological data set (shown in Table 3.1.5).

The two last components of the meteorological data set, diffuse irradiance and wind, were also extracted from the databases available. Since these data are not necessary in order to perform a simulation, they were not compared with measurements from Lier, Ås or MET. Neither weather stations in Lier, Ås or Blindern provide diffuse irradiance data, however, they do provide wind data. There were two databases which supplied diffuse irradiation data, Meteonorm and NASA. There were two data series from Meteonorm, one from the default

location Hurum, and the other from Skøyen. Since the two Meteonorm sets were closest to the local sets considering global irradiation, these two data series where assumed closest also in this regard. The diffuse data series used in the second meteorological data set are, therefore, the average of these two Meteonorm data series.

There were three databases which supplied wind data: Meteonorm, NASA and RETScreen. RETScreen is a database with values from 1961 to 1990. When there are no ground measurements either because they are not reliable or available, the data is supplemented from the NASA database. From RETScreen there were available ground measurements from Blindern. When comparing the temperature data, RETScreens data was as good as a complete match to the measurements from MET (see Appendix B). No average was, therefore, made between the three databases and the data from RETScreen was assumed to be the most correct data.

Table 3.1.5: The second meteorological data set which will be used in the simulations

	Global	Diffuse	Temperature	Wind
Month	Met, L, A	Met	MET	RETScreen
January	11.09	7.5	-4.30	2.5
February	27.38	17.0	-3.99	2.6
March	67.47	36.0	-0.20	2.6
April	111.80	53.5	4.50	3.0
May	157.95	76.5	10.81	2.8
June	166.57	85.0	15.19	2.8
July	149.39	79.5	16.41	2.5
August	119.70	63.0	15.20	2.6
September	77.56	42.5	10.80	2.6
October	39.05	24.5	6.31	2.6
November	14.85	9.5	0.70	2.6
December	7.15	5.0	-3.10	2.6
Yearly	949.97	499.5	5.70	2.65

3.2 Orientation

For this project it was chosen to use fixed tilted PV modules. Other options are seasonal tilted modules, tracking systems, one or two axis tracking systems or BIPV such as roof tiles or shades. Systems with one or two axis tracking

are mostly used for ground mounting. In addition, such systems are assumed to require more maintenance since there are more mechanical parts, and thus not very practical for roof installations. Furthermore, such mounting systems are more expensive. The modules should be directed towards south in order to obtain as much irradiation as possible. This corresponds to an azimuth angle of 0°. Magnetic and geographical south should in theory be the same. Due to the magnetic flux lines on Earth they deviate with varying degree depending on location. The modules should be directed towards geographic south, and not magnetic south, since this would affect the system yield [7, p.41].

3.2.1 Optimum Tilt Angle

The amount of radiation collected on the solar modules should be as large as possible. The tilt angle of fixed modules can be maximized with regards to seasonal performance or annual performance. The optimum tilt angle β_{opt}, illustrated in Figure 3.2.1 is defined as the tilt angle of highest annual irradiation and depends on both latitude (ϕ) and local climate. The rule of thumb with regards to the highest annual performance is a tilted angle approximately equal to the latitude of the site, $\beta_{opt} \approx \phi$ [7, p.39] [9, p.862]. The larger the latitude, the larger the difference between summer daytime and winter daytime and, therefore, the larger the difference between the summer and winter irradiation. As a result it can be anticipated that as the latitude increases, the optimal tilt angle should give priority to the collection of summer over the collection of winter irradiance. The system would be facing the equator and tilted at approximately $10° - 15°$ less than the local latitude by using Equation 3.2.1 [9, p.1014].

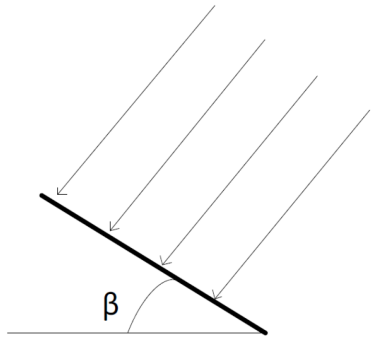

Figure 3.2.1: Tilt angle β

$$\beta_{opt} = 3.7 + 0.69 \mid \phi \mid \tag{3.2.1}$$

It is argued in [15, p.38] that for optimum spring, fall or optimum annual performance, the collector should be mounted at about 0.9ϕ. It is also argued in [24] that the optimum tilt angle is approximately 0.9ϕ, however, only for latitudes less than 65°. In [25] it is confirmed that the rule of thumb applies for nearly all regions in the world, i.e. optimum tilt angle should equal the latitude angle. However, larger deviations are given for regions of latitude higher than 45° N or lower than 45° S. This is a consequence of significantly more clouds, hence more diffuse irradiation which is best captured by flat tilted modules. A difference between latitude and optimum tilt angle can be defined as [26]

$$w = \phi - \beta_{opt} \tag{3.2.2}$$

In a simulation of 217 typical meteorological year data sites in the United States [26] it was found higher w values associated with higher latitudes and lower annual average clearness index $k_{t,a}$. The values for w for fixed south-facing panels, ranged between 0° and 14°. The results showed that the greatest values of w occurred at locations in the coastal Northwest and the Great Lakes regions with low $k_{t,a}$ values. These results were from the United States with highest latitude reaching 50° north. Equation 3.2.3 is based on the results done in [26] for fixed south-faced panels:

$$w = 0.0083\phi^2 - 0.1928\phi \tag{3.2.3}$$

When using equation 3.2.3 with the latitude for Oslo, it yields a w of 17.5171°. However, this would be a result of extrapolation since the latitude in Oslo is above 50°, and the reliability of this result is therefore uncertain. By using equation 3.2.1 w becomes 14.59°. When using PVsyst the optimal tilt angle is suggested to be 40°, facing geographical south. This corresponds to $w = 19°$. This is with regards to the highest annual performance of the PV modules.

3.2.2 PVsyst and Orientation

In PVsyst an information panel indicates the corresponding Transposition Factor (TF), the difference with respect to the optimum orientation, and the available irradiation on this tilted plane. When the TF is zero, the optimal tilt angle is found. PVsyst uses monthly meteorological calculations, which perform quick transpositions. Solar data is often only available for the horizontal plane, transposition from the horizontal irradiance to the tilted and oriented plane is, therefore, preformed [27]. The calculation for the curves is performed for several situations, in both directions from the point chosen (tilts at fixed azimuth, and azimuths at fixed tilt). The Hay model [28] is used as the transposition model in PVsyst, while the Erbs model (or the EKD model, Erbs, Klucher and Duffie model) is the diffuse fraction model used [27]. The diffuse fraction model is used to split the global irradiance into diffuse and beam components.

As a result the optimal tilt of the PV modules is not equal to the latitude, $\beta_{opt} \neq 59°$. The optimal tilt is instead in the range of $40° - 44.41°$, due to local weather of more clouds, more diffuse radiation and a larger difference between summer and winter irradiation. The lowest optimal tilt angle is chosen as the starting point to use in the simulations, since it is a rooftop where the PV modules are to be placed and, therefore, it is a limited area. Increasing the tilt angle of the modules results in a larger pitch distance between the rows in order to maintain the same length of shading from other rows. Decreasing the tilt angle further from 40° should be tested in order to observe the effect this has on the energy production and the Performance Ratio (PR) of the system. This will be further discussed in Section 3.4.4.

3.3 Shade

Shade on the modules result in a reduction of irradiation on the cells, which has a substantial influence on the current produced in the cell and module. The irradiance deficit is one of the losses when considering shading. The irradiance loss induces a non-linear electrical loss.

3.3.1 Electrical Effect of Shading

In every module there are placed bypass, or anti-parallel, diodes in order to prevent "hot spots" on the cells. A "hot spot" can occur under certain operating conditions where for example one cell is shaded and heated to the extent that the cell material is damaged [8]. When shade occurs on one cell this does not generate any currents. Instead the characteristics in this cell reverses, and the cell becomes a load which absorbs energy from the circuit. The amount of currents driven through the cell is converted into heat which could lead to "hot spots". When a module is then integrated into an array without bypass diodes, the array may force an even larger current through the cell. The bypass diodes prevent large voltages from building up across the solar cells in the reverse-biased direction (see Figure 3.3.1). The modules would obtain the largest shading tolerance if each cell had a bypass diode connected across it. However, due to manufacturing reasons bypass diodes are usually connected across $18-20$ solar cells. A standard module with $36 - 40$ cells would have two bypass diodes [8, p.73]. A module with one bypass diode could be explained as a module consisting of two sub-modules.

Shading which gives a lower amount of irradiance on the cell, results in a decreasing current. With the bypass diode, the current does not decrease in the first sub-module (the first $18 - 20$ cells) which are not shaded. However, it decreases when reaching the second sum-module with the shaded $18 - 20$ cells, as seen in Figure 3.3.2. The figure illustrates a standard module with 36 cells under STC conditions in which one cell is shaded by 75 %.

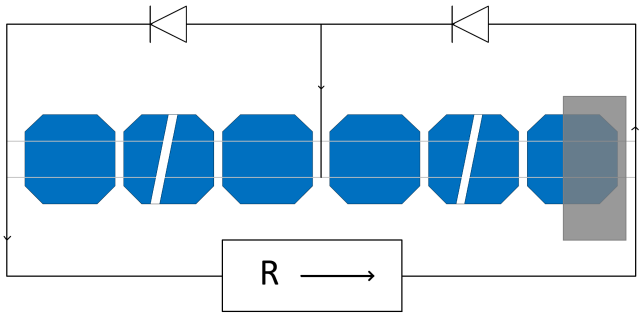

Figure 3.3.1: Connection of bypass diodes

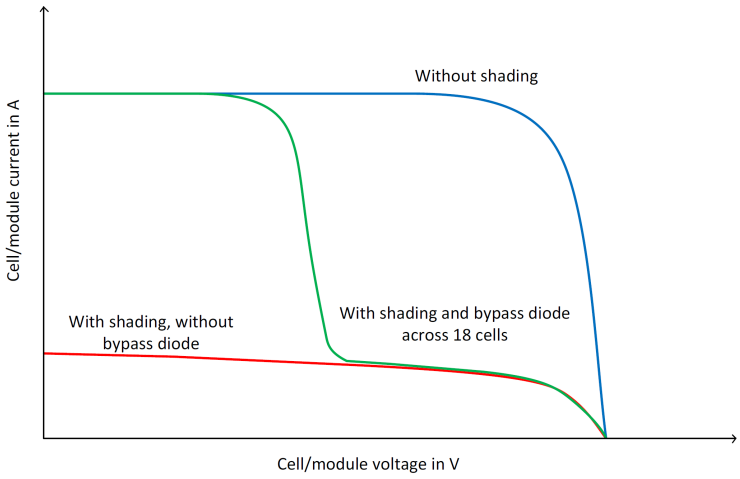

Figure 3.3.2: Module I-V curves with and without bypass diodes

Figure 3.3.3, 3.3.4 and 3.3.5 show how the I-V characteristic and the power characteristic curve is affected as multiple modules or sub-modules are shaded either in a series or a parallel connection. As seen in Figure 3.3.3, shades in series connection gives two possible power point maxima. Both are possible operating points if they lie within the inverter MPPT range. Which power maxima becomes the operating point depends on the course of shading over time and the behaviour of the MPPT [8, p.123]. The left operating point would with increasing number of shaded modules not be within the inverters MPPT range.

The characteristic curves for arrays with parallel connections vary depending on whether the shades cover several different strings or cover more modules within few stings (illustrated in Figure 3.3.4 and 3.3.5). The power loss remains almost constant for an array with parallel connections when shaded modules (or sub-

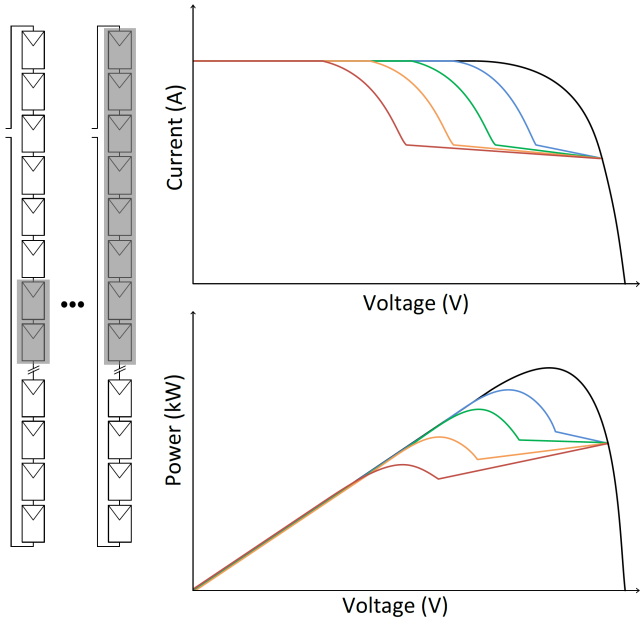

Figure 3.3.3: Shading situation where two to eight modules in a string is shaded, where the black curves = no shading, blue curves = 2 modules shaded, green curves = 4 modules shaded, orange curves = 6 modules shaded and the red curves = 8 modules shaded.

modules) on the same string increases. The power loss for parallel connections increases when the numbers of shaded strings increase. Comparing Figure 3.3.4 and 3.3.5 it is seen that a shading situation covering fewer modules in several strings is preferable to several modules in few strings. Considering the power loss in a string connection, it is greater than the loss for a parallel connection.

Considering the case where the size of the array is not set, another argumentation is called for. Considering only one string with only one module shaded, the loss is stable independent of how many modules are connected in that string [29]. However, with other strings in parallel, the shaded cell distorts the array I-V characteristics and displaces the MPP. As a consequence there occurs additional loss in the other strings (not more than the production of one module). With several shaded sub-modules within an array, consisting of series and parallel connections, the loss increases rapidly. It was shown that the energy loss (in percent of the normal production of the shaded string) increased significantly in the array when it had several parallel strings, and one of the strings was shaded [29]. The shaded string displaces the MPP operating point of the entire array, so that the other parallel coupled strings do not work at their own MPP any longer. This result is in accordance with a single cell shaded in one string and

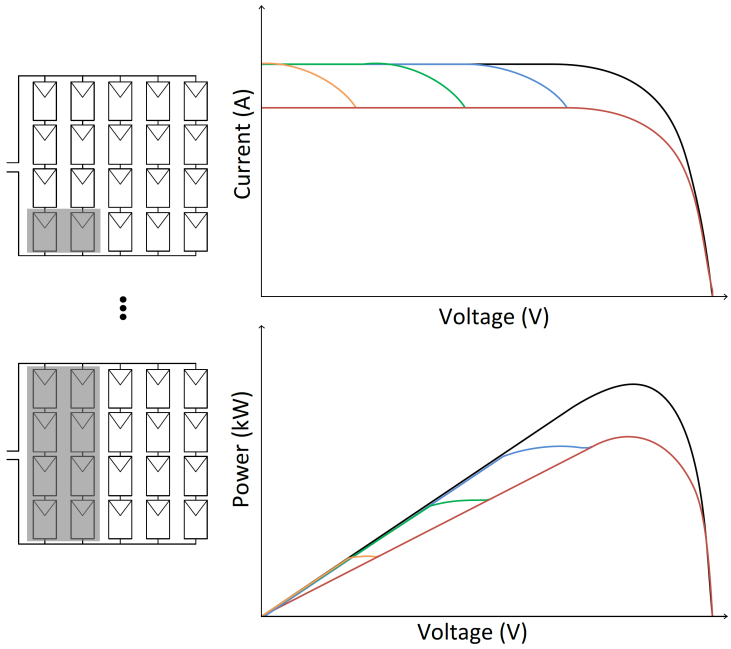

Figure 3.3.4: Shading situation of an array where two of the strings are shaded from two to eight modules, where the black curves = no shading, blue curves = 2 modules shaded, green curves = 4 modules shaded, orange curves = 6 modules shaded and the red curves = 8 modules shaded

then connecting it to other non-shaded strings.

As a design criteria it would, therefore, be most beneficial to have the modules with equal shading in the same string with a separate MPPT from the other strings in order to get the maximum amount of energy produced from the entire system. Fewer modules per string would in addition make sure that more module strings would operate at a MPP closer to their own.

3.3.2 Site Assessment

A site assessment of the roof where the PV installation is proposed in Oslo was performed January 27th, 2012. The commercial building is located at Skøyen in Oslo, 59°55′23.49″ N and 10°40′49.54″ E which can be seen in Figure 3.3.6.

On the roof the shading conditions were evaluated. The ideal installation of a PV system is where there are no shadows at all. When considering shadows on the site the following was evaluated [7, p.161]:

- Natural landscapes, e.g. surrounding mountains

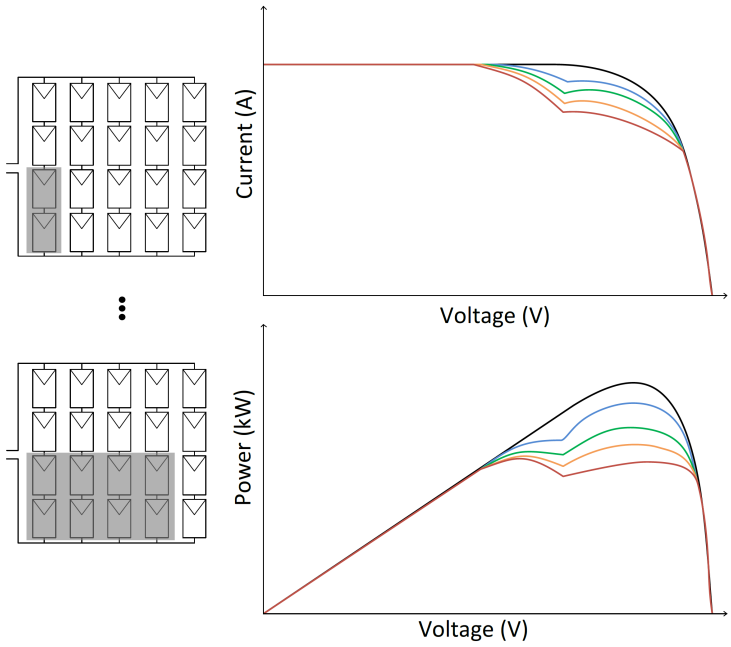

Figure 3.3.5: Shading situation of an array where two modules on one to four strings are shaded, where the black curves = no shading, blue curves = 2 modules shaded, green curves = 4 modules shaded, orange curves = 6 modules shaded and the red curves = 8 modules shaded

- Trees or other vegetation
- Other buildings
- Parts of the actual building where the system is to be located, chimneys etc.

The roof is approximately 1200 m^2. Figures 3.3.7 and 3.3.8 show the space where the PV modules should be placed and the present elements located on the roof. These elements will cast shadows and reduce the area where the modules could be placed. In Figure 3.3.7 there is seen a twelve storey building which also could cast a shadow on the PV installation. It is considered that neither the vegetation nor the natural environment could be considered a great contributor of shadow.

Mounting system

The type of mounting system chosen for the installation and the distance between these greatly affects the amount of shadow on the modules. Figure 3.3.9 shows two different mounting systems where Figure 3.3.9a shows aerodynamic

Figure 3.3.6: Location of the commercial building in Oslo marked with a red circle [30]

mounting system, and Figure 3.3.9b shows a ballasted mounting system. With these two mounting systems there is no need to penetrate the roof which could cause problems with regards to isolation etc. Roof penetrating mounting system exists, but is not taken into consideration in this study. The roof has been dimensioned for heavy snow loads and it is, therefore, assumed that the weight of the installation is not a problem. The issue of weight requirements on the roof has not been considered further in this study.

The amount of shading on the modules depend on the spacing between them, the module height, row length, tilt angle and latitude location. Figure 3.3.10 and Equation 3.3.1 describes two modules and the shadow cast by the first onto the second when oriented towards the equator [33].

$$H_S = A\left(1 - \frac{D + A\,cos\,\beta}{A\,cos\,\beta + A\,sin\,\beta\,cos\,\psi/tan\,\alpha}\right) \tag{3.3.1}$$

In equation 3.3.1; H_S describes the length onto the second module cast by the first, with a distance D between them, a tilt β, and a width of the modules A on a given time marked by azimuth ψ and solar altitude α. Equation 3.3.1 was solved with respect to the distance D between the modules and $H_S = 0$, and tested in Matlab with different types of modules at different days, time of day and with different tilt (see Appendix C). As a dimensioning criterion the modules should

Figure 3.3.7: Horizon north west

not shade each other at the equinoxes. Since this marks when day and night is equally long, either of the equinoxes could be used. In the Matlab calculation spring equinox was used, March 21st.

Table 3.3.1: Spring equinox pitch distances in meters, NASA

March 21st	20°	30°	40°	53°	59°
Mono					
10:00	1.661	1.897	2.076	2.213	2.239
11:00	1.648	1.878	2.051	2.182	2.205
12:00	1.649	1.878	2.053	2.185	2.209
Poly					
10:00	1.574	1.780	1.967	2.097	2.121
11:00	1.561	1.779	1.943	2.067	2.089
12:00	1.562	1.781	1.946	2.070	2.092

Table 3.3.1 shows the pitch distance between the rows in order not to shadow

Figure 3.3.8: Horizon south west

(a) Knubix [31]

(b) DPW [32]

Figure 3.3.9: Two different mounting systems one in landscape, the other in portrait

each other on spring equinox. The NASA numbers for azimuth and solar altitude has been used in this table. As seen, a higher tilt angle results in a larger pitch distance. The pitch distance is illustrated as D + A cos β in Figure 3.3.10. The required distance D to avoid shading during March 21st for a polycrystalline module with 40° tilt is between $1.08 - 1.2$ meters (pitch of $1.95 - 1.97$ meters). The distance close to December 21st is in a larger range of $5.1 - 10.4$ meters (pitch

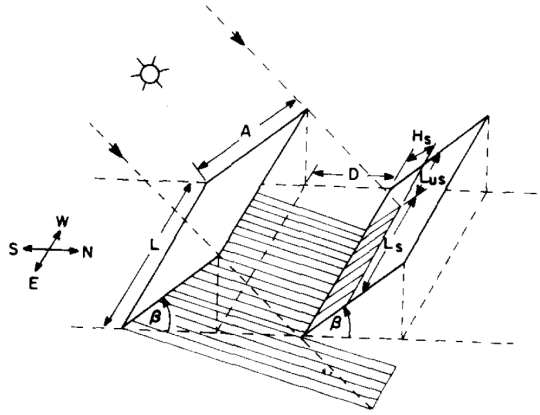

Figure 3.3.10: Shading of modules in rows [33]

of 5.8 to 11.2 meters) depending on which time period the modules are supposed to be shade free (see Appendix C). The distance for a monocrystalline module would be somewhat extended due to a larger width. When having a limited space to place the modules it, therefore, becomes critical that the modules are placed as the Knubix modules in landscape, not as the DPW modules in portrait, in order to decrease the distance between the module rows. Since the difference between the mono- and the polycrystalline modules is so small when tilted 40 degrees on the March 21st a pitch distance of 2 meters will be used in the 3D representation of the PV field.

The choice of mounting system would have an effect on the edge zones surrounding the modules and the module tilt. The edge zone is the distance from the installation to the edge of the building. Table 3.3.2 shows the mounting systems manufacturers that have been looked into in this study and their specifications. The different mounting types have not been considered as a limiting factor of which modular tilt the installation should have. These are simply used as an illustration of some of the manufacturers within ballasted and aerodynamic mounting systems. The edge zone specifications from Solar Dock arise from the State of California's building and fire safety codes (6 feet). DPWs edge zone requirements are based upon the American Society of Civil Engineers (ASCE) Code (require at least 3 feet). The edge zone requirements from Knubix are based on a calculation considering the height of the building. The edge zone for the SolarSTEP mounting system is stated to be valid for buildings with maximum 18 meters, however, could be valid for buildings up to 40 meters. The building in question is approximately 22.5 meters high.

The edge zone for the Skøyen installation is assumed to be approximately 2 meters, since this is the middle value of the five options in Table 3.3.2.

Table 3.3.2: Different mounting types and some specifications

Type	Edge zone minimum	Modular tilt		
Knubix	4.48	10° - 20°	Landscape	Aerodynamic
DPW	0.91	20° - 45°	Portrait	Ballasted
SolarSTEP	2.00	5° - 20°	Landscape	Aerodynamic
SunPower		5° - 10°	Landscape	Aerodynamic
Solar Dock	1.83	15° - 35°	Landscape	Ballasted

3.3.3 PVsyst: Horizon and Near Shadings

In PVsyst there has been made a distinction between far and near shadings. The far shadings are defined as shades cast by the horizon while the near shadings are defined as shades cast by near objects which change during the day.

Horizon

The far shadings are supposed to act globally on the PV plane. Acting globally would mean that it would not give any partial shading on the installation. The sun would either be or not be visible on the field. Horizon defining shadows would naturally consist of surrounding environment such as mountains and are defined with a horizon line in PVsyst (illustrated in Figure 3.3.11). The obstacles should be limited to approximately twenty times the PV-array size [10]. The length of the PV installation is approximately 40 meters, which gives a radius of approximately 800 meters before obstacles could be defined as horizon. The reason for this is that the horizon line is supposed to be viewed in the same way from any point of the field.

When a horizon line is accounted for in PVsyst the beam component of the irradiance is or is not visible on the field. PVsyst determines the exact time when the sun crosses the horizon line and weights the beam hourly value before performing the transposition. The diffuse part of the irradiance is assumed isotropic in the program. The diffuse part does, therefore, not depend on the position of the sun, it is the same irradiance which is coming from any direction of the sky and is therefore a constant factor during the year [29]. The albedo contribution in PVsyst is considered to be linearly decreasing according to the horizon height. When using meteorological data from ground stations the horizon effect is already taken into account for that station. A comparison of the measuring station horizon with respect to the field horizon could be accounted for.

A horizon line for the Skøyen field is not drawn, because of low mountains surrounding the site. In addition some horizon could already have been taken into account in the two measured data sets from Lier and Ås.

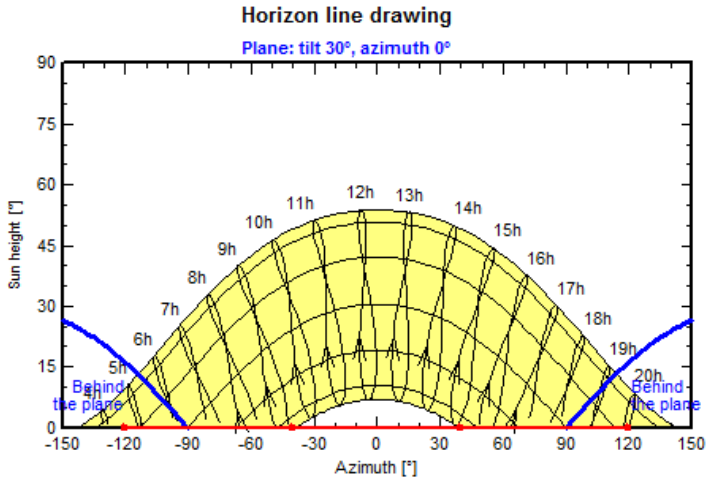

Figure 3.3.11: Horizon line drawing in PVsyst

Near Shadings

Shadings which change during the day and the season and only partly affect the PV field are the near shadings. The fraction of how the PV field is effectively shaded is defined in PVsyst by shading factors. In order to calculate the shading factor at any time as a function of the position of the sun requires a full 3D representation of the field and its surroundings.

The 3D representation of the building (Figure 3.3.12) was constructed mainly by the help of drawings of the building and Google Earth. Some assumptions were in addition made when considering the height of roof top shading elements with the assistance of photos taken during the site assessment. As mentioned there is a 800 meter radius where near shading objects should be taken into account. Inside this radius the twelve storey building illustrated in Figure 3.3.7 is located. This building was, therefore, represented in 3D, with measurements from drawings provided by *plan-og bygningsetaten* in Oslo. Moreover, Google Earth was used in order to place the building in approximate accordance with the PV field.

Within PVsyst the user has three options regarding shade:

1. No shadings
2. Linear shadings
3. Shading according to module strings

The first option would not give any shading and would, therefore, not require a 3D representation of the PV field and the surroundings. The second option, linear shadings, uses the table of shading factors as a function of the altitude

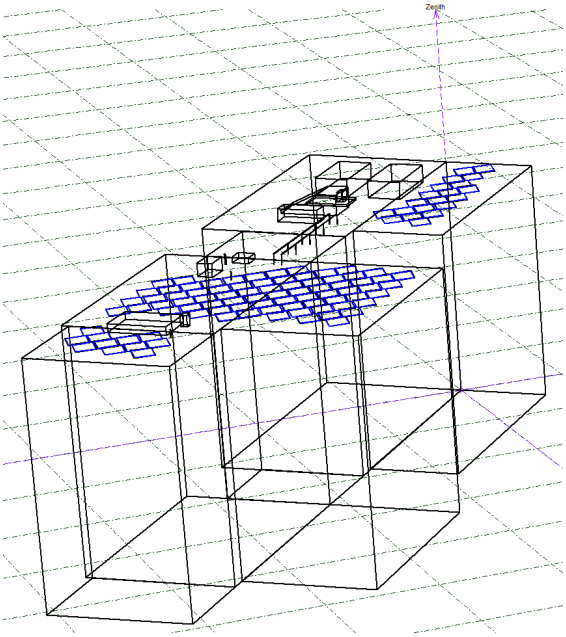

Figure 3.3.12: The 3D representation of the building with a PV installation on the roof in PVsyst

of the sun and azimuth. The table is used since calculation of a shading factor for each hour would take a considerable amount of time. However, the hourly shading factor can be calculated fast by interpolation during the simulation [10]. The shading factors are applied to the beam component of the irradiance and allow for an evaluation of the irradiance deficit on the PV plane were the effect is proportional to the shaded area. Claiming that the shaded area on the field is proportional to the irradiance deficit is, however, not representative for the real energy losses. The electrical behaviour also represents a loss. In order to take into account the electrical behaviour a third option is given to the user: shading according to module strings. The PV field is split into rectangular areas (as seen in Figure 3.3.13), each representing a whole string of modules. When calculating the shading factors the corresponding string becomes unproductive if a rectangle is shaded. It is stated that the real shading loss should lie between linear loss and the loss caused by shading according to module strings.

In order to calculate the shading factor table the program first carries out a transformation of the coordinates of the whole system in order to point the z-axis in the direction of the sun. For each sensitive element of the PV field, the program projects each elementary surface of the system on the plane of the field being considered. The intersections between the field elements and the positive projections are calculated for each element. The global shading on the field

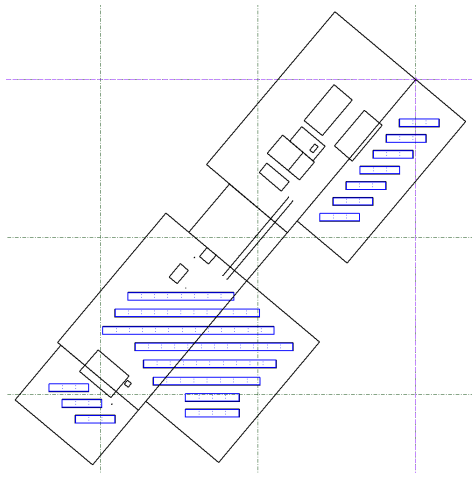

Figure 3.3.13: The modules on the roof drawn with rectangles

element consists of these elementary shadows which forms a polygon. The ratio of the area of the shadow polygon, to that of the sensitive element is the shading loss factor. For each sensitive field element (PV elements) this process is repeated [10].

Shading factor table according to strings, for the beam component

Azimuth / Height	-180°	-160°	-140°	-120°	-100°	-80°	-60°	-40°	-20°	0°	20°	40°	60°	80°	100°	120°	140°	160°	180°
90°	1.000	1.000	1.000	1.000	1.000	1.000	1.000	1.000	1.000	1.000	1.000	1.000	1.000	1.000	1.000	1.000	1.000	1.000	1.000
80°	1.000	1.000	1.000	1.000	1.000	1.000	1.000	1.000	1.000	1.000	1.000	1.000	1.000	1.000	1.000	1.000	1.000	1.000	1.000
70°	1.000	1.000	1.000	1.000	1.000	1.000	1.000	1.000	1.000	1.000	1.000	1.000	1.000	1.000	1.000	1.000	1.000	1.000	1.000
60°	1.000	1.000	1.000	1.000	1.000	1.000	1.000	1.000	1.000	1.000	1.000	1.000	1.000	1.000	1.000	1.000	1.000	1.000	1.000
50°	1.000	0.999	1.000	1.000	1.000	1.000	1.000	1.000	1.000	1.000	1.000	1.000	1.000	1.000	1.000	1.000	1.000	1.000	1.000
40°	0.999	0.999	0.999	1.000	0.999	0.999	0.999	1.000	1.000	1.000	1.000	1.000	1.000	1.000	1.000	1.000	0.999	0.999	0.999
30°	0.999	0.997	0.995	0.996	0.998	0.997	0.999	1.000	1.000	1.000	1.000	1.000	1.000	1.000	0.995	0.987	0.988	0.993	0.999
20°	0.999	0.997	0.994	0.982	0.991	0.994	0.997	0.999	0.872	0.870	0.869	0.997	0.998	0.988	0.973	0.959	0.982	0.990	0.999
10°	Behind	Behind	Behind	0.976	0.959	0.987	0.875	0.750	0.609	0.598	0.588	0.718	0.839	0.916	0.894	0.942	Behind	Behind	Behind
2°	Behind	Behind	Behind	Behind	0.942	0.767	0.448	0.380	0.100	0.136	0.117	0.278	0.401	0.569	0.833	Behind	Behind	Behind	Behind

Shading factor for diffuse: 0.962 and for albedo: 0.273

Figure 3.3.14: The shading factors of a PV system with a 20 ° modular tilt and a 2 meter pitch and a 2 meter edge zone, calculated in PVsyst

The diffuse irradiance component is assumed isotropic as in horizon, and is therefore constant during the year. The value is, however, not necessarily the same value as in horizon, since it is affected by near shading objects. In near shadings the diffuse irradiation could be explained as the integral of the shading factor of the visible part of the vault of heaven seen from the module [10]. This integral is the same during the year, but depends on the 3D representation of the field. The albedo component is also considered as a constant during the year in PVsyst. The diffuse and albedo shading factors are the same for linear shading and for

shading according to module strings. Reflections are not taken into account in PVsyst due to their very special hourly presence and since the reflection usually only hits a few modules within a string.

Along with having the choice of which type of shading is to be considered, a fraction for electrical effect in percentage is also possible to adjust in PVsyst. The difference between the value given by the linear loss (deficit of irradiance) and the loss according to module strings (taking into account the electrical effects) is due to electrical mismatch. The fraction of electrical effect acts on this difference and is adjusted by a percentage of intensity of the real effect. A percentage of 0 would equal pure linear shading, while 100 percent would equal full shading according to strings. The fraction for electrical effect is dependent on the shade distribution on the field and the electrical array configuration [29]. For shade arrangements where the shades are regular (mutual shadings of sheds) a sufficient set of sub-modules are shaded at the same time, completely suppressing the production of the full string, which would be close to 100 percent of shading according to strings. In cases where there are more distributed shades (for example from a chimney) where only some sub-modules are affected, some of the energy could be recovered due to the bypass diodes, and the fraction of electrical effect could be in the order of $60-80$ % [10]. A fraction of electrical effect of 60 % is assumed to be a realistic value with as many shading objects as there is on the roof.

Shade analysis

With the help of the shading animation during a day which is a possibility in PVsyst, a shade analysis was performed. The shading simulation in PVsyst gives a graphical view of the shading situation for every half hour of a chosen day. For each half hour during the day the modules that where shaded was recorded as either partially shaded or fully shaded. A shading analysis was performed for March 21st since this is the day when there is not supposed to occur module shading owning to other modular rows. The shading analysis would, therefore, only illustrate the shading caused by the shading elements on the roof. There has been made a distinction between partially shaded modules and fully shaded modules. However, the elimination of redundant modules is to be done on account of the longest duration of shade, not depending on if it is partially or fully shaded. A shade analysis was done for the final alternatives, since a change in modular tilt and pitch distance would change the shading lengths.

3.4 System - Matching Array and Inverter

In PVsyst the main components in the PV system are chosen: the module and inverter type and manufacturer. Type of cable and mounting system is indirectly chosen when determining or calculating the ohmic loss, and when drawing the 3D representation of the PV field.

3.4.1 Choosing Module

Hopesolar, BestSolar, King-Pv, Upsolar, Schuco, Kyocera, REC, Innotech Solar, LG, Samsung, SolarWorld, Boch and SunPower are some of the many manufacturers of poly- and monocrystalline modules today. In order to narrow down the selection of modules, three different module manufacturers where chosen:

1. Renewable Energy Corporation (REC)
2. Innotech Solar (ITS)
3. SunPower

REC was chosen since it is originally a Norwegian based company. However, it is now a worldwide organisation with several material factories in the USA and wafer and module production in Singapore. From each of the three manufacturers one module series was chosen to be evaluated further in this study. From REC the Peak Energy EU Series was chosen. From ITS the EcoPlus series was chosen since the module is manufactured in Sweden. SunPower was chosen since they manufacture high efficiency monocrystalline modules, and the series chosen was the E20 series. One module type was chosen from each of the three series. In order to produce as much energy as possible the module type from each series with the highest watt peak (Wp) was chosen. From REC REC250PE was chosen (250 Wp, polycrystalline, 15.1 % module efficiency), from ITS EcoPlus-PolyUp (250 Wp, polycrystalline, $15.2 - 15.8$ % module efficiency) and from SunPower SPR-327NE-WHT-D (327 Wp, monocrystalline, 20.1 % module efficiency).

When choosing a module within a kilometre from the coastal line a module certified with IEC61701 should be used [7, p.166]. IEC61701, "salt mist corrosion testing of PV modules", ensures that the modules are salt tested. The building in question at Skøyen is located $500 - 600$ meters from the coastal line. The certification IEC61215 could be extended to a higher load capacity rating of 5400Pa which could be relevant in regions that are subjected to heavy snow loads. When investigating the module certifications these two certifications were checked for explicitly. However, going into depths of finding out whether the manufacturer has chosen to increase the load capacity has not been investigated further.

Both series chosen from REC and ITS has the IEC61701 and IEC61215 certifications. The SunPower series chosen is certified with UL1703 which is an American certification standard. It is assumed that the SunPower certification corresponds to the IEC61701 and IEC61215.

3.4.2 Choosing Inverter

There are different choices between inverters, such as central inverters, multi-string inverters, string inverters, modular inverters, three and one phase inverters

and inverters with or without galvanic isolation in form of transformers. When the inverters are selected the following has to be taken into account [7, p.168]:

- The peak rating of the PV array
- Whether the solar modules are all in the same plane that is the same angle and direction.
- The type of shading that occurs on the array
- The average annual yield

The peak rating of the PV array vary depending on how many modules that are placed on the roof and whether it is a polycrystalline or a monocrystalline module. With the modules placed as illustrated in Figure 3.3.12, the array has a peak rating of 26 kWp with poly crystalline modules, and a peak rating of 34 kWp. Since the array has a peak rating above 20 kWp a central inverter could be chosen. However, due to the amount of shading elements on the roof string inverters were chosen. If the modules were not all in the same plane, this would also have been a reason to use string inverters instead of central inverters.

As with the modules the list of inverter manufacturers is long, and has been narrowed down to the three following:

- Eltek
- SMA Solar Technology AG
- Danfoss

The string inverters THEIA TL String, and THEIA HE-t by Eltek were chosen since they have high efficiency and one MPPT. The multi-string inverters Sunny Tripower of SMA was chosen since it has two MPPT inputs and high efficiency. Danfoss TLX series was chosen since they manufacture multi-string inverters with as much as three MPPT inputs per inverter and has high efficiency. For further information see the technical information in Appendix F.

For each of the three modules chosen, inverters from one of the three inverter series were chosen. In order to choose inverters all possible inverters (which are not over- or undersized) were simulated in the system as close up to 104 modules which is the limit when maintaining the edge zone of 2 meters. The system had otherwise 20° module tilt angle, 60 % electrical effect and was simulated with the new meteorological data set.

3.4.3 Matching Module and Inverter

The array and the inverter have to match in three areas: voltage, current and power. First, by taking voltage into account the array should be within the MPPT range of the inverter. Second, the number of strings in parallel cannot

exceed the maximum input current of the inverter. Third, the output power of the inverter limits how many modules in total that can be connected to it. In the simulations, the single-diode model explained in Section 2.2 is the model used to describe a PV module in PVsyst. By using this model to describe a module, it implies that all cells in the module are identical. More complicated models for the PV cell exists, such as the two-diode model. The single-diode model is considered sufficiently accurate in PVsyst, since there is a moderate accuracy of the input parameters (supplied by the manufacturers) and the fact that mismatch losses are taken into account separately [10]. Mismatch losses will be explained in Section 3.4.4.

Matching the PV array to the voltage specifications of an inverter

As explained in Section 3.1.1 the module voltage is dependent on the temperature. When arrays are matched with inverters the extreme temperatures of winter and summer are used in order to establish the size of the strings in terms of minimum and maximum number of modules.

Determining the minimum amount of modules in a string, the maximum cell temperature is used. The minimum inverter voltage is divided by the module maximum temperature voltage in order to find the minimum amount of modules in a string. The reason for this is that the MPP voltage of the array should not fall below the minimum operating voltage of the inverter, since the inverter could switch off or not operate at the arrays maximum possible output (see the red characteristics in Figure 3.4.1). The minimum amount of modules in a string is defined by

$$n_{min} = \frac{V_{MPP\ inverter\ min}}{V_{MPP\ module\ max\ temp}} \tag{3.4.1}$$

where

$$V_{MPP\ module\ max\ temp} = \left(1 + \Delta T \cdot \frac{\gamma_{V_{MPP}}}{100}\right) \cdot V_{MPP\ STC} \tag{3.4.2}$$

and where ΔT is the temperature difference between the highest module or cell temperature and the STC temperature (for example 70° C - 25° C) and where γ_V is the voltage temperature coefficient of the module [8].

The inverter may not always be operating at the ideal MPP, because of shading, less irradiance etc. A safety margin of 10 % could, therefore, be allowed. In addition a factor for the voltage drop expected across the DC cables could be taken into consideration in this calculation [7, p.187]. Equation 3.4.1 is used in PVsyst without a safety margin of 10 %. The voltage drop across the DC cables is taken into consideration in another calculation in PVsyst as explained

in Section 3.4.4 and it should, therefore, not be taken into consideration twice. If taken into account, the safety margin of 10 % would increase the minimum amount of modules. This consideration has not been taken into account in this study.

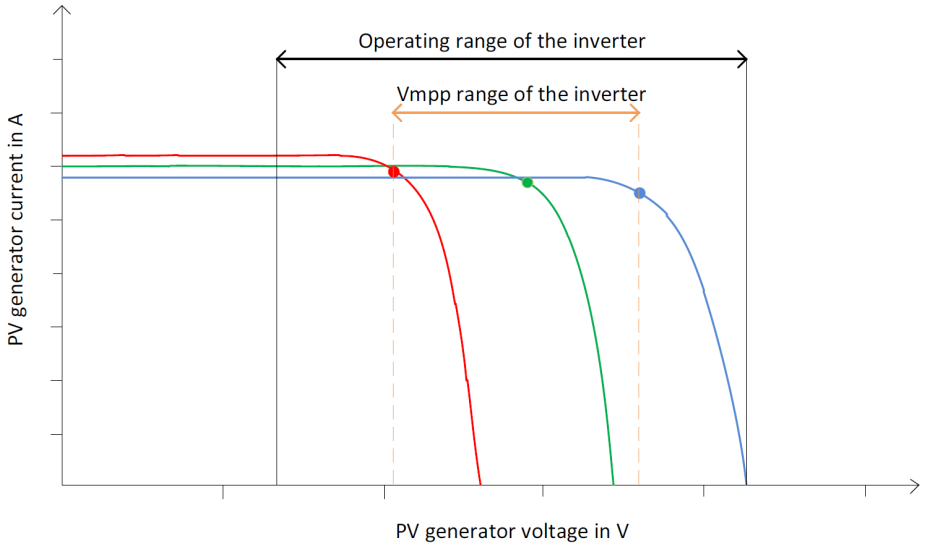

Figure 3.4.1: PV module characteristic curves and operating range of an inverter. The red module temperature 70° C, green module characteristic = 20° C, blue characteristic -20° C

The maximum amount of modules in series is determined by the minimum temperature of the modules since it is at this temperature the voltage of the array is largest. At first light in the morning the cell temperature will be close to the ambient temperature since the sun has not had time to heat the modules. The open circuit voltage has to be lower than the maximum voltage at the inverter in order to stay within the MPP voltage of the inverter (see the blue characteristic in Figure 3.4.1). The maximum amount of modules in series is, therefore, computed as

$$n_{max} = \frac{V_{max\ inverter}}{V_{OC\ module\ min\ temp}} \tag{3.4.3}$$

where

$$V_{OC\ module\ min\ temp} = V_{OC\ STC} - \left(\frac{\gamma_{V_{OC}}}{100} \cdot V_{OC} \cdot \Delta T\right) \tag{3.4.4}$$

and where $\gamma_{V_{OC}}$ is the open circuit temperature coefficient of the module (in V/° C) and ΔT is the temperature difference between the STC of 25° C and the lowest cell (or module) temperature (for example -20° C, -25° C) [8]. Equation 3.4.3 is used in PVsyst. It is recommended in [7, p.190] that a safety margin of 5 % below the specified maximum inverter voltage should be allowed to account for manufacturer tolerances and in case of extremely cold weather. This safety margin is not taken into account in PVsyst. The two sizing criteria are shown in Figure 3.4.2 as the two vertical lines marking the V_{MPP} range of the inverter.

Matching the PV array to the current specifications of an inverter

The current of the modules is only vaguely affected by temperature changes as explained in Section 3.1.1. The largest current of the modules has to be smaller than the maximum inverter current in order to function. By evaluating the current of the modules the number of strings in parallel can be assessed in accordance with

$$n_{strings\ in\ parallel} = \frac{I_{max\ inverter\ input}}{I_{SC\ STC} + (\gamma_{I_{SC}} \cdot \Delta T)} \tag{3.4.5}$$

where $\gamma_{I_{SC}}$ is the short circuit current temperature coefficient of the module in A/° C and ΔT is the temperature difference between the STC and the highest cell (or module) temperature[8]. The current criteria is shown in Figure 3.4.2 as the horizontal line of 210 A.

Matching the PV array to the power specifications of an inverter

In the inverters specification it is common to include maximum PV array rated power and maximum DC input power. The dotted line in Figure 3.4.2 show the inverter maximum DC input power, which is the maximum amount of DC power that the inverter can convert to AC. This number is usually lower than the maximum PV array power due to the losses in the system before it reaches the inverter. Finding how many modules that can be connected to an inverter the maximum PV array rated power or maximum DC input power is divided by the peak effect of the module in question. In PVsyst it is assumed that the division is done with respect to the maximum DC input power on account of Figure 3.4.2.

3.4.4 Losses

The losses that occur in a PV system could be explained as the cause of a reduction of the available array output energy with respect to the nominal power of the PV module stated for STC conditions [10]. The dimensioning criteria

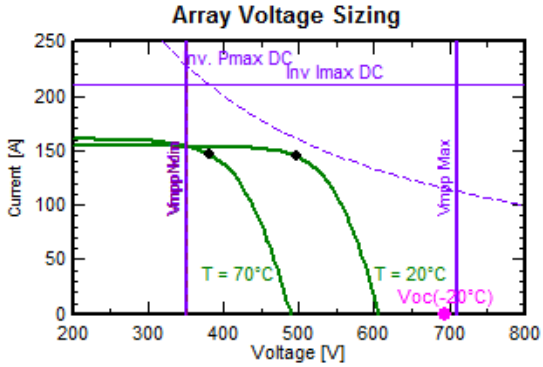

Figure 3.4.2: Array or inverter sizing in PVsyst, 16 REC245PE modules in series and 18 strings, using a Eltek inverter, Theia 7200TL

of the performance ratio is discussed first followed by the losses which are taken into account in PVsyst (irradiance loss, thermal loss, ohmic loss, mismatch losses, quality loss, soiling loss and incidence angle modifier loss) A summary of the final parameters used during the simulations are found in Appendix D.

Performance ratio

PR is defined in [34] as

$$PR = \frac{Y_f}{Y_r} \tag{3.4.6}$$

where Y_f is the final system yield, and Y_r is the reference yield. The reference yield which is the system yield without losses, while the final system yield is taking into account the losses in the system. The PR as a result indicates the overall effect of losses. The losses are affected by array temperature, incomplete utilisation of the irradiation and system component inefficiencies or failures [34]. Since the PR is normalized it can be used in order to compare PV different system types for the same location, as well as identical systems installed in different locations [7, p.247].

It was presented operational performance results of 368 grid-connected PV installations in [35]. PV systems installed during $1991 - 1994$ and $1996 - 2002$ were compared, and an increase of the annual PR values where observed from an average mean PR of 0.65 to 0.74. The maximum PR range of the systems installed in $1991 - 1994$ was 0.65 to 0.7. For the newer installations $(1996 - 2002)$ the maximum PR was in the range of 0.75 to 0.8. It was stated that by taking into account the efficiency values of inverters of today (article published in 2004),

optimum values of annual PR between 0.81 and 0.84 could be achieved [35]. An annual PR of 0.6 to 0.8 for a grid-connected system was the result of the performance analysis of 260 PV plants in the IEA-PVPS Task 2 database [12], which is in the same range as indicated range for a grid-connected system in [9] 0.65 to 0.75. However, it is also stated in [9] that well designed PV installations, with high performance have a PR in the range of 0.7 to 0.8.

Taking the arguments above into account the PV installation in Oslo should have a PR optimally above 0.8 and if lower, not below 0.78. This should be used as a dimensioning criteria in the simulations.

Irradiance Loss

Irradiance loss describes the loss which is caused when the irradiance differs from the STC conditions. The nominal efficiency for the modules are specified for STC conditions. This efficiency decreases when the irradiance reaching the module decreases, that is going below 1000 W/m^2.

Thermal losses

The thermal losses describe the loss as a result of the temperature difference between the modules in the array and the 25° C which is the temperature at STC conditions. The operating temperature of modules are normally much higher than 25° C. They can reach as much as $60 - 70$° C as calculated in Section 3.1.1. In PVsyst the thermal loss is calculated following the single-diode model (as explained in Section 2.2).

In PVsyst there are two ways to influence the calculations of the thermal loss, either by defining the field thermal loss factor, or the standard NOCT coefficient. The program gives the equivalence between the two. The energy balance between ambient temperature and the cell temperature is due to irradiance as seen in Equation 3.4.7

$$U \cdot (T_m - T_a) = A \cdot G \cdot (1 - \eta_m) \tag{3.4.7}$$

Equation 3.4.7 describes the thermal behaviour, where A is the absorption coefficient of solar irradiation, and η_m is the module efficiency. The default value for the absorption coefficient is 0.9. However, this value can be changed in PVsyst. PVsyst calculates the PV efficiency according to the operational conditions of the module when possible. PVsyst uses 10 % as the PV efficiency if calculation is not possible.

The thermal loss factor is described by

$$U = U_c + U_v \cdot v \tag{3.4.8}$$

where U_c is the constant component of the thermal loss factor, U_v is a factor proportional to the wind velocity v. These factors depend on the mounting of the modules, sheds, roofing, façade, etc. The mounting gives an idea of how well the system is ventilated, e.g. sheds would give free circulation of air on both sides of the module. For the field thermal loss factor there are three default options which could be chosen:

1. "Free" mounted modules with air circulation
2. Semi-integrated with air duct behind
3. Integration with fully insulated back

The standard NOCT coefficient can be defined instead of the field thermal loss factor. In such a case PVsyst uses Equation 3.4.7 with the definitions of the NOCT conditions (described in Section 3.1.1).

The NOCT coefficient is usually specified by the manufacturers. The NOCT coefficient is the temperature attained by the PV modules with free air circulation all-around the module under the conditions described above. There are two ways of defining NOCT, as an open circuit (at V_{oc}) or loaded (at P_{mpp}) [10]. In the definition of NOCT the operating state is not clear. As a result PVsyst assumes that the definition concerning open-circuit modules has a $\eta_m = 0$ and $\eta_m = 10$ % when the system is loaded. PVsyst lets the user choose how the thermal loss should be defined, either by the NOCT coefficient of the module or by the thermal loss factor. In this study it has been chosen to use the NOCT coefficients defined as open-circuit in order to define the thermal losses.

Ohmic losses

Ohmic losses ($R \cdot I^2$) taken into account in PVsyst are the ones caused by the wiring resistance. In PVsyst the user has the option of including transformer losses if an external transformer exists. When determining the global wiring resistance of the DC circuit it can be done by either setting the ohmic loss ratio or by explicitly defining the loss in mOhm. There is also the option of performing a computation in PVsyst in order to calculate the global wiring resistance.

The two wiring layouts which are taken into account in PVsyst are shown in Figure 3.4.3, a layout with parallel strings and Figure 3.4.4, a layout with groups of parallel strings. The blue lines illustrate the string module connections. The pink lines show the connections to the main box or the connection box, while the green lines illustrate the wiring between the connection boxes of the strings to the inverter. The wiring connection most similar to the one in Skøyen would be the one illustrated in Figure 3.4.3. In the Skøyen case there would not be any

need for a connection box, the string module connections would go straight to the inverters.

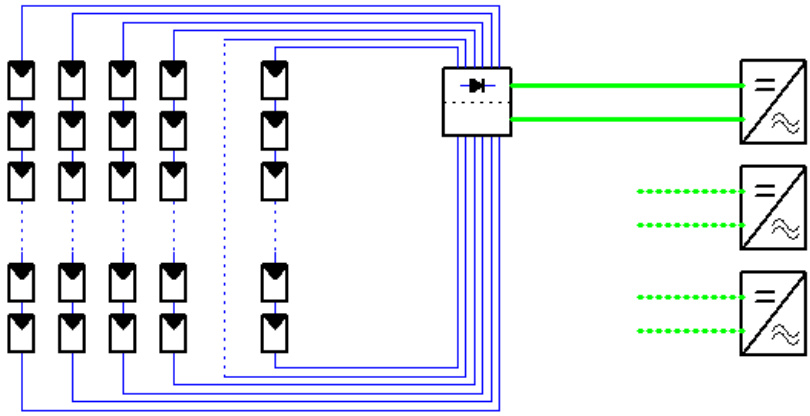

Figure 3.4.3: Wiring connections for parallel strings

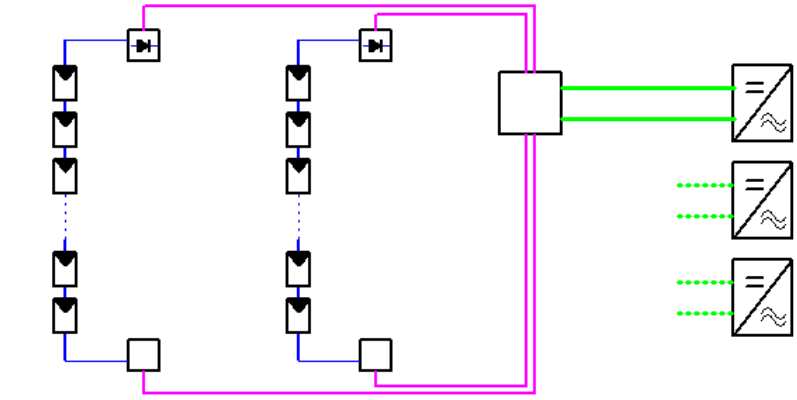

Figure 3.4.4: Wiring connections for groups of parallel strings

In addition to taking DC cable lengths into account the user has the option of including the AC circuit which is the wiring from the inverter to the injection point. If it is of significant length this should be taken into account. If there is an external transformer present in the system then, iron loss and resistive/inductive losses can be taken into account as well. The ohmic loss ratio is the ratio between the wiring ohmic loss $P_{wir} = R_{wir} \cdot I_{sc}^2$ and the nominal power $P_{nom}(array) = R_{array} \cdot I_{sc}^2$. Where $R_{array} = \dfrac{V_{mp}}{I_{mp}}$ at STC and R_{wir} is equal to the global wiring resistance of the system. The global wiring resistance is obtained by placing

the sub-array wiring resistances in parallel. The amount of wiring loss could be adjusted for by choosing an alternative cross section. In this case a resistive wiring loss of 1.5 % is chosen as an upper limit which can be altered with other cross sections were the prices of different wires could be taken into account.

Module quality - mismatch

Module efficiency loss describes the deviation of the average effective module efficiency with respect to the manufacturers' nominal specification. This used to be a great uncertainty when evaluating PV system performance. Now modules are sold with guaranteed power assertions, a given tolerance and flash-test assertions. The module efficiency loss default is 0.1 %. However, it is stated that this value should express the users own confidence in the modules performance [10]. With respect to the manufacturers' specifications this value is, therefore, set to 0 % in this study.

Mismatch losses take into account that real modules in an array does not necessarily present the same I-V characteristics. PVsyst has made a graphical tool for determining the effect of parameter mismatch, for either the cells in a module or the modules in an array. In this tool there is used a random dispersion of the characteristics of the short-circuit current for each module by Gaussian distribution or square distribution. The tool gives the power loss at MPP and the current loss at 90 % of V_{MPP}. The simulation asks for a mismatch loss factor which is different for MPP or fixed-voltage operation. This is taken as a constant during the simulation. The type of module used would give different mismatch losses. Performing the simulation the default values for the mismatch losses are considered sufficient and are, therefore, proceeded with in the simulation.

Soiling loss

In PVsyst there is the possibility of defining either a yearly soiling loss factor or monthly values all expressed in percent. Soiling could behave as mismatch losses since some cells are shaded and, therefore, give a different I-V characteristic than normally. The soiling loss is defined as a percentage of the STC power. It corresponds to a global diminution of the array power and is equivalent to irradiance diminution. It is not assumed soiling on the modules. Even if Oslo is the largest city in Norway, the air is considered clean. What is known, is the possibility of snowfall (se Figure 3.3.7 and 3.3.8). January is assumed to be the month with most snow in Oslo, still it is possible to observe snow in December, February and March. Snow around the modules would improve the efficiency due to a reduction in temperature, and the reflections from the snow cover could affect the modules in a positive manner. With increasing tilt angle of the modules it could be argued that the snow would simply slide off the modules or melt. However, if the snowfall is heavy during night and does not slide off the

modules the snow would act as soil and cause a diminution of irradiance. As a result monthly soiling losses has been assumed to 35 % in December and February and 50 % in January. It could be argued that soiling losses should also be added in March. A discussion or an evaluation whether snow should be considered as soiling loss and not taken into account in another manner in PVsyst could be done in a later stage. The snow is taken into account as soiling loss in this study with the assumption that it would give a more conservative perspective on the energy production during winter.

Incidence Angle Modifier (IAM) losses

IAM could be called reflection loss. The reflection loss is an optical effect which occurs when the irradiation reaches the glass which is protecting the PV cells which lie underneath. The loss follows Fresnel's laws with regards to transmission and reflection on the protective layer (the glass), and on the cell's surface. In PVsyst this loss is taken into account by Equation 3.4.9

$$F_{IAM} = 1 - b_0 \cdot (\frac{1}{cos\, i} - 1) \tag{3.4.9}$$

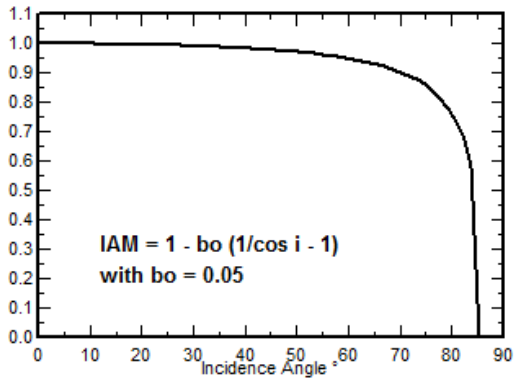

Figure 3.4.5: Incidence angle modifier

where i equals the incidence angle on the plane. Equation 3.4.9 is the Fresnel laws by using a parameterisation called ASHRAE. The default value for b_0 is 0.05. This value is set for crystalline PV modules. For thermal solar modules $b_0 = 0.1$ [10].

3.4.5 Cable sizing

Cable sizing is indirectly considered in PVsyst when defining the ohmic losses in the system. In this study where only the maximum ohmic loss has been defined in the program, approximate cable sizing was done after the simulation. Cable sizing was only done for the final alternatives since it has to be done after all the strings have been assigned their string. In order to size the wirings to have a loss below 1.5 %, all lengths of the string wirings have to be measured. Choosing the wiring path several factors could be taken into account, such as:

- The Current Carrying Capacity (CCC)
- Practical considerations
- Aesthetic consideration
- Economic considerations
- Voltage loss

The CCC refers to the maximum amount of current a conductor can have flowing through it without causing damage. The CCC is affected by the cross sectional area of the conductor, type of insulation around it and the environment in which the cable is installed. A reduction factor of the CCC could be added if several conductors were placed together causing heat between the conductors [36]. Here only practical considerations were taken into account due to the vast amounts of assumptions which would have to be made in order to evaluate both the CCC and the economic considerations. The upper limit of the voltage loss is taken into account in PVsyst which leaves the practical and aesthetic considerations. The aesthetic considerations are evaluated as not important due to the fact that the installation is on a roof where only a few people have access.

The minimum cross section size was calculated with Equation 3.4.10:

$$A_{DC\ cable} = \frac{2 \cdot L_{DC\ cable} \cdot I_{DC} \cdot \rho}{Loss \cdot V_{MPP\ string}} \tag{3.4.10}$$

where $L_{DC\ cable}$ is the route length of the DC cable, I_{DC} is the string current, ρ is the resistivity of the wire, $Loss$ is the percentage of maximum voltage loss in the conductor and $V_{MPP\ string}$ is the string voltage. The route length of the DC cable is adjusted for with the factor of 2, since this is closer to the total circuit wire length.

3.5 Module Layout

Module layout is a descriptive tool in the version of PVsyst which has been tested during this study. In a future version this will be related to the 3D representation

of the PV field. The module layout is independent of the electrical design and the simulation of the PV system. In module layout the user has the possibility to recreate the PV field where each module is represented. Once all the modules in the system have been placed, defining the electrical configuration of the field can be performed. Each module is assigned to a string which then is assigned automatically to a MPPT input. The number of bypass diodes per module is defined by the user as well as the coupling of them resulting in sub-modules in length or width. When all modules have been assigned the electrical shading effects of a string can be observed. Shades are drawn manually over the modules, and the global and diffuse irradiance on the plane can be set manually as well as the temperature. The effect of the shading drawn is given in percentage for the linear shading factor on the beam component, on global irradiance and the additional electrical non-linear loss. Results of the shading test are given for the whole system as well as for each inverter. In addition I-V and power characteristic curves are shown for each inverter.

Since the shadings are drawn manually in module layout the results would be for that specific shading situation in that exact moment in time. It would require several shading situations during different times of the day and different days during the year in order to get an idea of the shading effect on each inverter and on the whole field. The module layout has, therefore, not been used in this study. However, when module layout could be used with the 3D representation of the field and its surroundings it would give a more realistic result and more details concerning the effect of shading on each string and the whole system.

A layout of the module string configuration has been made for the final alternatives. The module constellation in near shadings have been the basis for the set up with its initial modules. In cases where the 3D representation had to many modules, evaluating which modules which would not be part of the final layout was done with the shading analysis which was made in near shadings.

3.6 Connection to the Grid and Metering

3.6.1 Connection to the Grid and Customer Status

End users producing energy is relatively new in Norway. Nonetheless, in March 2010 there was given a general dispensation to simplify the processes related to customers with an energy surplus. Such customers, so called surplus customers, are defined by NVE as:

End users of electricity that have an annual generation that normally does not exceed their consumption, but have during certain hours a surplus of electricity that can be fed back to the grid. Generation which requires licensing or producers that supply electricity to other end-users are not covered by the dispensation.[37, p.32]

The dispensation from NVE entails that the local network company buys the surplus energy from the customer. The surplus customer does then not have to enter into a balance agreement with the TSO of the Norwegian electric power system. The dispensation also entails that the surplus customers could be excluded from trade concession (omsetningskonsesjon). Per now it is voluntary for the local network company to offer the suggested arrangement for surplus customers. If connection of new surplus customers demands a reinforcement of the network, then the local network companies may require a connection charge from the surplus customer [37, p.33]. All new surplus customers would have to contact their local network owner in order to investigate whether they would like a surplus customer in their grid. The regional network owner and operator for Skøyen is Hafslund Nett AS.

Hafslund Nett does not demand a specific size of energy surplus from the surplus customer other than that it is small enough that it does not fall under NVEs trade concession. Technical demands from Hafslund involve for example that the surplus customers plant cannot contribute to a reduction in voltage quality of other customers in the network. Other demands which are set by Hafslund are due to security considerations. In addition, Hafslund requires a four quadrant meter which can measure the exchange of energy in both directions. Other requirements when connecting to the Hafslund $230 - 400$ V network are found in [38] which is in accordance with *Forskrift om Leveringskalitet* (FoL).

One important question which would arise when considering connection to the grid is: does the PV installation result in a surplus situation of energy during the year? If it does, it could be considered a surplus customer if Hafslund agrees to the connection. If the PV installation does under no circumstances during the year produce more than the building consumes, then the installation would be considered a private installation.

3.6.2 Metering

In case the production exceeds the consumption the location of the meter must be considered. There are many different types of meters, depending on what the consumer needs to measure with respect to the purchasing agreement with the electrical distributor, in this case Hafslund. Figure 3.6.1 illustrates two different metering, net metering and gross metering. With a gross metering system the main switch solar supply would be shifted to the point in front of the meter measuring the solar supply production, marked with a dotted line.

A net-metering agreement would allow the customer to use all the electricity produced by their own PV system and only be charged for any excess electricity which is consumed. This would mean that the electricity distributor purchases the electricity at the same rate as they are selling to the consumer [7, p.144]. The net metering schematic could or could not measure the solar production,

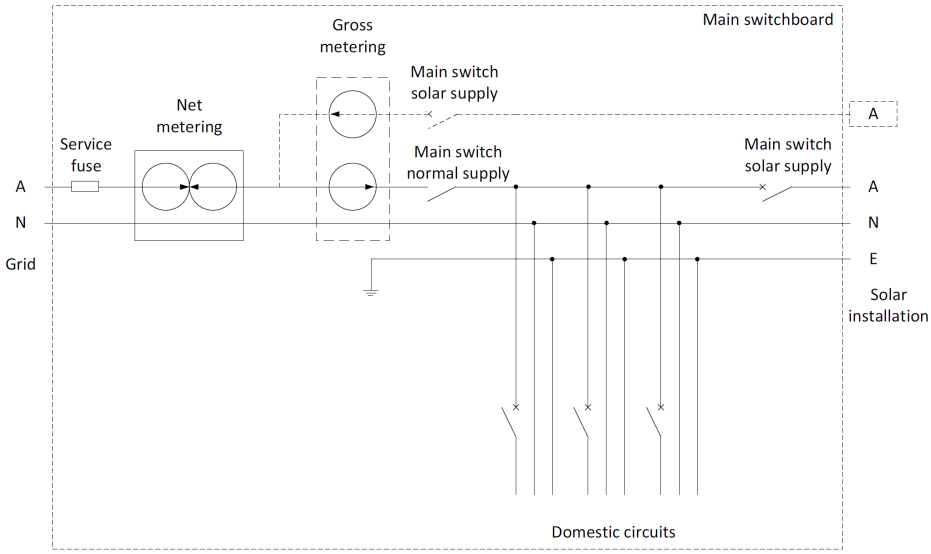

Figure 3.6.1: Net and gross metering systems in the same diagram

due to its placement after the domestic circuits. A net import meter would bill the consumer only for the units that are imported. Using an import meter and an export meter or a corresponding dual-element electronic meter, provides the opportunity for the electrical distributor to pay a different tariff for the electricity exported than the one imported. A gross metering would on the other hand provide information concerning the solar production, this could also be supplied by the inverter chosen. Gross metering could either consist of two meters, a generation meter measuring the solar supply and a consumption meter measuring the consumption or it could be one dual-element electronic meter functioning in the same manner. Which meter set up and which metering agreement that is to be used, should be discussed with Hafslund. This would only be necessary in case the PV installation changes the customer status to a surplus customer.

3.7 Economics

A simple overview of the economic aspects of the final alternatives should be done in order to get an idea of the costs of such an installation. All manufacturers of modules and inverters should receive a request concerning the selling price of the module or inverter used in order to give the most realistic picture of the price situation per now. However, such prices could change in a possible next phase of implementation and would only be valid for the time when or if such a request

was to be answered. The income aspect of the installation would depend on whether the installation would cause the Hafslund customer to become a surplus customer in accordance with the definition given by NVE.

Two methods which take into consideration the economic aspects of the installation are:

1. Simple payback
2. Life cycle costing

Simple payback is calculated by the following formula

$$T = \frac{C}{S} \tag{3.7.1}$$

where T is the payback period in years, C is the initial investment cost and S is the annual cost savings of electricity that does not need to be purchased [7, p.307].

In order to perform life cycle costing, a life cycle cost analysis is used in order to determine the cost per kilowatt-hour for the PV system. The life cycle cost analysis has been made in order to determine the investment cost of the equipment, the operation and maintenance cost. In addition component life time and replacement costs should be taken into consideration. To determine the cost per kWh the following equation is used [7]:

$$cost/kWh = \frac{Present\ value\ of\ the\ system\ over\ X\ years}{Yield\ (kWh)\ generated\ over\ X\ years} \tag{3.7.2}$$

In this study a analysis period (X years) of 20 years has been used, since it has been assumed a lifetime of approximately 20 years of the modules. Determining the present value of the system over 20 years requires knowledge concerning maintenance, repair and replacement costs during the period of analysis, which is here set to 20 years. The PV modules and the BoS components have been taken into account. There are small maintenance costs associated with a PV system as a whole. The maintenance cost of the PV modules is set to be 1 % yearly of the investment cost. With the assumed lifetime of the modules to be approximately 20 years there would be no replacement costs. Inverters can last $10-20$ years [7, p.314]. They would, however, need a repair during this period. A repair cost of the inverters as well as the rest of the BoS components is included every five years. The repair cost is assumed to be 1 % of the investment costs of the BoS investment costs. In these calculations it is assumed that the inverters are repaired every 5 years and would, therefore, not need replacing until after the analysis period of 20 years. In a more thorough calculation in a possible next phase of such a project, the manufacturer of the inverters and modules should

be consulted on how long expected life time their product has and take possible replacement costs into account.

Two different situations that would generate an income has been considered in these calculations:

1. The production is lower than the buildings consumption, which leads to no energy surplus situations. The income can be considered as the savings for the energy which is not supplied by Hafslund.
2. If the installation produces more than the building consumes, Hafslund will then pay for the surplus energy which is produced. The income would be the market price and a small addition.

The market price for electricity changes hourly on Nord Pool. Nord Pool organize and operate the main market place for trading spot power and is owned by the Nordic TSOs. For simplicity it is in this study assumed that the market price in the future will correspond to the average spot price for the last three years with delivery in Oslo, 0.34 NOK/kWh [39]. The small addition is a reimbursement which at least private customers in the Haflund grid gets for the network tariff. This addition would change, however, could be approximately 0.0425 NOK/kWh [40]. For the situation where the production is lower than the building consumption the prices are set each year with a tariff. The tariff consists of a fixed price and two variables depending on the power consumption peak and the amount of energy used. Table 3.7.1 illustrates the tariff which the building pays in 2012. This is valid for buildings with overload protection over 125 A with a 230 V supply, and 80 A with a 400 V supply. It also includes buildings with an expected yearly consumption above 100 000 kWh. The power variable in the tariff is charged with regards to the highest power peak within a month.

Table 3.7.1: The tariff in 2012 for low voltage connections (230 V and 400 V) to Hafslunds grid [41]. Summer = April - October, Winter = November - March.

Fixed price	Power variable		Energy variable	
NOK/month	NOK/kW/month		øre/kWh	
	Summer	Winter	Summer	Winter
415	25	74	5.25	7.40

In the calculations of life cycle costing, the inflation rate and the discount rate is set to is 2.5 % and 6 % respectively. The inflation rate is set based on the long term target in the monetary policy set by the Government in Norway [42]. The project discount rate should reflect the risk in the project and the expected return of investment. The discount rate is individual and would, therefore, vary depending on how the project is regarded with respect to these two factors. In the handbook of socio-economic analysis of energy projects by NVE it is proposed a discount rate of $6 - 8$ % for end user initiatives [43, p.25]. 6 % is to be used

if the initiative is considered to have a clear environmental advantage, while 8 % should be used for other initiatives. Based on this, a discount rate of 6 % has been used in the economic calculations in this study.

Chapter 4

Simulations

This chapter documents the process of finding the final three systems providing the best PR and energy production. Parameters which have been altered are the modular tilt angles, pitch distance, fraction of electrical effect and multiple inverters. A base case was used in order to compare the effect of varying these parameters. The base case consisted of REC modules (type REC250PE) and inverters from SMA (Sunny Boy SB 5000 TL-20). The base case system consisted of 100 modules, 10 modules in each string connected to five inverters where each inverter has a two MPPT inputs. The NOCT coefficient specified in accordance with that of the REC module (29° C), wiring loss at 1.5 % at STC and the soiling loss specified 50 % for January and 35 % for February and December. The modules were placed with an edge zone of two meters and all modules had an azimuth of 0°. With a module tilt of 40°, the default meteorological data set and linear shading gave the following results illustrated in Figure 4.0.1 and Figure 4.0.2. These figures also illustrates how a general simulation report is presented in PVsyst.

As seen the base case system is simulated to produce 23.17 MWh/year with a specific production of 927 kWh/kWp/year and a performance ratio of 77.0 %. The losses within the system are illustrated in the loss diagram in Figure 4.0.3. It is seen in Figure 4.0.3 that there is a gain of 22 % due to the tilt of the modules, a loss of 8.1 % due to the near shadings calculated as linear shades, a 2.9 % loss due to the IAM factor. The the efficiency of the PV modules are then taken into account, following with the losses due to irradiance level, temperature, soiling, mismatch and wiring loss. Finally the inverter losses are taken into consideration.

	GlobHor kWh/m²	T Amb °C	GlobInc kWh/m²	GlobEff kWh/m²	EArray MWh	E_Grid MWh	EffArrR %	EffSysR %
January	11.0	-1.70	25.7	17.4	0.195	0.174	4.61	4.11
February	28.0	-2.40	54.1	42.4	0.663	0.628	7.43	7.04
March	66.0	0.30	94.0	85.1	2.073	1.996	13.37	12.87
April	106.0	4.70	127.9	118.3	2.807	2.706	13.30	12.82
May	172.0	10.10	185.2	172.2	3.971	3.831	13.00	12.54
June	166.0	13.90	165.5	152.6	3.463	3.338	12.68	12.22
July	169.0	17.00	174.6	161.7	3.621	3.489	12.56	12.11
August	131.0	16.20	147.5	136.3	3.076	2.965	12.64	12.18
September	78.0	13.20	105.5	97.1	2.220	2.137	12.75	12.27
October	37.0	8.70	59.3	49.9	1.170	1.120	11.96	11.44
November	15.0	3.70	36.8	25.1	0.599	0.569	9.87	9.37
December	8.0	0.80	28.4	16.1	0.241	0.221	5.14	4.71
Year	987.0	7.10	1204.5	1074.2	24.099	23.174	12.13	11.66

Legends:			
GlobHor	Horizontal global irradiation	EArray	Effective energy at the output of the array
T Amb	Ambient Temperature	E_Grid	Energy injected into grid
GlobInc	Global incident in coll. plane	EffArrR	Effic. Eout array / rough area
GlobEff	Effective Global, corr. for IAM and shadings	EffSysR	Effic. Eout system / rough area

Figure 4.0.1: Main results of the base case system

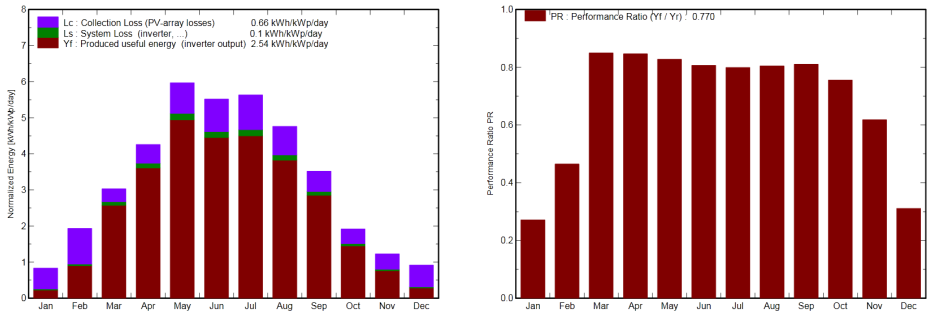

Figure 4.0.2: Normalized energy production and the performance ratio of each month, base case system

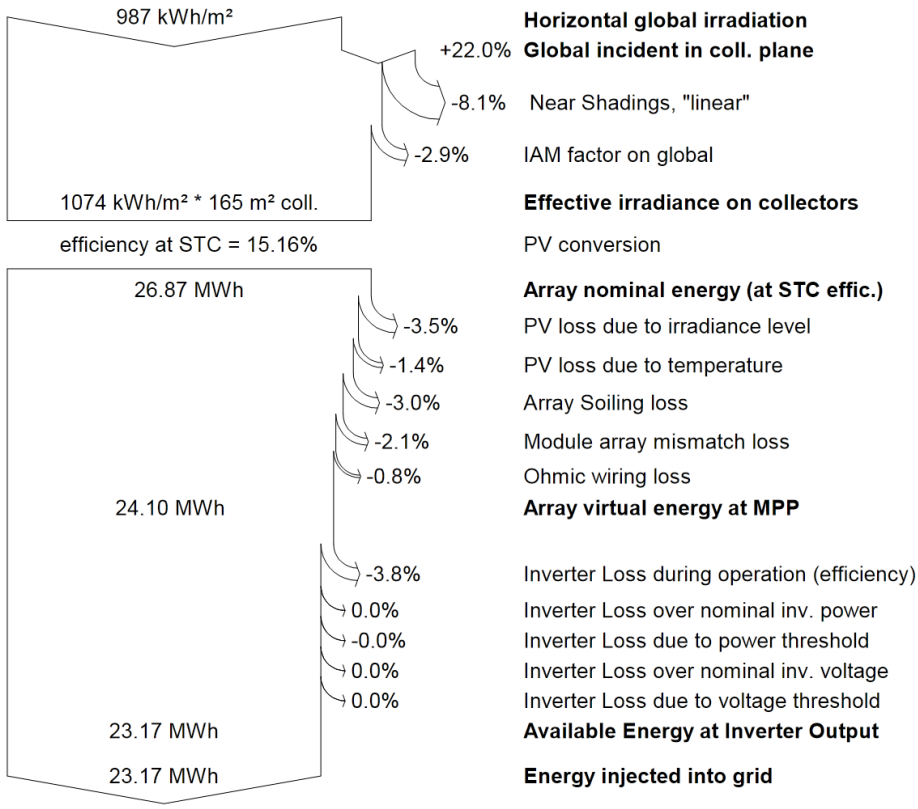

Figure 4.0.3: Loss diagram for the base case, from PVsyst

4.1 Fraction of Electrical Effect

Table 4.1.1 shows the main results when varying the fraction of electrical effect from 0 % electrical effect (linear shadings) to 100 % electrical effect. The system is otherwise unchanged from the base case, which means that the loss diagram in Figure 4.0.3, is unchanged except from the near shading loss which is shown in Table 4.1.1.

Table 4.1.1: The main results when varying the fraction of electrical effect. Tilt angle: 40°, azimuth: 0°, EF: electrical effect

	Produced energy MWh/year	Specific production kWh/kWp/year	Performance ratio (PR) %	Near shading loss %
Linear shadings	23.174	927	77.0	-8.1
20 % EF	22.884	915	76.0	-9.3
40 % EF	22.592	904	75.0	-10.6
60 % EF	22.296	892	74.0	-11.8
80 % EF	21.999	880	73.1	-13.1
100 % EF	21.700	868	72.1	-14.3

4.1.1 Discussion

As seen in Table 4.1.1, when the fraction of electrical effect is taken into account the near shading loss increases, decreasing the performance ratio, specific production and produced energy. This is an expected result since a higher fraction of electrical effect influences the production of every module in the affected string. A 100 % electrical effect fraction represents the whole string being equally affected as the shaded module in that string, as mentioned in Section 3.3.3. A 100 % electrical effect would be an incorrect representation of partial shadings on the modules due to the bypass diodes in the modules and the module layout. The fraction of electrical effect is set to 60 % in the next simulations since this is considered a more realistic fraction when taking into consideration the shades on the roof. Varying the electrical effect does, however, illustrate the range where the shading loss lies.

Limitations to the electrical effect calculation

In order to calculate a realistic electrical effect, all modules would have to be exactly positioned in the 3D representation with a clear notion of which modules

belong to which strings, how many bypass diodes that are used in each module etc. The creators of PVsyst have started this process with "module layout". In the article for the 25th European Photovoltaic Solar Energy Conference in Spain, 2010 [29] the creator of PVsyst stated that the implementation of joining module layout with the near shadings would be realized by the end of 2010. Nevertheless, it is not implemented in the version used during this study (V5.54).

4.2 Module Tilt Angles

Table 4.2.1 illustrates the losses in the systems where the modular tilt angle has been changed. Table 4.2.2 shows the main results with different module tilt angles. *Global addition* in the table describes the global irradiance addition on the plane due to the module tilt.

Table 4.2.1: Losses in % with variable module tilt angles

Module tilt	40°	30°	25°	20°
Global addition	22.0	20.2	18.3	15.8
Shading loss	-11.8	-8.5	-6.5	-4.6
IAM	-3.0	-3.1	-3.3	-3.5
Irradiance level	-3.7	-3.6	-3.6	-3.7
Temperature	-1.4	-1.4	-1.3	-1.2
Soiling loss	-2.4	-2.3	-2.3	-2.3
Mismatch loss	-2.1	-2.1	-2.1	-2.1
Wiring loss	-0.7	-0.7	-0.7	-0.7
Inverter loss	-3.9	-3.9	-3.8	-3.8

Table 4.2.2: Main results with variable module tilt angles, done with the base case and a 60 % fraction of electrical effect

Tilt angle °	Produced energy MWh/year	Specific production kWh/kWp/year	Performance ratio (PR) %	Global addition %	Shading loss %
40	22.30	892	74.0	22.0	-11.8
30	22.82	913	77.0	20.2	-8.5
25	22.94	918	78.6	18.3	-6.5
20	22.87	915	80.0	15.8	-4.6

Table 4.2.3 presents the main results when the pitch distance has been increased

from 2 meters to 2.5 meters (illustrated in Figure 4.2.1). In order to reduce the pitch distance the number of modules were reduced from 100 to 72 modules, requiring another type of inverter in order to match the new number of modules. In this case an Eltek inverter, type Theia 2.9 HE-t was chosen. Both the Eltek inverter and the SMA base inverter have a maximum efficiency of 97 %.

Table 4.2.3: Increasing pitch distance between the module rows to 2.5 meters

Tilt angle °	Produced energy MWh/year	Specific production kWh/kWp/year	Performance ratio (PR) %	Global addition %	Shading loss %
40	16.58	921	77.2	22	-8.7

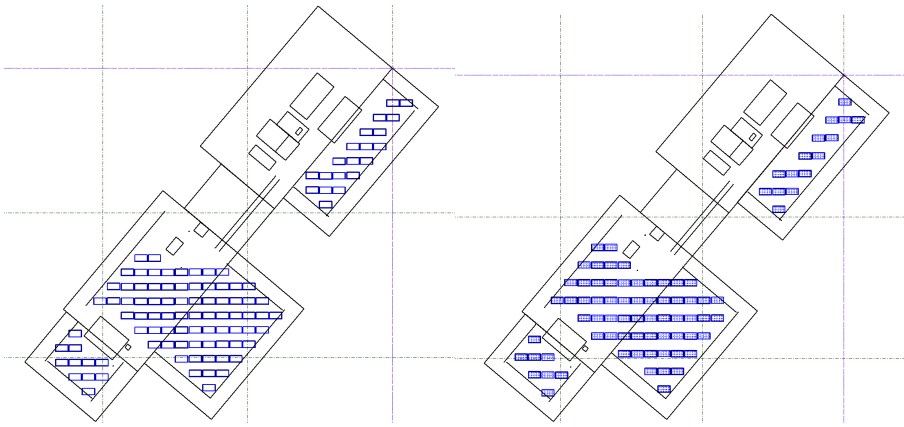

(a) 2 meter pitch (b) 2.5 meter pitch

Figure 4.2.1: Overview of 2 meter and 2.5 meter pitch distance

4.2.1 Discussion

Investigating Table 4.2.1 reveals that there is little change of the following losses; IAM, loss due to irradiance level, loss due to temperature, soiling loss, mismatch loss, wiring loss and inverter loss. More considerable changes are seen in the losses due to shading and the gain due to module tilt. Considering the difference in shading loss of a system with a modular tilt of 40° and 20° there is a change of 7.2 %. The gain of global irradiance on the tilted planes varies in a range of 7.6 %. Since these are the two loss components that change the most, they are displayed with the main results in Table 4.2.2.

As seen in Table 4.2.2 the shading loss decreases with decreasing tilt angle of the modules. This is a result of the pitch distance maintained at 2 meters while the

module tilt is decreased. The global irradiance addition decreases with decreasing modular tilt, due to a larger difference from the optimal tilt of 40°. The specific production and the produced energy increases with decreasing tilt angle from a tilt angle of 40° to 25°, and decreases somewhat from 25° to 20° tilt angle. The reason for this could be explained by adding up the gain from the global irradiance with the shading loss. This results in a gain which increases from 10.2 %, 11.7 % and to 11.8 % at 40°, 30° and 25° modular tilt angles receptively. It then decreases to 11.2 % gain at a 20° modular tilt. How this gain and loss is weighted with respect to importance in the system is, however, not necessarily the same. A difference could be assumed, since the resulting gain between the gain and shading loss at 20° decreases to a gain value lower than the one at 30° modular tilt. This is not reflected in the specific production or the produced energy. The possible weight difference between the two factors could also be the reason for the increasing performance ratio with decreasing tilt angle.

Comparing the same tilt angle of 40° with s pitch distance of 2.5 meter (seen in Table 4.2.3) it is seen that the global addition due to the tilt of the modules are the same as for the 2 meter pitch distance. The shading loss and the performance ratio for the system with 40° tilt angle and 2.5 meter pitch distance is approximately the same as for a tilt angle of 30° with a 2 meter pitch distance. The specific production for the system with 2.5 meter pitch distance has increased as a result of both high gain of global irradiance due to the tilt of the modules and the relatively low shading loss. However, since this system had to remove modules in order to maintain an edge zone of 2 meter the kWp of the system has decreased from 25 kWp to 18 kWp and the produced energy has decreased from 22.30 MWh/year to 16.58 MWh/year. When dimensioning the PV system for a performance ratio above 80 % and having limited amount of space on the roof it is, therefore, considered more functional to reduce the tilt angle of the modules and not operate with an optimal tilt angle than increase the pitch and reduce the number of modules further. The following simulations will, therefore, be performed with a system of a modular tilt angle of 20° and a pitch distance of 2 meter (and an electrical effect of 60 %).

4.3 Meteorological Data Set

Table 4.3.1 shows the main results of a year of production with the two different meteorological data sets. Figure 4.3.1 shows the normalized productions per month for both meteorological data sets. The purple in Figure 4.3.1 illustrates the collection loss (the PV array losses), the green part illustrates the system loss (mainly the inverter loss) while the red illustrate the produced useful energy (the inverter output). The collection loss for the default case is 0.53 kWh/kWp/day compared to 0.51 kWh/kWp/day for the new case. The system loss is equal in the two cases with 0.1 kWh/kWp/day. The inverter output for the default case is 2.51 kWh/kWp/day compared to 2.44 kWh/kWp/day for the new case. Table

4.3.2 shows the losses in the systems with the two different meteorological data sets.

Table 4.3.1: Main results with the default and the new meteorological data set (Meteo2), 20° tilt angle, 60 % electrical effect

Meteo set	Produced energy MWh/year	Specific production kWh/kWp/year	Performance ratio (PR) %
Default	22.87	915	80.0
Meteo2	22.28	891	80.1

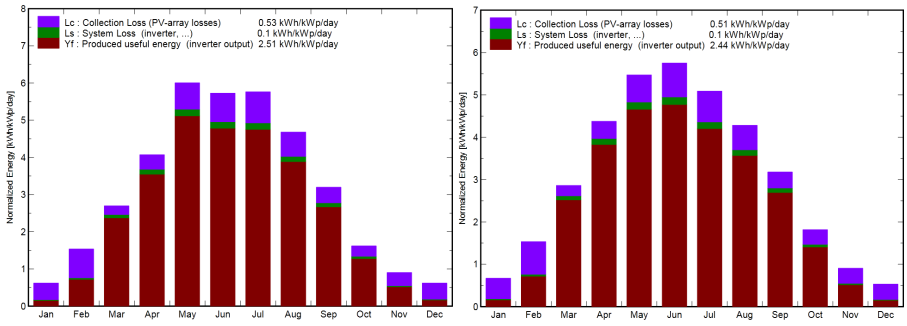

(a) Default meteorological data set (b) New meteorological data set

Figure 4.3.1: The normalized productions (per installed kWp): nominal power 25.00 kWp for 20° tilt angle, 60 % electrical effect

4.3.1 Discussion

As seen in Table 4.3.1 both the produced energy and the specific production per year are higher for the default meteorological data set. It is also possible to see the same tendency in Figure 4.3.1, keeping in mind that the ordinate axis is larger for Figure 4.3.1a than for Figure 4.3.1b.

The performance ratio for the simulation with the new meteorological data set is 0.1 % higher than the simulation with the default data set. In order to explain this, the losses in Table 4.3.2 has to be taken into consideration. The inverter loss, wiring loss, mismatch loss, soiling loss, irradiance level loss and loss due to IAM has only changed by 0.1 % or none at all and will, therefore, not be discussed further. The losses due to temperature, shading and the gain due to increasing global irradiance due to the tilt of the modules display a more considerable change. The temperature loss is decreased to half from 1.2 % to

Table 4.3.2: The losses in the system with the default and the new meteorological data set, 20° tilt angle, 60 % electrical effect

Loss, %	Default	Meteo2
Global addition	15.8	17
Shading loss	-4.6	-4.9
IAM	-3.5	-3.6
Irradiance level	-3.7	-3.8
Temperature	-1.2	-0.6
Soiling loss	-2.3	-2.3
Mismatch loss	-2.1	-2.1
Wiring loss	-0.7	-0.7
Inverter loss	-3.8	-3.9

0.6 %. This can be explained with the yearly average of temperature in the two meteorological sets which are 7.04° C and 5.7° C for the default meteorological data set and the new data set respectably. As explained in Section 3.1.1, the modules function with a higher voltage and efficiency when the temperature is lower. Therefore, the loss is decreased with the new data set. The shading loss increases with 0.3 % from the default to the new meteorological data set. The global irradiance in the new meteorological data set is 37 kWh/m^2 less than the global irradiance in the default set. However, the gain due to the tilt of the modules has increased with 1.2 %. The two meteorological datasets are very similar comparing the global irradiance except for May, July and August where the default dataset has a higher global irradiance. Comparing the gain of more irradiance by tilting the modules results in a higher gain for the new dataset in all the months except for May, July and August. The reason for this is that the new meteorological data set has overall a lower global irradiance and still obtain higher gain in 9 out of 12 months (for further information see Appendix G).

4.4 Inverters

4.4.1 Homogeneous System

A homogeneous PV system is where all the module and inverters types, module tilt and azimuth direction are the same for the whole system. Table 4.4.1, Table 4.4.2 and Table 4.4.3 show the main results from simulation of a homogeneous PV system with different types of inverters with the two types of polycrystalline modules and the one type of monocrystalline module. The tables only display the inverters which matched the PV system such that a minimum of 90 modules

were included. Table 4.4.4 shows the main results and the main difference from the base case with the difference of using REC modules in one simulation and ITS modules in the other simulation. Figure 4.4.1 and Figure 4.4.2 illustrate the corresponding I-V curve for different amounts of irradiance for the REC module and the ITS module respectively.

Table 4.4.1: The main results from simulation with inverters from Eltek, SMA and Danfoss with the polycrystalline REC module: REC250PE

	Inverter type	Produced energy MWh/year	Performance ratio (PR) %	Number of modules	Series/ Strings/ Inverters
SMA	SunnyBoy	22.28	80.1	100	10/10/5
Eltek	Theia 4300 TL	22.81	80.4	102	17/6/6
	Theia 4800 TL	22.83	80.5	102	17/6/6
	Theia 5300 TL	22.40	**80.6**	100	20/5/5
	Theia 2.0 HE-t	22.15	80.5	99	11/9/9
	Theia 2.9 HE-t	21.46	80.4	96	12/8/8
SMA	Tripower 8000TL	22.92	**80.8**	102	17/6/3
Danfoss	TLX Pro 6k	23.15	80.1	104	13/8/4
	TLX Pro 8k	22.80	80.4	102	17/6/3
	TLX Pro 12.5k	22.75	80.2	102	17/6/2

4.4.2 Heterogeneous System

A heterogeneous system of different Eltek inverters was simulated and resulted in the main results displayed in Table 4.4.5. The modules have the same 20° modular tilt and azimuth direction the only difference is, therefore, that more than one type of inverters are used in the PV system. The roof was divided into three fields where each field have their inverter type. Fields A, B and C are as displayed in Figure 4.4.3.

4.4.3 Discussion

Considering the homogeneous simulations done for the polycrystalline alternatives it is seen that changing the base inverter (Sunny Boy) with one of the other high efficiency inverters gave a higher performance ratio in most cases. The base

Table 4.4.2: The main results from simulation with inverters from Eltek, SMA and Danfoss with the polycrystalline ITS module: EcoPlus PolyUp, 250W

	Inverter type	Produced energy MWh/year	Performance ratio (PR) %	Number of modules	Series/ Strings/ Inverters
SMA	SunnyBoy	21.92	78.9	100	10/10/5
Eltek	Theia 4300 TL	22.44	79.2	102	17/6/6
	Theia 4800 TL	22.46	79.2	102	17/6/6
	Theia 5300 TL	22.04	**79.3**	100	20/5/5
	Theia 2.9 HE-t	22.84	79.0	104	13/8/8
SMA	Tripower 8000TL	22.55	**79.5**	102	17/6/3
Danfoss	TLX Pro 6k	22.77	78.8	104	13/8/4
	TLX Pro 8k	22.43	79.1	102	17/6/3
	TLX Pro 12.5k	22.77	78.8	104	13/8/4

inverter was undersized for the monocrystalline alternative and could, therefore, not be used in a simulation. It is, however, seen from the monocrystalline case that the performance ratio is higher than both of the other polycrystalline cases even when the same inverter is used. This could be explained by the high module efficiency of the monocrystalline modules. Due to the high power of the monocrystalline modules it is also seen that approximately only half of the inverters within the chosen series of inverters were possible to use when taking into consideration the voltage, power and current conditions where the modules and the inverters should match. Sizing the systems such that each string should have its own MPPT input also limited the amount of possible inverters, since several inverters have a set up which allows parallel couple strings such that the parallel coupling has a MPPT instead of each string.

Comparing the base cases when using REC modules and ITS modules it is seen that the performance ratio in the ITS simulation is 78.9 % while 80.1 % for the REC simulation. This can be explained by Table 4.4.4 and the I-V curves of the two modules, illustrated in Figure 4.4.1 and Figure 4.4.2. The two simulations are identical except for the inverters and the module types, there are equally many modules in series, number of strings and number of inverters. The reason for the deviation of performance ratio is due to the array loss caused by a reduction in the irradiance level, which differs with 3.3 %. As explained in Section 3.4.4 this loss is caused by a reduction in the nominal efficiency when the irradiance level falls below 1000 W/m^2. According to the technical data on the two modules,

Table 4.4.3: The main results from simulations with inverters from Eltek, SMA and Danfoss with the monocrystalline SunPower module: SPR-327NE-WHT-D

	Inverter type	Produced energy MWh/year	Performance ratio (PR) %	Number of modules	Series/ Strings/ Inverters
SMA	SunnyBoy				
Eltek	Theia 2.0 HE-t	30.71	81.2	104	8/13/13
SMA	Tripower 8000TL	31.06	**82.1**	104	13/8/4
Danfoss	TLX Pro 6k	29.60	81.4	100	10/10/5
	TLX Pro 8k	30.89	81.7	104	13/8/4

Table 4.4.4: Main results and main differences from base case simulations with the polycrystalline REC and ITS modules

	Produced energy MWh/year	Specific production kWh/kWp/year	Performance ratio (PR) %	Irradiance level loss %
REC base	22.28	891	80.1	-3.8
ITS base	21.92	877	78.9	-7.1

the REC module has a module efficiency of 15.1 % while the ITS module has a module efficiency between $15.2 - 15.8$ %. It is also seen from Figure 4.4.1 and Figure 4.4.2 that the ITS module has a higher MPP than the REC module for irradiations of both 1000 and 800 W/m^2. However, when the incident irradiation decreases to 600 W/m^2 and below, the REC module has the higher MPP.

Concluding from the results of the simulation the irradiance level is most often in the lower range of measured irradiance in W/m^2, when disregarding the influence on the I-V curve with changing temperatures. The mean annual global horizontal irradiance in Oslo and Ås estimated from cloudiness during $1931 - 1960$ was 109 and 104 W/m^2 [44] which corresponds to 954.84 kWh/m^2 and 911.04 kWh/m^2. At least for Oslo these numbers correspond nicely to the value in the new meteorological data set.

The maximum produced energy per year for the heterogeneous case is 22.826 MWh (102 modules, corresponding to 25.5 kWp), while for the homogeneous case it is 22.40 MWh (100 modules, corresponding to 25 kWp). The performance ratio of the heterogeneous case would lie between 80.5 and 80.6 %, while it could be

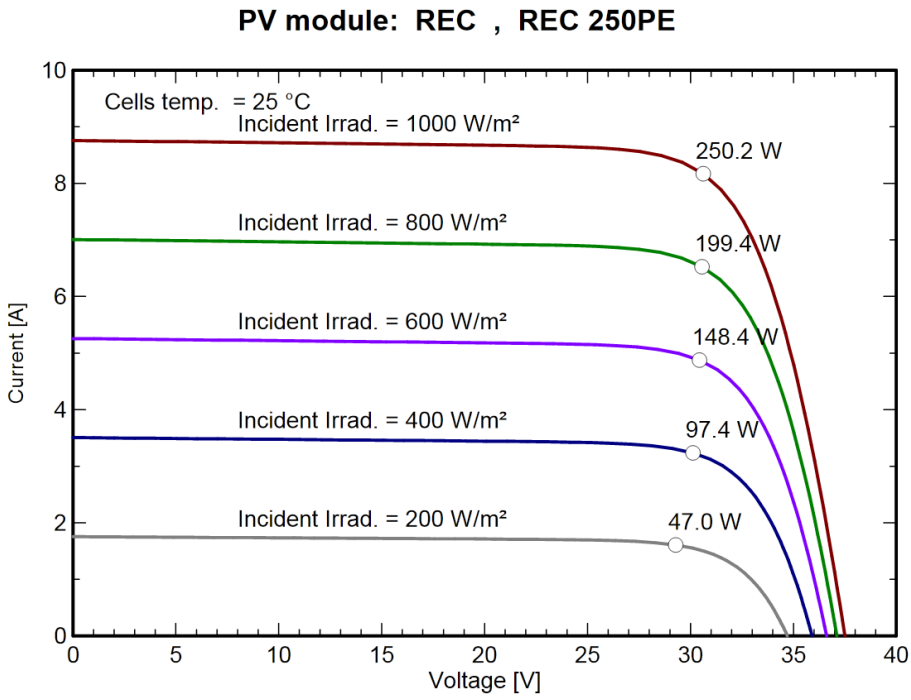

Figure 4.4.1: The REC module I-V curve with different irradiation, from PVsyst

80.6 % as for the homogeneous case. As seen, there is not a considerable difference between these two cases. Nevertheless, it was chosen not to go further with other heterogeneous cases due to the limited amount of inverters which were chosen for this study. The inverters from SMA and Danfoss which are chosen are e.g. oversized for field A. A wider range of inverters should be taken into account in order to optimize the production from each sub-field. An advantage of designing a heterogeneous case where the field is divided into smaller fields on account of physical location is that it could increase the practicality when cabling and connecting the modules into strings.

Since the simulation with the ITS modules revealed that these modules most likely are not as well suited for the irradiation levels in Skøyen an alternative including ITS modules will not be considered further. On account on the highest performance ratio, the Eltek inverter Theia 5300 TL and the SMA inverter used in the homogeneous REC case are taken further. The SMA inverter in the monocrystalline system is also taken further on account of the high performance ratio.

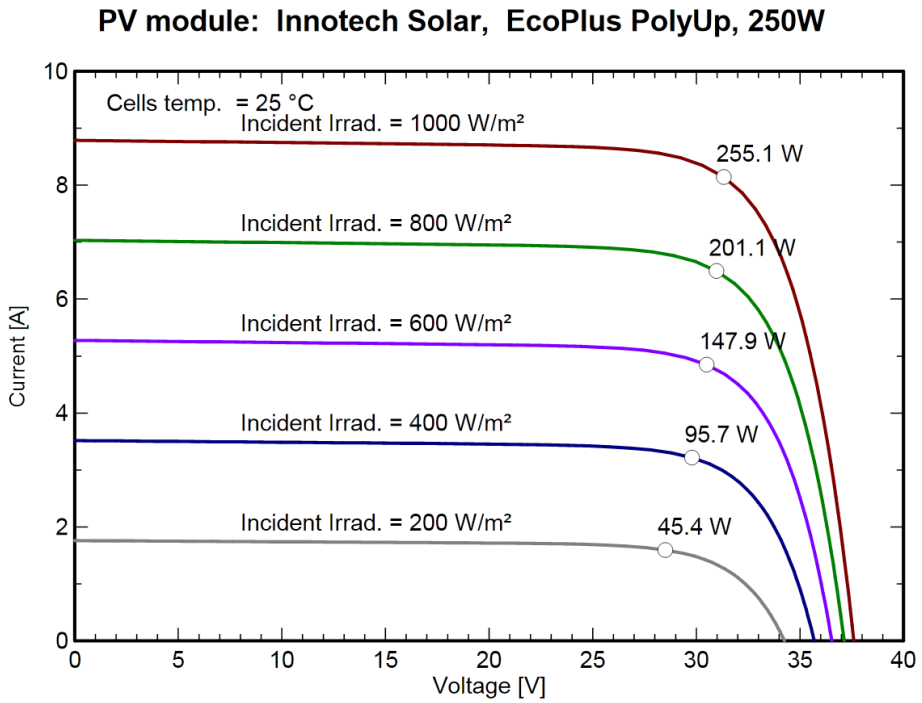

Figure 4.4.2: The ITS module I-V curve with different irradiation, from PVsyst

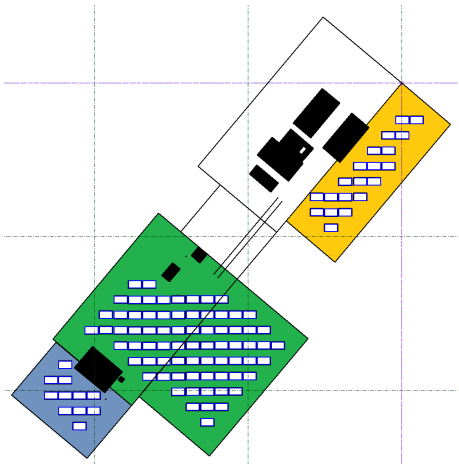

Figure 4.4.3: Overview of the roof divided into three fields. Field A = blue, field B = green, field C = yellow, black objects = shading objects

Table 4.4.5: Main results when simulating a heterogeneous system with different Eltek inverters with the polycrystalline REC module

	Inverter type	Produced energy MWh/year	Performance ratio (PR) %	Number of modules	Series/ Strings/ Inverters
Field A	Theia 2.0 HE-t	2.24	80.6	10	10/1/1
Field B	Theia 4300 TL	16.1	80.4	72	18/4/4
	Theia 4800 TL	16.11	80.5	72	18/4/4
Field C	Theia 4800 TL	4.476	80.5	20	20/1/1
	Theia 5300 TL	4.475	80.5	20	20/1/1

4.5 Shade Analysis and Module Layout

The three final alternatives are systems consisting of a total of 100, 102 and 104 modules. In order to assign all modules to their string, four and two modules would have to be removed from the original 104 module maximum on the roof. In order to decide which redundant modules should be removed, the results from the shade analysis was taken into account.

Table 4.5.1: The main result from the shade analysis, displaying the modules with the longest duration (in hours) of shade from the three fields. * marks modules that are fully shaded a period during the day

Module no.	Shade duration
A-11	3.0*
A-8	2.5
B-18	4.0*
B-19	2.5*
B-28	3.0
C-17	2.5*
C-19	2.5*

Table 4.5.1 presents the main results from the shade analysis of the field with 20° modular tilt and 2 meter pitch distance. For a fully detailed analysis see Appendix C. For the polycrystalline alternative with Eltek inverters there are four redundant modules. There are 20 modules per string in this alternative. For the second polycrystalline alternative with SMA inverters there are two redundant

modules which has to be removed. For the last alternative, the monocrystalline alternative with SMA inverters there is no need to remove modules. Figure 4.5.1 to Figure 4.5.3 illustrate the module layout.

4.5.1 Discussion

For the first polycrystalline alternative with Eltek inverters four modules were removed: B-18, B-28, A-11 and A-8. Module B-18, B-28 and A-11 were the modules with longest duration of occurring shade, while the fourth module had several alternatives which could be removed. Modules A-11, B-19, C-17 and C-19 were candidates which could be removed. Since field C consists of 20 modules with a similar shading pattern, it was considered best if these were to be placed in the same string. Modules C-17 and C-19 were, therefore, not eliminated. Module A-11 was simulated without being fully shaded during the day and the string from field A would have to connect to field B due to the low amount of modules on field A. Removing B-10 would give a module layout which perhaps is not practical when considering the coupling of the modules. Module A-8 was, therefore, the fourth module which was removed.

For the second polycrystalline alternative with the REC modules and the SMA inverters only two modules were removed based on the same arguments when removing four: B-18 and A-11. Module B-28 was considered removed. However, A-11 was chosen since this module is fully shaded during the day. Removing module A-11 would give a longer coupling distance from field A to field B. A more thorough analysis of which modules that are to be removed could be reconsidered in a possible next step in this project.

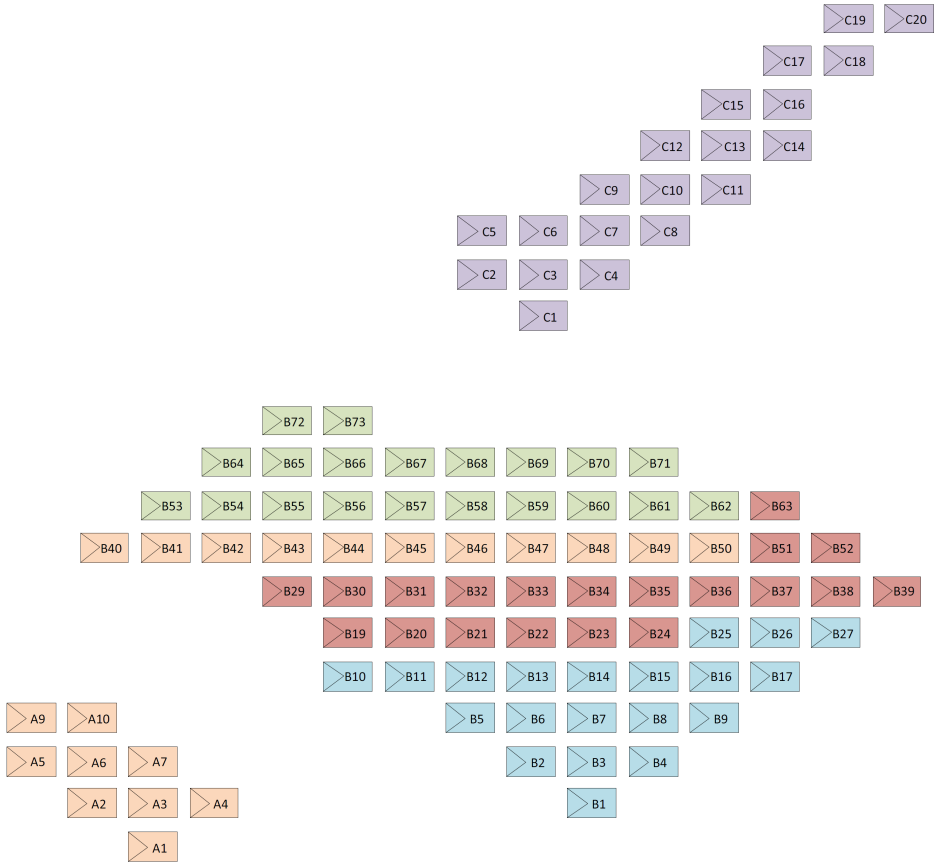

Figure 4.5.1: Module layout of the REC alternative with Eltek inverters, 100 modules in total

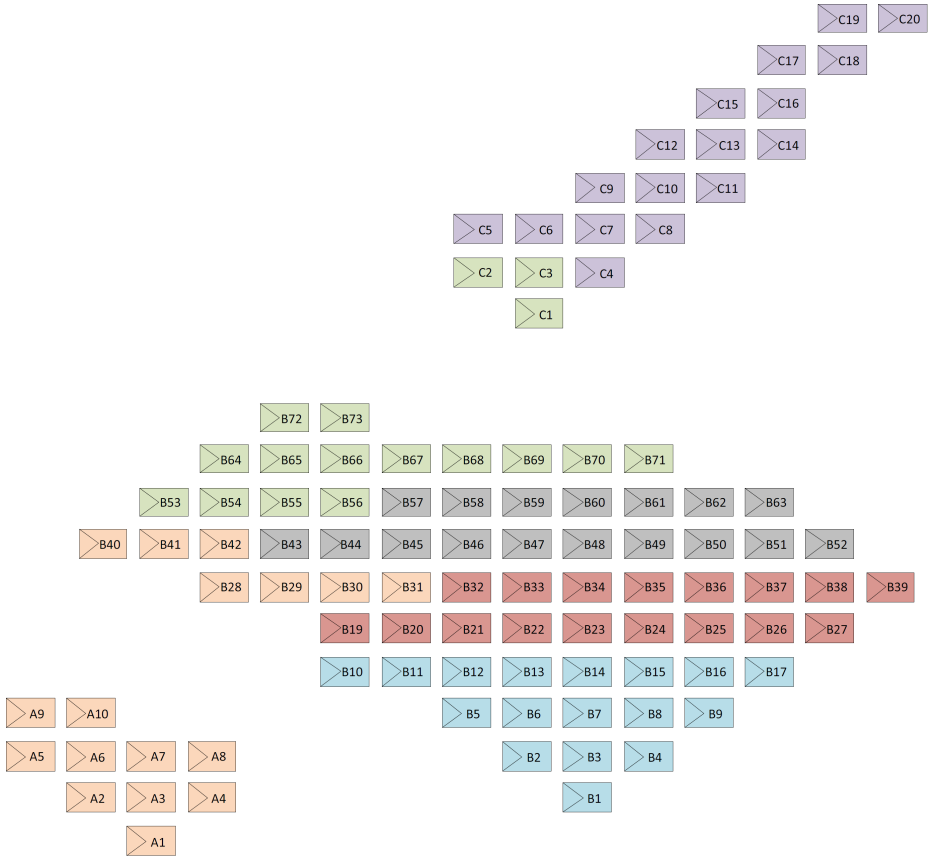

Figure 4.5.2: Module layout of the REC alternative with SMA inverters, 102 modules in total

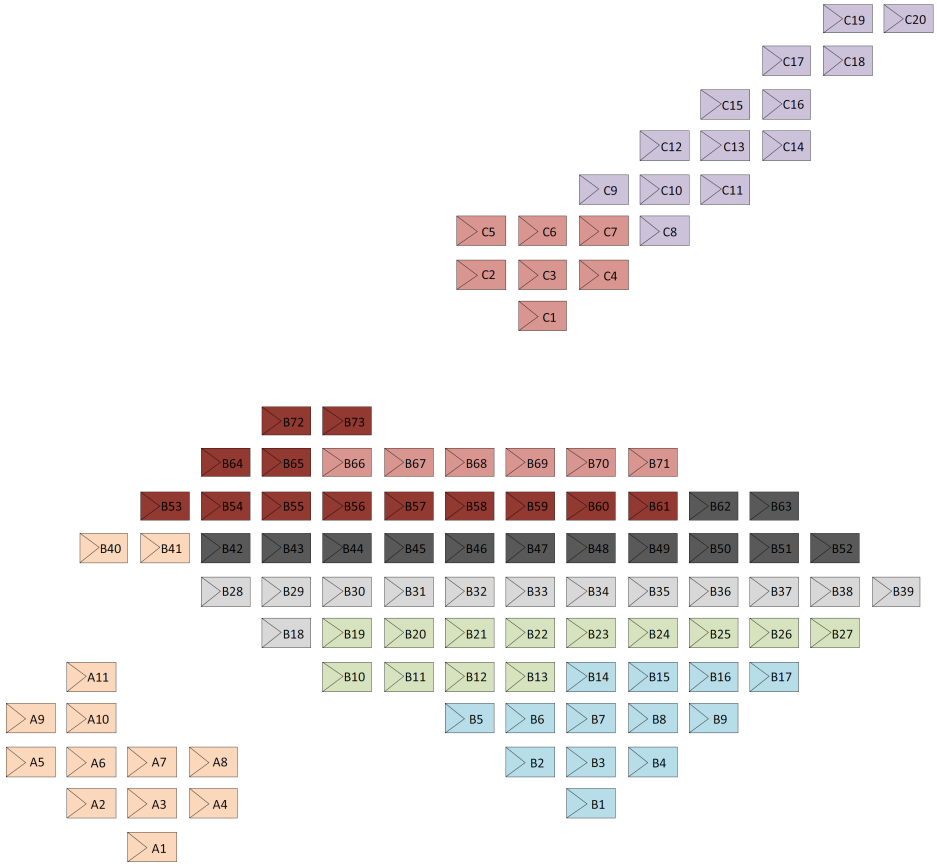

Figure 4.5.3: Module layout of the SunPower alternative with SMA inverters, 104 modules in total

4.6 Cable Sizing

As mentioned, cable sizing is not done explicitly in PVsyst. However, it is based on the resulting simulations done in the program. Table 4.6.1 to 4.6.4 show the minimum cross sectional area (CSA) of proposed DC cable paths for the three alternatives. Only the DC cables have been sized in this study. The loss in percent is of the standard size cable which is found closest in size with the calculated CSA. The inverters are assumed placed in the stair house on the roof. The proposed cable paths and more detailed calculations of the cable lengths are found in Appendix E.

Table 4.6.1: Minimum CSA (mm^2) and loss for the polycrystalline alternative with Eltek inverters

Eltek	String 1	String 2	String 3	String 4	String 5
Minimum CSA	2.96	3.25	2.53	2.43	2.24
Closest CSA	4	4	4	4	4
Loss	1.11 %	1.22 %	0.95 %	0.91 %	0.84 %

Table 4.6.2: Minimum CSA (mm^2) and loss for the polycrystalline alternative with SMA inverters

SMA	String1	String2	String 3	String 4	String 5	String 6
Minimum CSA	3.89	3.42	3.31	2.80	2.77	2.19
Closest CSA	4	4	4	4	4	2.5
Loss	1.46 %	1.28 %	1.24 %	1.05 %	1.04 %	1.31 %

Table 4.6.3: Minimum CSA (mm^2) and loss for the five first strings of the monocrystalline alternative

SunPower	String1	String2	String 3	String 4	String 5
Minimum CSA	1.69	1.63	1.45	1.33	1.10
Closest CSA	2.5	2.5	1.5	1.5	1.5
Loss	1.01 %	0.98 %	1.45 %	1.33 %	1.10 %

4.6.1 Discussion

The CSA depend on the cable path and the amount of modules that are to be connected in series. The minimum cross section of the two polycrystalline

Table 4.6.4: Minimum CSA (mm^2) and loss for the three last strings of the monocrystalline alternative

SunPower	String 6	String 7	String 8
Minimum CSA	1.21	1.20	1.03
Closest CSA	1.5	1.5	1.5
Loss	1.21 %	1.20 %	1.03 %

alternatives is in the same range since they have 20 and 17 modules in series (see Table 4.6.1 and 4.6.2). The monocrystalline alternative with 13 modules in a string has the smallest CSA (illustrated in Table 4.6.3 and 4.6.4). Both the SunPower and REC modules are supplied with $1 - 2$ meters of solar cables and MC4 connectors (se Appendix F). These connectors match solar cables with a CSA of 4 mm^2. Using higher cross section in the cables would diminish the ohmic loss in the system. However, higher cross section would result in higher price. These calculations apply only for one proposed cable path for each of the alternatives, altering the cable paths would alter these calculations. If all of the cables were to have a cross section of 4 mm^2, all strings in all alternatives would have a loss below the defined maximum of 1.5 % in PVsyst.

Chapter 5

Customer Status and Economics

In order to determine whether the company in the building can be classified as a surplus customer, the production from the PV installation has to be compared with the consumption within the building. It is possible to compare production and consumption since the building has a meter which measures the energy and power each hour and since PVsyst generates hourly plots of the production of simulated system. Furthermore, the results of the economic calculations are presented in this chapter.

5.1 Production and Consumption

The production in kWh from the three alternatives is drawn per month in Figure 5.1.1. The yearly production from the polycrystalline alternative with Eltek inverters is 22.4 MWh, 22.9 MWh for the polycrystalline alternative with SMA inverters while the yearly production is 31 MWh for the monocrystalline alternative. For further details see Appendix H. Table 5.1.1 presents the production as percentage of the energy use within the building. The consumption figures are from the year 2011. Consumption vary on account of several factors, for example how many people that use the building, the weather situation etc. The consumption figures from 2011 were chosen since this is the last full year with consumption data that will visualise to some extent the relation between energy production and consumption.

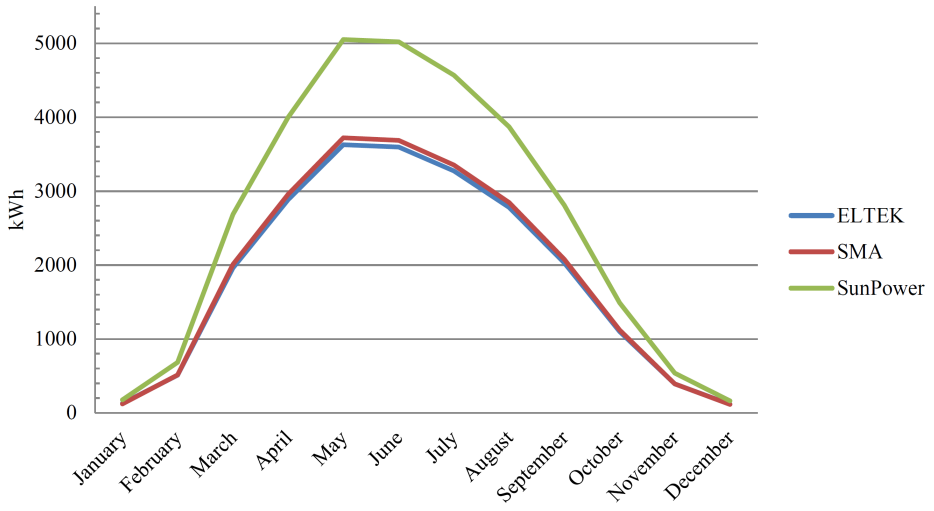

Figure 5.1.1: Simulated energy production per month of the three alternatives

Table 5.1.1: The energy production as percentage of the total energy use in the building, 2011

	REC Eltek	REC SMA	SunPower SMA
January	0.08 %	0.07 %	0.11 %
February	0.02 %	0.02 %	0.42 %
March	1.06 %	1.08 %	1.45 %
April	1.71 %	1.76 %	2.38 %
May	1.78 %	1.82 %	2.47 %
June	1.49 %	1.53 %	2.08 %
July	1.44 %	1.48 %	2.02 %
August	1.03 %	1.05 %	1.43 %
September	0.89 %	0.91 %	1.23 %
October	0.51 %	0.52 %	0.69 %
November	0.19 %	0.19 %	0.26 %
December	0.07 %	0.07 %	0.10 %
Yearly	0.92 %	0.94 %	1.27 %

5.1.1 Discussion

Both the energy and power production have been compared to the energy and power consumption in the building in order to establish the effect of the PV

Table 5.1.2: The energy production as percentage of the energy used for cooling in the building, 2011

	REC Eltek	REC SMA	SunPower SMA
January	14.04 %	13.43 %	19.34 %
February	62.06 %	14.91 %	83.50 %
March	180.46 %	184.73 %	247.00 %
April	106.14 %	108.82 %	147.21 %
May	25.90 %	26.57 %	36.06 %
June	9.23 %	9.46 %	12.89 %
July	7.31 %	7.49 %	10.20 %
August	6.11 %	6.26 %	8.51 %
September	8.26 %	8.46 %	11.43 %
October	6.26 %	6.39 %	8.48 %
November	3.42 %	4.70 %	4.70 %
December	2.64 %	2.57 %	3.67 %
Yearly	10.83 %	11.08 %	15.02 %

installation. The customer status would only change if there is an export of energy out on the grid, which can been observed when evaluating the power production and consumption. Evaluating the energy production first, it is seen from Figure 5.1.1 that the monocrystalline alternative produces most energy. The production from the polycrystalline alternatives show that the SMA inverter produces the most, as mentioned in Section 4.4. The SMA inverter has the highest efficiency, which could be on account of the galvanic isolation that the Eltek inverters provide. An average household in Norway uses approximately 20.4 MWh a year, where approximately 16 MWh/year is for electricity [1]. Table 5.1.1 presents the energy production of the PV installation in percentage of the energy consumption in the building. As seen, The production per year is less than 1 % in the polycrystalline cases and about 1.3 % in the monocrystalline case. Since the building is a six storey building, it has a considerable energy consumption. For the monocrystalline case it is at most covering approximately 2.5 % of the buildings consumption (in May).

As this is a commercial building its weekly consumption profile would be high during the weekdays and low during the weekends. The most probable time when production would exceed the consumption would, therefore, be during the weekend in summer. Evaluating the average and maximum power production in Table 5.1.3 and Table 5.1.4 it is seen that the consumption in the building does not go below 78 kW, while the highest power production for the PV installation

Table 5.1.3: The average and maximum power produced during the simulated year

	REC/Eltek		REC/SMA		SunPower/SMA	
	Average	Max	Average	Max	Average	Max
	kW	kW	kW	kW	kW	kW
January	0.67	3.15	0.68	3.21	0.96	3.81
February	2.20	9.38	2.28	9.63	2.98	12.57
March	5.58	17.66	5.78	18.19	7.64	24.19
April	7.00	18.88	7.39	19.43	9.86	26.41
May	*7.24*	19.73	*7.53*	20.31	*10.13*	27.80
June	6.82	19.68	7.27	20.26	9.72	28.00
July	6.25	**20.21**	6.52	**20.81**	8.85	**28.72**
August	6.20	19.95	6.48	20.54	8.69	28.41
September	5.52	17.24	5.75	17.75	7.72	24.22
October	3.88	16.88	4.03	17.38	5.28	23.07
November	1.99	9.27	2.11	9.52	2.75	12.33
December	0.79	3.12	0.78	3.18	1.11	4.41

is approximately 29 kW (for the monocrystalline alternative). Consequently the PV installation would not change the customer status to a surplus customer. As seen in Table 5.1.4 the minimum power during a year is within a range of 21 kW, while the maximum power during a year is in a range of 195 kW. The minimum load in the building is, therefore, much more stable than the maximum load which has its power peak during the summer. Analysing the consumption of the building (Appendix H) shows that there is an increase in the main consumption. However, the cooling measurements show that this is the post that is increasing the most during summer, which could only be considered natural. Comparing the energy production with the cooling consumption during a year it is seen from Table 5.1.2 that the production from the PV installation cannot cover the cooling consumption in the building either. The simulated production would cover the cooling demand during March and April 2011, since little cooling is used and the production is increasing. When reaching June the production can only cover about $7 - 10$ % of the cooling demand.

Table 5.1.4: The minimum and maximum power consumed for each month in 2011

	Min kW	Max kW
January	81	369
February	84	378
March	81	384
April	81	435
May	87	480
June	93	537
July	99	510
August	99	564
September	96	471
October	84	462
November	84	420
December	78	429

5.2 Economics

Table 5.2.1 shows the approximate evaluation of the investment cost for the three alternatives. An enquiry regarding prices were sent out to REC, SunPower, Eltek and SMA. The module price for the REC modules were obtained from REC and the inverter price for the Eltek inverter was provided from Eltek. The module price for the SunPower modules were obtained from Photon International [45] as well as the price for the SMA inverters [46]. The remaining BoS costs for the different alternatives were considered to be equal and are based on previously calculated figures from Multiconsult. The difference in BoS costs for the monocrystalline alternative is because of the price being in cost/kWp, which depends on the efficiency of the modules used. For an equal mounting system only with modules with higher efficiency and higher Wp would have BoS cost/kWp which would be lower since the kWp of the entire system would be higher.

The power variable in the tariff paid today is calculated by using the maximum load power peak within the building during one month. In order to be able to reduce the power variable the production from the PV installation would have to reduce the load power peak in the building at that exact time and day when the load peak occurs. Since the PV installation does not produce more than the building consumes during a year (in this case the consumption in 2011) the income generated from the PV installation is the same as saved costs from importing the energy from Hafslunds grid (seen in Table 5.2.2). A theoretical alternative was

Table 5.2.1: Investment cost for the three alternatives. Rate per May 11th, 2012: 7.62 EUR/NOK

	REC Eltek	REC SMA	SunPower SMA	Unit
Module price	750	750	1140	€/kWp
Length	1.665	1.665	1.559	m
Width	0.991	0.991	1.046	m
Power	250	250	327	Wp
Efficiency	15.15	15.15	20.05	%
Inverter	297.14	210.00	210.00	€/kWp
Mounting system	250.00	250.00	188.90	€/kWp
Montage	200.00	200.00	151.12	€/kWp
DC cables	214.00	214.00	161.69	€/kWp
AC cables	131.20	131.20	99.13	€/kWp
Communication	40.00	40.00	30.22	€/kWp
Total BoS cost	1 132.34	1 045.20	841.06	€/kWp
Module + BoS cost	1 882.34	1 795.20	1 981.06	€/kWp
	14 347.12	13 682.93	15 099.56	NOK/kWp

made illustrating the income if the energy production was sold for market price, which is illustrated in Table 5.2.3. The simulated results from the three PV alternatives represent the production based on the meteorological data set which should represent a normal year. Since the meteorological data set represents normal weather it would not be realistic to compare the production data with the exact time and dates when a load power peak occurs in the building. During 2011 the load power peaks occurred between 11:00 and 15:00 (see Appendix H). The PV modules produce the most within this time range. In Table 5.2.2 there is presented a best and a worst case scenario with respect to reducing the maximum power production in the building. The best case scenario is considering that the total amount of the maximum power production peak that month reduces the maximum load power peak that month. The scenario where the minimum reduction in effect is considered is when all the simulated power measurements during a day is averaged. And then averaging these values to get one value for each month. The value for each month is then the reduction in the maximum load power peak occurring that month. The real reduction in load power peaks is considered to be located in between the minimum and maximum scenarios taken into account in this study.

Table 5.2.4 illustrates a present value calculation over 20 years. The same as-

sumptions for duration of the analysis period, inflation rate, discount rate, etc., made for the life cycle costing are used in this calculation. For more details see Appendix I.

Table 5.2.2: Calculated income (NOK) for a worst (minimum) and a best case scenario (maximum) when considering the power production

	Energy	Power		Total		
		Min.	Max.	Min.	Max.	Unit
REC/Eltek	1 243	1 904	6 465	3 147	7 708	NOK
REC/SMA	1 271	1 985	6 647	3 256	7 918	NOK
SunPower/SMA	1 722	2 649	8 906	4 370	10 627	NOK

Table 5.2.3: The theoretical income if the total amount of energy was sold at spot price on Nord Pool

	Income (NOK)
REC/Eltek	7 648
REC/SMA	7 826
SunPower/SMA	10 605

Table 5.2.4: Main results of the present value calculations

	REC/Eltek		REC/SMA		SunPower/SMA	
	Best	Worst	Best	Worst	Best	Worst
Investment	358 678	358 678	348 915	348 915	513 506	513 506
Maintenance	23 595	23 595	21 591	21 591	43 769	43 769
Repair	5 970	5 970	5 621	5 621	6 032	6 032
Income	114 163	46 607	117 284	48 227	157 411	64 733
	-274 080	-341 636	-258 842	-327 899	-405 895	-498 573

5.2.1 Simple Payback

Table 5.2.5 presents the payback time for the two scenarios with the tariff savings and the payback time if all the produced energy were to be sold in the market.

Table 5.2.5: Payback time in years when using the simple payback method

	Best case Years	Worst case Years	Market price Years
REC/Eltek	46.5	114.0	46.9
REC/SMA	44.1	107.2	44.6
SunPower/SMA	48.3	117.5	48.4

5.2.2 Life Cycle Costing

Table 5.2.6 presents the cost per kWh for the three alternatives, when the yield is assumed degraded 13.3 % during the 20 year analysis period (0.75 % degradation each year).

Table 5.2.6: The cost per kWh of the three alternatives

	NOK/kWh
REC/Eltek	0.93
REC/SMA	0.88
SunPower/SMA	0.97

5.3 Discussion

There are limited investment figures based on previous calculations from (similar) PV installations in Norway. The prices for the BoS components excluding the inverters in Table 5.2.1 are, therefore, figures based on previous calculations from other European countries. The figures of the DC cables are e.g. from a German roof installation of 60 kWp. The figures used in this table are, therefore, highly uncertain. In the cases where an offer has been made it should be kept in mind the fluctuations in the solar market could cause the offer to change in a later stage. The figures do, however, give an impression of what the costs could be for these alternatives, which was the intention. Evaluating the calculated income for a worst and a best case scenario (Table 5.2.2) it is seen that with the current tariff with Hafslund there is most to save in reducing the power variable. Comparing

with the theoretical income where all of the energy is sold on the spot market it is seen that the income here incidentally matches the best case scenario in the current tariff agreement. As seen in Table 5.2.4 there is a negative present value for all of the alternatives with the current tariff agreement. This is when using the tariff of 2012 and considering it to be fixed only to be adjusted by inflation. As seen in the table, it is the polycrystalline alternative with SMA inverters that results in the least negative present value of the alternatives. There are a lot of variables influencing the electricity market, amongst others the global electricity market which could possibly increase profitability of the PV alternatives. National regulations could also change and subsidies for PV could be given. As it is today there are no subsidies for PV installations in Norway. Disregarding possible political changes as subsidies, it is seen that in the worst cases the income during the 20 years barely covers the maintenance and repair costs.

The simple payback method is inaccurate since it does not take into account the maintenance, repair costs, inflation and discount rate. However, it gives an idea of the payback time, which is above the assumed lifetime of the modules (20 years), seen in Table 5.2.5. During 50 years, some reinvestment costs would have to be taken into consideration, which would then further increase the payback time. As seen there is a variation of $50 - 70$ years depending on alternative and whether the income is a best or worst case scenario. The theoretical income alternative, selling the energy on the spot market, is comparable to the best case income scenario. The life cycle costing method takes into consideration the factors that the simple payback does not and, therefore, give a more realistic view of the economics in the alternatives. Comparing Table 5.2.6 to the average spot price of energy delivered in Oslo the last three years of 0.34 NOK/kWh (44.8 €/MWh), it is seen that the energy from the PV installation is approximately triple the spot price. Comparing with the energy variable in the Hafslund tariff, which is on average 0.06 NOK/kWh, would not be correct since this is only one variable within the tariff that results in a part of the overall energy price which is paid today.

Chapter 6

Further Work

This thesis should be considered a preliminary study of the possibilities of installing a PV system on a commercial building, in Oslo. In this thesis, there has been an overall focus on the electrical aspects of PV systems. There are, therefore, electrical aspects which could be investigated further as well as mechanical considerations that also should be taken into account in possible further studies of this installation. For example, the wind pressure should be calculated when evaluating the modular angle tilt and the edge zone of 2 meters. If ballasted mounting systems were to be chosen for the installations, an investigation should be performed on how much weight the roof holds. With regards to the electrical aspects it would be interesting to simulate the systems with different types of modules and inverters. It could be investigated further the existing circuits in the building and evaluating if the connection point could be shifted from the main switchboard to one of the circuits providing electricity to the top floors. Other interesting aspects would be fire safety when having a PV installation on the roof, and protection equipment and settings.

In this thesis only the consumption of 2011 was compared with the production of the PV installations. There is complete yearly data for the consumption in 2009 and 2011 which could be considered if a more thorough study should take place. A comparison study of similar PV installations (with regards to installed Wp) would also be of use in order to evaluate the difference in production due to meteorological conditions (location). Further, it would be interesting to investigate the production and consumption trends and the system which is already built in the Hafslund grid and match this with a simulation done in PVsyst in order to see the deviation. Evaluating the system in this study in a different simulation program could shed light on other aspects which are not considered in PVsyst.

With regards to economics it would be interesting to examine the socio-economic benefits of a PV installation and including these figures into the calculations.

Furthermore, it would be interesting to investigate subsidies in Norway and the effect green certificates would or could have on a PV installation.

In case this study is taken further it should be considered to invest in measurement equipment such as reference cells or pyranometers. A pyranometer measures irradiance (global and diffuse irradiation can be measured) and could be placed with the same tilt angle as the modules or placed horizontally in order to evaluate the horizontal irradiance. Such measuring equipment could be used after some time (months or years) in order to evaluate the simulation results provided by PVsyst (with the measured irradiance and temperature) with the output and actual production from the installation.

Chapter 7

Conclusion

The optimum tilt angle of the fixed modules considering the annual yield of a system is 40° at Skøyen, Oslo. However, due to the limited amount of space on the roof it was found that the tilt angle resulting in both an acceptable performance ratio and production was 20°. Designing the distance between modular rows such that there would not occur shading from other modular rows during spring equinox resulted in a pitch distance of approximately 2 meters. Increasing the pitch distance further would increase the performance ratio somewhat, except result in reducing of the total amount of modules and, therefore, also reducing the production and the installed capacity of the installation. The final installation oriented towards geographical south with an edge zone of 2 meters has in this study a capacity of 104 modules on the roof. With the choice of three inverter series to match the maximum amount of modules and three types of modules, the three alternatives which provided the best production and performance ratio were:

1. A polycrystalline alternative with REC modules and Eltek inverters
2. A polycrystalline alternative with REC modules and SMA inverters
3. A monocrystalline alternative with SunPower modules and SMA inverters

Since Norway is located so far north the incident irradiation will, therefore, not be very high. The choice of modules with a higher MPP at lower irradiance is, therefore, more suited here than modules with high MPP at the highest incident irradiation. The REC modules were on account of this chosen for both the polycrystalline alternatives instead of one ITS polycrystalline alternative.

The three final alternative PV installations produce 22.4, 22.9 and 31 MWh/year, which is more than an average household in Norway consumes during a year (20.4 MWh/year). The monocrystalline alternative produces approximately 1.5 times that value. However, this production is not enough to cover the consump-

tion of a six storey commercial building. The production from the three systems only covers about 1 % of the total energy consumption in the building. The production would have covered approximately 11 % of the cooling load during 2011. On account of the high consumption in the building, there are no situations where the installation produces more power than the building uses (consumption of 2011). The customer status will, therefore, not change to surplus customer on account of the PV installation on the roof.

With the assumptions and simplifications done regarding the economic situations investing in a PV installation is found unprofitable. Using the simple payback method, it would take about 50 years for the system to pay itself back. The cost per kWh is calculated to be about triple the spot price on electricity. The preferred alternative to proceed with, would with the information and the assumptions of this study, be polycrystalline modules with SMA inverters. This alternative produces most of the two polycrystalline alternatives and has a lower investment cost. The monocrystalline alternative would be the preferred system to proceed with when regarding the production, however, not with regards to costs.

References

[1] Magnussen I.H. Killingland, M. and D. Spilde. Energibruk, energibruk i fastlands-norge. Report 9/2011, Norges vassdrags- og energidierktorat, Middelthunsgate 29, Postboks 5091 Majorstua, 0301 Oslo, May 2011. http://www.nve.no/Global/Publikasjoner/Publikasjoner%202011/Rapport%202011/rapport9-11.pdf.

[2] U.S. Energy Information Administration. International energy outlook 2011. http://205.254.135.7/forecasts/ieo/pdf/0484%282011%29.pdf, September 2011. Accessed: June 5th, 2012.

[3] Heck S. Aanesen, K. and D. Pinner. Solar power: Darkest before dawn. Can be accessed at http://www.mckinsey.com/Insights, May 2012.

[4] F. Drevon. Solar power (pv) covered half of germanys energy demand. http://www.tu.no/energi/2012/05/29/solkraft-dekket-halvparten-av-tysklands-energibehov, May 2012. Accessed: June 5th, 2012.

[5] F. Drevon. This dwelling has an energy surplus. http://www.tu.no/bygg/2012/03/19/dette-bolighuset-gar-i-pluss, March 2012. Accessed: May 5th, 2012.

[6] J. Seehusen. Kraftbygg skal sette verdensrekord. http://www.tu.no/bygg/2012/03/16/kraftbygg-skal-sette-verdensrekord, March 2012. Accessed: June 6th, 2012.

[7] B. Neill S. Garrett S., McLean and Stapleton G. *Grid-Connected PV Systems Design and Installation*. Global Sustainable Energy Solutions Pty Ltd, 2010.

[8] The German Solar Energy Society. *Planning and Installing Photovoltaic Systems - A Guide for installers, architects and engineers*. Number ISBN: 1-84407-131-6. James and James Ltd, 2005.

[9] S. Hegedus and A. Luque. *Handbook of Photovoltaic Science and Engineering*. Number 978-0-470-72169-8. John Wiley and Sons, 2nd edition edition, September 2011.

[10] University of Geneva. *PVsyst Contextual Help*, 1994-2010. Also available on the website: www.pvsyst.com.

[11] Spagnuolo G. Teodorescu R. Veerachary M. Petrone, G. and M. Vitelli. Reliability issues in photovoltaic power processing systems. *Industrial Electronics, IEEE Transactions on*, 55(7):2569 –2580, july 2008.

[12] M.A. Eltawil and Z. Zhao. Grid-connected photovoltaic power systems: Technical and potential problems—a review. *Renewable and Sustainable Energy Reviews*, 14(1):112 – 129, 2010.

[13] `www.pvsyst.com`.

[14] T. Markvart. *Solar Electricity*. John Wiley and sons, ltd., 2000.

[15] R.A Messenger and J. Ventre. *Photovoltaic Systems Engineering*. Number 0-8493-1793-2. CRC Press LLC, 2nd edition edition, 2004.

[16] Nielsen H.K. Norum L.E. Saetre T.O. Midtgård, O.M. and G.H. Yordanov. Over-irradiance (cloud enhancement) events in high latitudes, 2011. Extended abstract submitted for the 38th IEEE PVSC, 3-8 of June 2012.

[17] E. Barstad. The solar resource in norway. `http://www.fornybar.no/sitepageview.aspx?sitePageID=1648`. Accessed: April 3rd, 2012.

[18] Ossenbrink H.A. Dunlop E.D., Huld T.A. and Šúri M. Potential of solar electricity generation in the european union member states and candidate countries. `http://re.jrc.ec.europa.eu/pvgis/`, 2007. Solar Energy, 81, 1295-1305.

[19] Norwegian Institute of Meteorology. eklima. `www.eklima.met.no`. Statistical database.

[20] M. Behnia and S. Odeh. Improving photovoltaic module efficiency using water cooling. *Heat Transfer Engineering*, 30(6):499–505, 2009. cited By (since 1996) 8.

[21] Meteo data sources. `http://www.pvsyst.com/en/publications/meteo-data-sources`. Accessed: April 2nd, 2012.

[22] Müller S. Remund J. Kunz, S. and C. Schilter. *Handbook part 1: Software*. Meteonorm, version 6 edition, December 2012.

[23] Meteo data comparisons. `http://www.pvsyst.com/en/publications/meteo-data-comparaisons$\#$fig$\_$yearly$\_$globh$\_$diff`. Accessed: April 2nd, 2012.

[24] T.P. Chang. The gain of single-axis tracked panel according to extraterrestrial radiation. *Applied Energy*, 86(7–8):1074 – 1079, 2009.

[25] C. Breyer and J. Schmid. Global distribution of optimal tilt angles for fixed tilted pv systems. 3-936338-26-4, pages 4715–4721, September 2010. 25th

European Photovoltaic Solar Energy Conference and Exhibition/ 5th World Conference on Photovoltaic Energy Conversion.

[26] W.D. Lubitz. Effect of manual tilt adjustments on incident irradiance on fixed and tracking solar panels. *Applied Energy*, 88(5):1710 – 1719, 2011.

[27] P. Ineichen. Global irradiance on tilted and oriented planes: Model validations. February 2011. University of Geneva.

[28] J.E. Hay. Calculation of monthly mean solar radiation for horizontal and inclined surfaces. *Solar Energy*, 23(4):301 – 307, 1979.

[29] T. Lejeune and A. Mermoud. Partial shadings on pv arrays: By-pass diode benefits analysis. Institute for the Environmental Science, University of Geneva, September 2010.

[30] Google Maps. `maps.google.no`, March 2012.

[31] Knubix. Image gallery. `http://www.knubix.com/english/flachdach-solaranlagen/index.asp`.

[32] DPW solar. Ballasted roof mounts. `http://www.dpwsolar.com/pdf/lit/SL-SS-1094-1DPWBRM.pdf`.

[33] J. Appelbaum and Bany J. The effect of shading on the design of a field of solar collectors. *Solar Cells*, 20(3):201 – 228, 1987.

[34] International Electrotechnical Commission (IEC), 3, rue de Varembe Geneva, Switzerland. *Photovoltaic system performance monitoring - Guidelines for measurement, data exchange and analysis*, first edition: 1998-04 edition, 1998. International Standard IEC 61724.

[35] U. Jahn and W. Nasse. Operational performance of grid-connected pv systems on buildings in germany. *Progress in Photovoltaics: Research and Applications*, 12(6):441–448, 2004. cited By (since 1996) 16.

[36] Norsk elektroteknisk norm (NEK). *Electrical low voltage installations*. Number NEK 400:2006. NEK, third edition edition, 2006.

[37] Jensen Lund P.T. and T.A Johansen. *Annual Report 2012, The Norwegian Energy Regulator*. Norwegian Water Resources and Energy Directorate, 2010.

[38] Hafslund Nett AS. Connection of production plants, 230-400 v. Guideline: 01-06-01.

[39] Nord Pool. Elspot prices. `http://www.nordpoolspot.com/Market-data1/Elspot/Area-Prices/ALL1/Hourly/`. Accessed: 11th of May, 2012.

[40] Hafslund Nett AS. Landets første plusskunde. `http://www.hafslundnett.no/omoss/artikkelarkiv/les_artikkel.asp?artikkelid=2156`, 2012. Accessed: June 13th, 2012.

[41] Hafslund Nett AS. Tariffs for firms and commerce - 2012. http://www.hafslundnett.no/nett/artikler/les_artikkel.asp?artikkelid=239. Accessed: 14th of March, 2012.

[42] Norges Bank Central bank of Norway. Inflation. http://www.norges-bank.no/no/prisstabilitet/inflasjon/, June 2006. Accessed: 27th of May, 2012.

[43] Jensen T. Haugen, S. and I. Magnussen. Handbook of socio-economic analysis of energy projects. http://www.nve.no/Global/Publikasjoner/Publikasjoner2003. Accessed: 27th of May, 2012.

[44] J.A. Olseth and A. Skartveit. The solar radiation climate of norway. *Solar Energy*, Vol. 37(No. 6):pp. 423–428, June 1986.

[45] J. Herron. Stay tuned. Photon International, the solar power magazine, 2012-03, March 2012.

[46] Spot market prices. Photon International, the solar power magazine, 2012-04, April 2012.

[47] G.C. Schwartz and K.V. Srikrishnan. *Handbook of Semiconductor Interconnection Technology*. Number 978-1-57444-674-6. CRC Press, second edition edition, May 2006, 2012.

[48] R.A. Freedmand and H.D. Young. *University Physics, with modern physics*. Pearson Addison-Wesley, 12th edition edition, 2008.

[49] REC. Rec peak energy series. http://www.recgroup.com/en/products/modules/recpeakenergyseries/. Accessed: May 30th, 2012.

[50] Innotech Solar. Product downloads. http://innotechsolar.com/eng/product_downloads/. Accessed: May 30th, 2012.

[51] SunPower. New sunpower e20 series: the world's first 20% efficiency solar panel. http://us.sunpowercorp.com/homes/products-services/solar-panels/e20/. Accessed: May 30th, 2012.

[52] Eltek. Solar products. http://www.eltek.com/wip4/products.epl?cat=&k1=25509&k2=&k3=&k4=. Accessed: May 30th, 2012.

[53] Danfoss. Tlx inverter range. http://danfoss.ipapercms.dk/Drives/DSI/Factsheets/UK/TLXrange/. Accessed: May 30th, 2012.

[54] SMA. Sunny tripower 8000tl/10000tl/12000tl/15000tl/17000tl. http://www.sma.de/en/products/solar-inverter-without-transformer/sunny-tripower-8000tl-10000tl-12000tl-15000tl-17000tl.html. accessed: May 30th, 2012.

[55] SMA. Sunny boy 3000tl/4000tl/5000tl. http://www.sma.de/en/products/solar-inverter-without-transformer/sunny-boy-3000tl-4000tl-5000tl.html. Accessed: May 30th, 2012.

Appendix A

Data Collection Process

The search engines that were used in order to find articles were Scopus and IEEE. The information regarding the geographical coordinates and distances between different locations was retrieved from Google Earth. Cases where Google Earth was used are for example:

- Locating the project site and measuring the distance between this site and the site of the default meteorological file for Oslo and the local weather stations Lier and Ås.
- Retrieving information concerning the size and dimensions of the roof where the PV installation is proposed installed.

Information concerning the size of the roof etc. was provided by Multiconsult. This information was used alongside with the information of the roof given from Google Earth. Information regarding the size of the twelve storey building which could shade for the PV installation was collected from "plan- og bygningsetaten" in Oslo, Brit Eikholt.

Publications on the PVsyst web page and the contextual help of the program gave insight into how PVsyst functions. In order to understand details, the author of the PVsyst software and founder André Mermoud was contacted by mail. Two of the mounting system suppliers were contacted by mail, since there was not specified an edge zone explicitly in the technical data on their web page. Eric Gilliland replied from DPW, and Kate Bayard replied from Solar Dock.

Hafslund, and Elvedin Grudic was contacted when the grid connection was investigated. The project work of master student Håkon Tranøy as well as his main sources has been looked into. His project concerned the technical requirements of end-users with energy surplus (surplus plus customers).

Appendix B

Meteorological Data

Meteorological data collection

When searching for local information concerning temperature and global horizontal irradiance, MET was contacted. In the Oslo area they have no functioning irradiation measuring station operative at the moment. It was, however, found information from Blindern (59.9423° N, 10.7201° E at an altitude of 94 meters), Oslo which showed they measured global horizontal irradiance up till the year 2006. The accuracy of the irradiation measurements were considered insufficient due to the fact that it had been measured at only four times a day at hour 1, 7, 13 and 19. Using these measurements would give maximum three values a day, resulting in an unrealistic high value of irradiation during a day. The temperature information from MET are based on daily normals from 1961 to 1990.

The irradiation measurements used in order to make the second meteorological set was collected from two Bioforsk stations; Lier and Ås, from the web site `http://lmt.bioforsk.no/agrometbase/getweatherdata.php`. Bioforsk is the Norwegian institute of agricultural and environmental research which was established in 2006. The weather stations in Lier and Ås are the two closest to Oslo, which measure irradiation. Figure B.0.1 show the measuring stations closest to Skøyen, where the green marker illustrates Lier and the blue illustrates Ås.

What could be an error in converting data from hourly to monthly values was discovered, with the help of Georgi H. Yordanov from the University of Agder, when working with the monthly extracted irradiance data from the two stations. The values resulted in annual irradiation of 1300 up to 1600 kW/m^2. Converting the hourly irradiance values to monthly values, the annual values were below 960 kW/m^2, which is considered a more reasonable value in southern Norway.

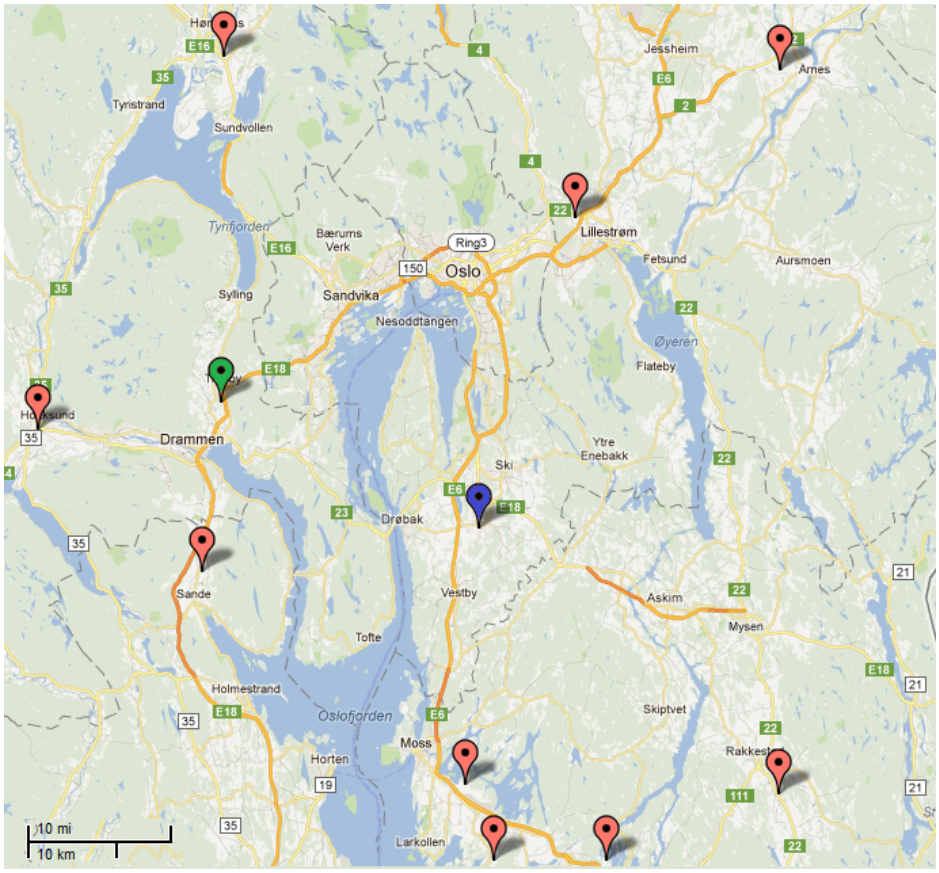

Figure B.0.1: The closest Bioforsk measuring stations to Skøyen.

Global Irradiation

Table B.0.1 and B.0.2 show the global horizontal irradiation of the free online databases Meteonorm, NASA-SSE, PVGIS and RETScreen and the global horizontal irradiation from the weather stations at Lier and Ås respectively.

Table B.0.1: Global irradiation (kWh/m^2)

Source:	Meteonorm D	NASA-SSE	PVGIS	RETScreen	Meteonorm
January	11	12.09	8.03	9.30	11
February	28	30.79	21.81	24.30	28
March	66	71.61	53.01	68.20	63
April	106	111.00	95.70	102.00	107
May	172	164.92	140.74	156.55	142
June	166	166.20	154.80	147.30	149
July	169	170.81	146.32	142.91	136
August	131	131.13	108.19	108.19	119
September	78	82.80	66.00	63.60	78
October	37	40.30	31.00	40.61	39
November	15	16.20	11.07	11.10	19
December	8	7.44	5.52	5.89	7
Yearly	987	1005.29	842.19	879.95	898

Table B.0.2: Global irradiation (kWh/m^2) from the local weather stations in Lier and Ås

	Lier	Ås
January	10.10296	12.26918
February	26.88368	26.65028
March	71.41158	69.47032
April	118.21084	115.97058
May	158.7409	159.05088
June	175.62776	175.66038
July	144.92432	147.63778
August	114.33588	114.48102
September	76.56544	77.68156
October	40.30082	39.9209
November	12.83348	12.54814
December	6.24626	7.34862
Yearly	956.18392	958.68964

Temperature

Table B.0.3 shows the monthly average and the mean yearly temperatures from Meteonorm, NASA, PVGIS and RETScreen.

Table B.0.3: Temperatures (°C)

	Meteonorm			NASA	PVGIS	RETScreen	
	Default	Open	City			Fornebu	Blindern
January	-1.7	-4.4	-3.3	-4.3	-3.1	-3.3	-4.3
February	-2.4	-4.1	-3.1	-3.9	-2.6	-2.8	-4
March	0.3	-0.2	0.6	-1.1	-0.2	1	-0.2
April	4.7	4.5	5.3	3.4	4.7	5.2	4.5
May	10.1	10.8	11.6	9.3	9.7	11.6	10.8
June	13.9	15.2	16	13.2	14	15.5	15.2
July	17	16.4	17.2	15.4	16.8	17.7	16.4
August	16.2	15.2	16.1	14.4	16.6	16.4	15.2
September	13.2	10.8	11.7	9.7	12.3	11.5	10.8
October	8.7	6.3	7.2	5.3	6.8	6.8	6.3
November	3.7	0.7	1.8	0.1	1.8	1.3	0.7
December	0.8	-3.2	-2	-3.3	-2.3	-2.2	-3.1
Yearly	7.1	5.7	6.6	4.9	6.3	6.6	5.7

Table B.0.4 shows the monthly normal values based on the daily normal values in between 1961 and 1990 measured by MET at Blindern in Oslo. Figure B.0.2 shows the lowest and highest temperature measured at Blindern between 2000-2011 in January and July respectively.

Table B.0.4: Monthly normal temperature values (°C), Blindern, Oslo

	MET
January	-4.30
February	-3.99
March	-0.21
April	4.49
May	10.80
June	15.19
July	16.40
August	15.19
September	10.80
October	6.30
November	0.70
December	-3.10
Yearly average	5.70

Daily extremes

Norwegian Meteorological Institute met.no

Stations

Stnr	Name	Operates from	Operates until	Altitude	Latitude	Longitude	Municipality	County	Region
18700	OSLO - BLINDERN	Feb 1937		94	59.9423	10.7201	OSLO	OSLO	SOUTHEASTERN NORWAY

Elements

Code	Name	Unit
TAN	Minimum temperature	°C

Elements

Code	Name	Unit
TAX	Maximum temperature	°C

18700 OSLO - BLINDERN WITH TAN
Period:2000-2011
10 lowest values

Mnth	Jan
1	-20.5
Date	09.01.2010
2	-20.1
Date	04.01.2003
3	-20.0
Date	08.01.2010
4	-19.6
Date	06.01.2010
5	-19.0
Date	07.01.2010
6	-17.7
Date	06.01.2003
7	-16.8
Date	10.01.2010
8	-16.7
Date	03.01.2010
9	-16.6
Date	01.01.2002
10	-16.2
Date	01.01.2001

18700 OSLO - BLINDERN WITH TAX
Period:2000-2011
10 highest values

Mnth	Jul
1	33.0
Date	03.07.2009
2	32.7
Date	02.07.2009
3	31.6
Date	28.07.2008
4	31.5
Date	01.07.2009
5	31.4
Date	11.07.2005
6	31.3
Date	08.07.2005
7	31.2
Date	09.07.2005
8	31.0
Date	26.07.2008
9	30.6
Date	12.07.2005
10	30.6
Date	27.07.2008

Figure B.0.2: Temperature maximums and minimums from 2000 – 2011 in January and July

Diffuse irradiation

Table B.0.5 shows the diffuse irradiation data which was possible to retrieve. As seen there are only data from two of the databases, the Meteonorm and NASA.

Table B.0.5: Diffuse irradiation data (kWh/m^2), D = default

	Meteonorm		NASA-SSE
	D		
January	8	7	8.4
February	18	16	19.5
March	39	33	41.5
April	59	48	60.3
May	72	81	77.8
June	84	86	83.1
July	80	79	81.5
August	66	60	69.1
September	44	41	44.4
October	25	24	25.1
November	10	9	11.1
December	5	5	5.6
Yearly	510	489	527.4

Wind

Table B.0.6 shows the wind data possible to derive from the databases.

Table B.0.6: Wind data (m/s)

	Meteonorm	NASA-SSE	RETScreen	
			Fornebu	Blindern
January	5.6	5.52	2.2	2.5
February	5.4	5.11	2.2	2.6
March	5.7	5.01	2.5	2.6
April	5.8	4.87	2.7	3
May	4.7	4.66	2.7	2.8
June	4.6	4.38	2.8	2.8
July	4.2	4.37	2.7	2.5
August	4.6	4.37	2.6	2.6
September	4.8	4.96	2.5	2.6
October	4.6	5.26	2.5	2.6
November	5	5.36	2.1	2.6
December	5.5	5.4	1.9	2.6
Yearly	5.1	5	2.5	2.7

Appendix C

Shade

Distance Between Modules

The distances between the module rows were calculated by using Equation 3.3.1, five different tilt angles (20°, 30°, 40°, 53° and 59°) at 10:00, 11:00 and 12:00 a clock. Table C.0.1 shows the azimuth and altitude numbers that was used from USNO and NASA. The numbers from USNO were calculated from the specific day and time in year 2011, while the NASA numbers are monthly averaged numbers.

Table C.0.1: Azimuth and altitude numbers from USNO and NASA

	Azimuth		Altitude	
	USNO	NASA	USNO	NASA
March 21st				
10:00	139.7°	140°	24.4°	22.0°
11:00	155.9°	155°	28.4°	26.0°
12:00	172.9°	172°	30.4°	28.0°
June 21st				
10:00	130.9°	131°	46.2°	46.0°
11:00	150.5°	151°	51.0°	50.7°
12:00	172.7°	173°	53.4°	53.0°
December 21st				
10:00	149.3°	150°	2.5°	3.03°
11:00	162.7°	163°	5.4°	5.95°
12:00	176.5°	177°	6.7°	7.15°

Table C.0.2: Spring equinox distances, D in meters, between rows, polycrystalline modules, USNO

March 21st	20°	30°	40°	53°	59°
10:00	0.570	0.834	1.071	1.331	1.429
11:00	0.573	0.837	1.076	1.337	1.435
12:00	0.574	0.839	1.078	1.339	1.437

Table C.0.3: Spring equinox distances, D in meters, between rows, polycrystalline modules, NASA

March 21st	20°	30°	40°	53°	59°
10:00	0.643	0.939	1.208	1.501	1.611
11:00	0.630	0.921	1.184	1.471	1.578
12:00	0.631	0.923	1.186	1.474	1.582

As seen from Table C.0.2 and C.0.3 the distance between the module rows are increasing as the clock is reaching noon when USNO numbers for the azimuth and altitude were used, in contrast to when the NASA numbers for azimuth and altitude were used. When considering June 21st (the day when the least amount of distance between the rows are necessary in order to have no shade on other rows, see Table C.0.4) both the numbers from USNO and NASA increases with increasing hour of the day. Then considering the day when the distance between the rows are as large as they can be, December 21st (see Table C.0.5), the distance is decreasing with increasing hour of the day. Only the numbers from NASA are shown in Table C.0.4 and C.0.5 since these numbers are considered more conservative. The numbers from NASA are consequently the ones used to set the pitch distance.

Table C.0.4: Distance D between rows June 21st, polycrystalline modules, NASA

June 21st	20°	30°	40°	53°	59°
10:00	0.215	0.314	0.404	0.502	0.539
11:00	0.243	0.355	0.457	0.567	0.609
12:00	0.254	0.371	0.477	0.592	0.636

During summer increasing altitude will decrease the shade, however, not much since the sun has an altitude above 45°. The azimuth is almost the same whether it is June or December. Increasing azimuth angle increases the length of the shade until its maximum length at approximately 180° is reached, before the shade decreases again. As the altitude is above 45° the altitude does not diminish

Table C.0.5: Distance D between rows December 21st, polycrystalline modules, NASA

December 21st	20°	30°	40°	53°	59°
10:00	5.545	8.107	10.422	12.949	13.898
11:00	3.11	4.547	5.845	7.262	7.794
12:00	2.698	3.945	5.071	6.301	6.762

the length caused by the azimuth to the same extent as in the autumn or winter months (September and March). The shade at noon will, therefore, be the largest in the time between March and September. The reason why the distances are increasing in Table C.0.2 and decreasing in Table C.0.3 are, therefore, due to the small differences in azimuth and altitude from the two sources USNO and NASA on the day of spring equinox.

Table C.0.6 illustrate the distance D in meters for both monocrystalline modules and polycrystalline modules, with azimuth and altitude numbers from NASA. Table C.0.7 show the pitch distance between monocrystalline and polycrystalline modules based on the azimuth and altitude numbers from NASA.

Table C.0.6: Spring equinox distances, D in meters, NASA

March 21st	20°	30°	40°	53°	59°
Mono					
10:00	0.678	0.992	1.275	1.584	1.7
11:00	0.665	0.972	1.249	1.552	1.666
12:00	0.666	0.974	1.252	1.556	1.67
Poly					
10:00	0.643	0.939	1.208	1.501	1.611
11:00	0.63	0.921	1.184	1.471	1.578
12:00	0.631	0.923	1.186	1.474	1.582

Table C.0.7: Spring equinox pitch distances in meters, NASA

March 21st	20°	30°	40°	53°	59°
Mono					
10:00	1.661	1.897	2.076	2.213	2.239
11:00	1.648	1.878	2.051	2.182	2.205
12:00	1.649	1.878	2.053	2.185	2.209
Poly					
10:00	1.574	1.78	1.967	2.097	2.121
11:00	1.561	1.779	1.943	2.067	2.089
12:00	1.562	1.781	1.946	2.07	2.092

Shade Analysis

Figure C.0.1 illustrates the results of the shade analysis seen in Tables C.0.8 to Table C.0.13. The shade analysis was performed with a module tilt of 20°, 60 % electrical shading effect with a pitch distance of 2 meters. The module size is set in the size of polycrystalline modules (1.665 x 0.991 x 0.043 m). The results are, however, considered to be equally valid for the monocrystalline case (1.559 x 1.046 x 0 046 m), because of to the small deviation in modular size. Sunrise was simulated to occur at 06:30 while sun set was at 18:30. Since the shade analysis is done by manually observing which modules that are shaded each half hour in PVsyst, there could occur faults. The resolution of the field could also have been too small in order to see exactly when modules are shaded which is another source of error. However, since the meteorological data set could be interpreted as a general year there will be deviations from the analysis in a live field.

Table C.0.8: The time and modules shaded in field A during March 21st, x = partially shaded module, f = fully shaded module

FIELD						
A	6	7	8	9	10	11
06:30	x	x	x	x	f	f
07:00		x	x		x	f
07:30			x			x
08:00			x			x
08:30			x			x
09:00						x

Table C.0.9: The time and modules shaded in field B, during March 21st, x = partially shaded module, f = fully shaded module

FIELD B	5	6	7	8	9	10	11	12	13	14	15	16	17
06:30													
07:00													
07:30													
14:30													
15:00													
15:30													
16:00													
16:30						x							
17:00						x	x						
17:30						f	f	x	x				
18:00	x	x	x	x	x	f	f	f	f	f	f	f	f

Table C.0.10: The time and modules shaded in field B, during March 21st, x = partially shaded module, f = fully shaded module

FIELD B	18	19	20	21	22	23	24	25	26	27
06:30										
07:00										
07:30										
14:30	x									
15:00	x									
15:30	x									
16:00	x	x								
16:30	x	x								
17:00	x	x	x							
17:30	f	f	x	x	x					
18:00	f	f	f	f	f	f	f	x	x	x

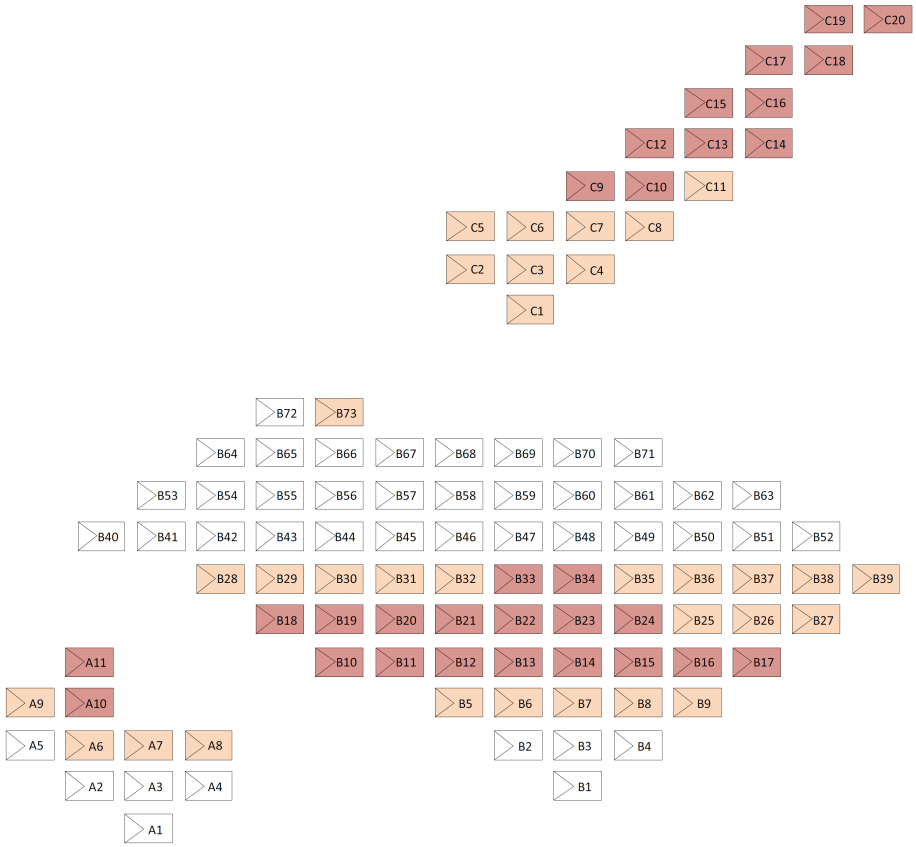

Figure C.0.1: Overview of the results of the shading analysis for March 21st with 2 meter pitch distance. The dark red modules are the ones that are fully shaded on some point during the day, while the peach coloured modules are partially shaded during the day.

Table C.0.11: Time and modules shaded in field B, during March 21st, x = partially shaded module, f = fully shaded module

FIELD													
B	28	29	30	31	32	33	34	35	36	37	38	39	73
06:30													
07:00													
07:30													x
14:30													
15:00													
15:30	x												
16:00	x												
16:30	x												
17:00	x	x											
17:30	x	x	x	x	x								
18:00	x	x	x	x	x	f	f	x	x	x	x	x	

Table C.0.12: Time and modules shaded in field B, during March 21st, x = partially shaded module, f = fully shaded module

FIELD										
C	1	2	3	4	5	6	7	8	9	10
16:00										
16:30										
17:00		x			x	x				
17:30	x	x	x	x	x	x	x	x	x	x
18:00		x	x	x	x	x	x	x	f	f

Table C.0.13: Time and module number shaded in field C during March 21st, x = partially shaded module, f = fully shaded module

FIELD										
C	11	12	13	14	15	16	17	18	19	20
16:00							x		x	
16:30					x		f	x	f	x
17:00		x			f	x	f	f	f	f
17:30	x	f	f	f	f	f	f	f	f	f
18:00	f	f	f	f	f	f	f	f	f	f

Appendix D

Simulation Settings

Orientation Parameters

Field type:	fixed tilted plane
Plane tilt:	40°, 30°, 25°, 20°
Azimuth:	0°

Loss Parameters

The three modules tested were one module from REC (REC250PE), one from Innotech Solar (ITS EcoPlus, poly-Up 250W_p) and one from SunPower (E20, SPR-327NE-WHT-D).

The thermal parameter was defined by using the NOCT coefficient, and then the corresponding constant loss factor was given by PVsyst (seen in Table D.0.1). The DC ohmic losses were the only one defined in PVsyst during the simulations, the option of defining the AC ohmic losses are as mentioned present in PVsyst.

Table D.0.1: Thermal parameter simulation settings

	REC	ITS	SunPower
NOCT coefficient	47.9°C (± 2°C)	47.9°C (± 2°C)	45°C (± 2°C)
Constant loss factor	25.8 (24.7)	25.8 (24.7)	28.8 (26.7)

Table D.0.2: Ohmic losses parameters

DC circuit	REC	ITS	SunPower
Global wiring resistance, mOhm	225	93.8	105.5
or loss fraction at STC, %	1.5	1.5	1.5
Voltage drop across series diode, V	0	0	0

Table D.0.3: Module quality and mismatch parameters

	REC	ITS	SunPower
Module quality:			
Module efficiency loss	0 %	0 %	0 %
Mismatch losses:			
Power loss at MPP	2 %	2 %	2 %
Loss when running at fixed voltage	4 %	4 %	4 %

Table D.0.4: Soiling losses parameters

January	February	March	April	May	June
50 %	35 %	0 %	0 %	0 %	0 %

July	August	September	October	November	December
0 %	0 %	0 %	0 %	0 %	35 %

Appendix E

Cable sizing

After each of the modules where assigned to their string, the lengths were measured in the 3D representation of the building with the modules placed on the roof. In order to find the total lengths Equation E.0.1 was used.

$$Cable\ length = N_{modules}(M_{length}+2M_{frame})+N_{spaces}(2height+pitch) \quad \text{(E.0.1)}$$

where $N_{modules}$ are the number of modules in the string, M_{length} is the length of one module, M_{frame} is the frame length, N_{spaces} are the number of spaces between the rows (two rows equals one space) and *height* is the height from the junction box to the ground. The junction boxes on the modules are assumed to be located on module width divided by two.

The minimum cross section of the cables were calculated by using Equation 3.4.10 from Section 3.4 with a cable loss of 1.5 %. The metal resistivity is highly dependent on temperature and is described by the following Equation

$$\rho = \rho_0[1 + \alpha_0(T - T_0)] \quad \text{(E.0.2)}$$

where ρ_0 is the metals resistivity (Ωcm) defined at a reference temperature (T_0) which is usually 0° C or 20° C and α_0 is the temperature coefficient of resistivity ($^\circ C^{-1}$). At a temperature T ρ is the resistivity. The bulk value of ρ_0 is 1.678 $\mu\Omega$cm at 20° C [47, p.320], resulting in $T_0 = 20^\circ$ C. The approximate temperature coefficient of copper close to room temperature is $0.00393^\circ C^{-1}$ [48, p.852]. Calculating the copper resistivity at a temperature of 50° C results in $\rho = 18.75$ mΩ/mm^2/m. A ρ of copper of 18.3 mΩ/mm^2/m is used in [7, p.221]. If the computational tool in PVsyst is used in order to calculate the wiring loss, a ρ may be defined by the user or a default value of 22 mΩ/mm^2/m can be used for a temperature of 50° C.

REC modules, Eltek inverters

The module distribution which was made for the REC modules with the Eltek inverter is seen in Figure E.0.1. The measured cable lengths are also displayed in this figure. Table E.0.1 shows the total lengths of the cables per string, with a 10 % safety margin added in the end due to uncertainty of the accuracy of the measuring tool in the 3D representation in PVsyst.

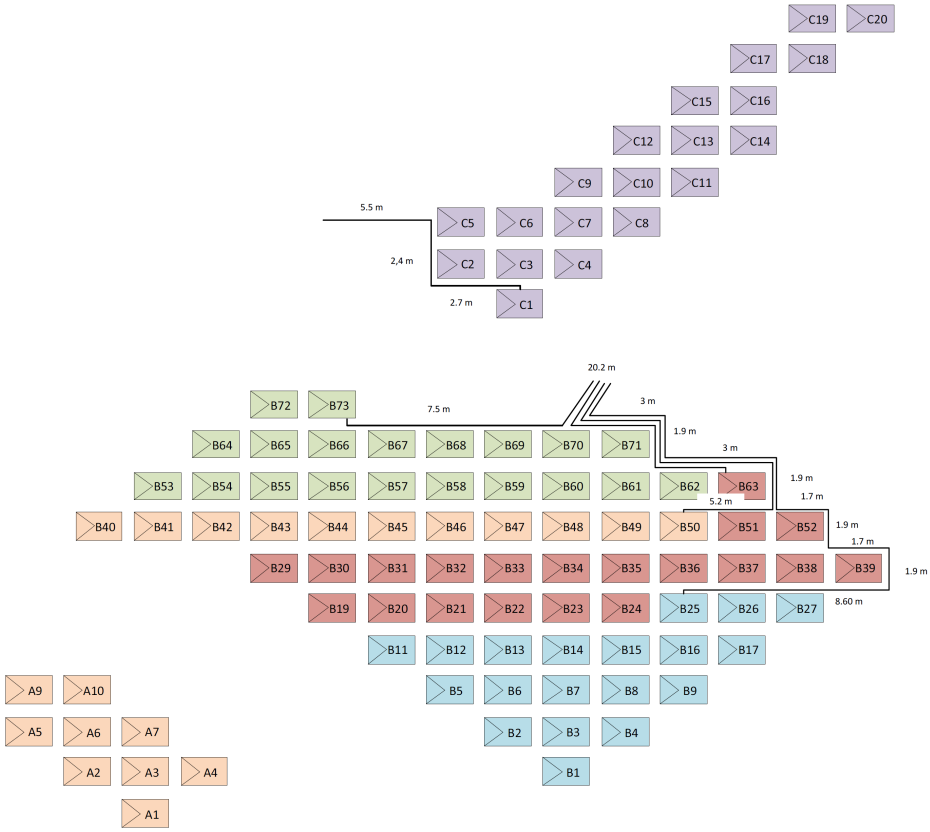

Figure E.0.1: Module string distribution with the REC module and the Eltek inverter

Table E.0.2 shows the minimum cross section area of the cables with 1.5 % loss, the nearest normal cross section area of PV module cables and the loss calculated with this cross section in percent. Standard cross sectional areas for PV module cables are 1.5 mm^2, 2.5 mm^2, 4 mm^2 and 6 mm^2.

Table E.0.1: Cable lengths for the alternative with the REC module and Eltek inverter

	String1	String2	String 3	String 4	String 5
Modules in a string	10	20	20	20	20
Number of spaces	0	4	3	2	7
Module tilt	20	20	20	20	20
Module length	1.665	1.665	1.665	1.665	1.665
Module width	0.991	0.991	0.991	0.991	0.991
Module frame	0.086	0.086	0.086	0.086	0.086
Pitch	2	2	2	2	2
Height, junction box	0.1695	0.1695	0.1695	0.1695	0.1695
Cable length	17.51	44.376	42.037	39.698	51.393
String colour	Peach	Blue	Red	Green	Purple
String part 1	24.527				
String part 2	17.51				
Length between fields	4.7				
Min lengths	46.737	44.376	42.037	39.698	51.393
Length to the door:	35.2	45.8	28.1	27.7	10.6
Total lengths	81.937	90.176	70.137	67.398	61.993
Safety margin, 10 %	90.1307	99.1936	77.1507	74.1378	68.1923

Table E.0.2: The minimum cross section area (CSA) with the measured lengths ($\rho = 18.3\text{m}\Omega/\text{mm}^2/\text{m}$)

	String 1	String 2	String 3	String 4	String 5
Minimum CSA, mm^2	2.96	3.25	2.53	2.43	2.24
Closest CSA, mm^2	4	4	4	4	4
Loss	1.11 %	1.22 %	0.95 %	0.91 %	0.84 %

REC modules, SMA inverters

The module distribution which was made for the REC modules with the SMA inverter is seen in Figure E.0.2. The measured cable lengths are also displayed in this figure. Table E.0.3 and Table E.0.4 show the total lengths of the cables per string, with a 10 % safety margin added in the end due to uncertainty of the

accuracy of the measuring tool in the 3D representation in PVsyst.

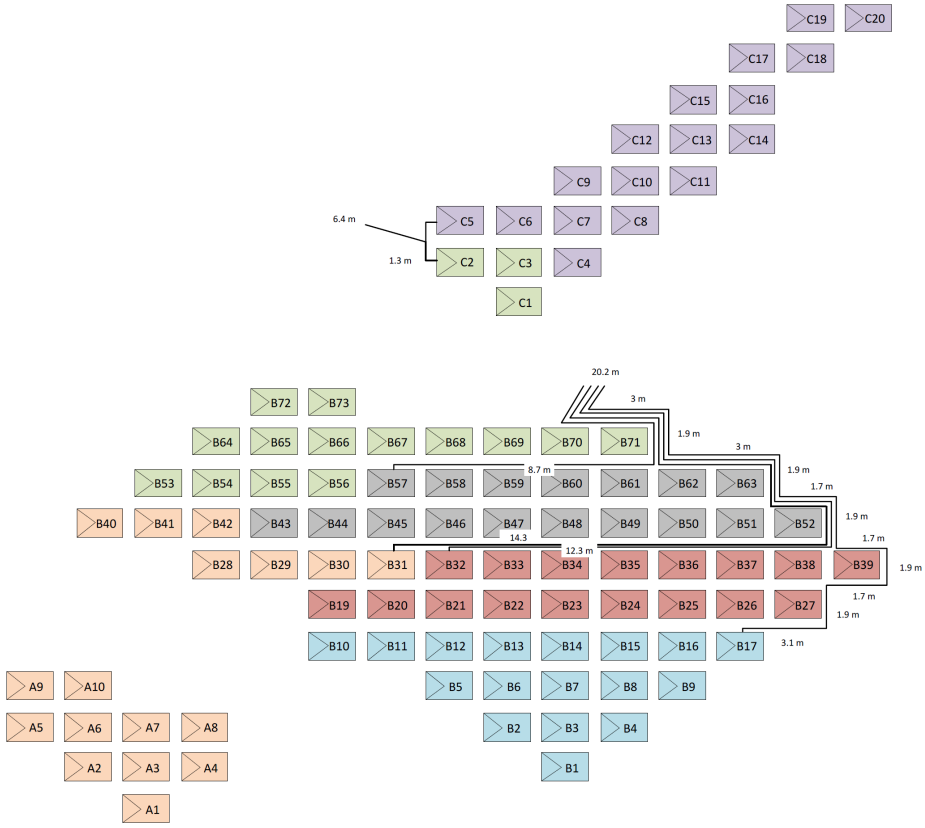

Figure E.0.2: Module string distribution with REC modules and SMA inverter

Table E.0.3: Cable lengths for the alternative with the REC module and SMA inverter

	String 1	String 2	String 3	String 4	String 5
Modules in a string	7	17	17	17	3
Number of spaces	1	3	1	1	1
Module tilt	20	20	20	20	20
Module length	1.665	1.665	1.665	1.665	1.665
Module width	0.991	0.991	0.991	0.991	0.991
Module frame	0.086	0.086	0.086	0.086	0.086
Pitch	2	2	2	2	2
Height, junction box	0.1695	0.1695	0.1695	0.1695	0.1695
Cable length	14.596	36.784	32.106	32.106	7.592
String colour	Peach	Blue	Red	Grey	Green
String part 1	24.527				29.192
String part 2	14.596				7.592
Length between fields	4.7				20.88
Min cable length	43.823	36.784	32.106	32.106	57.664
Lengths to the door	47.9	43.9	45.9	33.8	7.7
Total length	91.723	80.684	78.006	65.906	65.364
Safety margin, 10%	100.8953	88.7524	85.8066	72.4966	71.9004

Table E.0.4: Cable lengths for the alternative with the REC module and SMA inverter, string 6

	String 6
Modules in a string	17
Number of spaces	6
Module tilt	20
Module length	1.665
Module width	0.991
Module frame	0.086
Pitch	2
Height, junction box	0.1695
Cable length	43.801
String colour	Purple
String part 1	
String part 2	
Length between fields	
Min lengths	43.801
Lengths to the door	7.7
Total length	51.501
Safety margin, 10 %	56.6511

Table E.0.5 shows the minimum cross section area of the cables with 1.5 % loss, the nearest normal cross section area of PV module cables and the loss calculated with this cross section in percent. Standard cross sectional areas for PV module cables are 1.5 mm^2, 2.5 mm^2, 4 mm^2 and 6 mm^2.

Table E.0.5: The minimum cross section area (CSA) with the measured lengths ($\rho = 18.3 m\Omega/mm^2/m$)

	String1	String2	String3	String4	String5	String6
Minimum CSA	3.89	3.42	3.31	2.80	2.77	2.19
Closest CSA	4	4	4	4	4	2.5
Loss	1.46 %	1.28 %	1.24 %	1.05 %	1.04 %	1.31 %

SunPower modules, SMA inverters

The module distribution which was made for the SunPower modules with the SMA inverter is seen in Figure E.0.3. The measured cable lengths are also displayed in this figure. Table E.0.6 and Table E.0.7 show the total lengths of the cables per string, with a 10 % safety margin added in the end due to uncertainty of the accuracy of the measuring tool in the 3D representation in PVsyst.

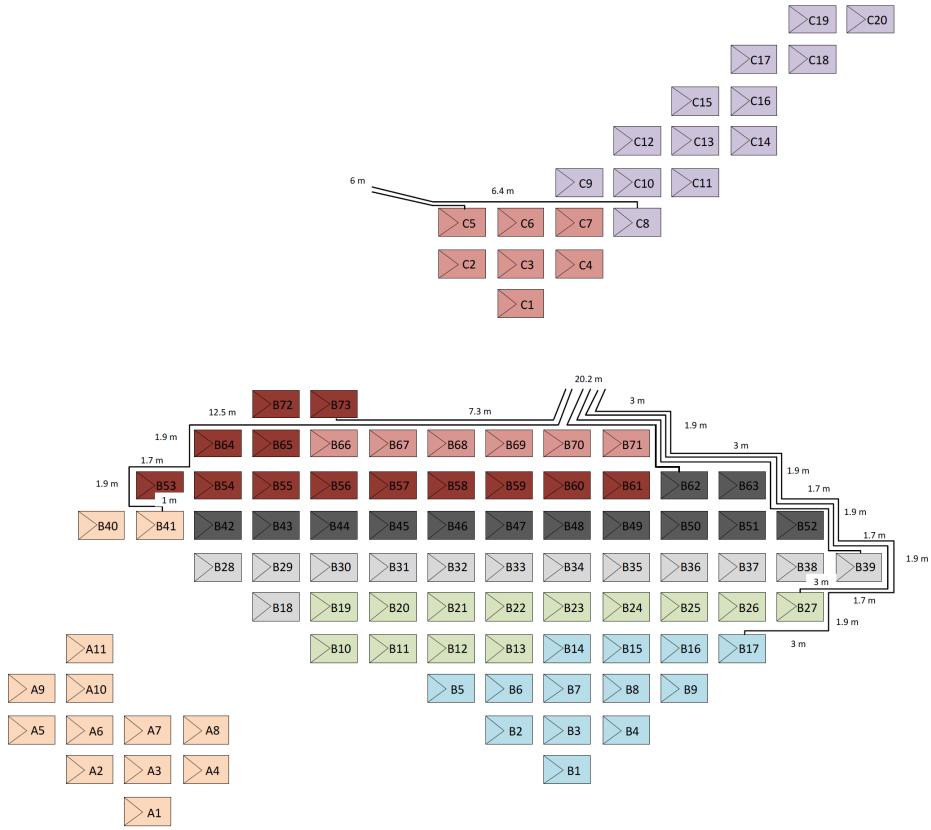

Figure E.0.3: Module string distribution with SunPower modules and SMA inverter

Table E.0.6: Cable lengths for the alternative with the SunPower module and SMA inverter, to string 5

	String1	String2	String 3	String 4	String 5
Modules in a string	11	13	13	13	13
Number of spaces	4	3	1	1	1
Module tilt	20	20	20	20	20
Module length	1.559	1.559	1.559	1.559	1.559
Module width	1.046	1.046	1.046	1.046	1.046
Module frame	0.092	0.092	0.092	0.092	0.092
Pitch	2	2	2	2	2
Height, junction box	0.1789	0.1789	0.1789	0.1789	0.1789
Cable length	27.5922	28.5364	23.8208	23.8208	23.8208
String colour	Peach	Blue	green	Grey	Dark grey
String part 1	27.5922				
String part 2	3.302				
Length between fields	4.7				
Min cable lengths	35.5942	28.5364	23.8208	23.8208	23.8208
Lengths to the door	39.2	43.8	40.2	35.3	25.1
Total length	74.7942	72.3364	64.0208	59.1208	48.9208
Safety margin, 10 %	82.27362	79.57004	70.42288	65.03288	53.81288

Table E.0.8 and Table E.0.7 show the minimum cross section area of the cables with 1.5 % loss, the nearest normal cross section area of PV module cables and the loss calculated with this cross section in percent. Standard cross sectional areas for PV module cables are 1.5 mm^2, 2.5 mm^2, 4 mm^2 and 6 mm^2.

Table E.0.7: Cable lengths for the alternative with the SunPower module and SMA inverter, to string 8

	String 6	String 7	String 8
Modules in a string	13	7	13
Number of spaces	2	2	5
Module tilt	20	20	20
Module length	1.559	1.559	1.559
Module width	1.046	1.046	1.046
Module frame	0.092	0.092	0.092
Pitch	2	2	2
Height, junction box	0.1789	0.1789	0.1789
Cable length	26.1786	16.2726	33.252
String colour	Red	Pink	Purple
String part 1		9.906	
String part 2		16.2726	
Length between fields		20.88	
Min cable lengths	26.1786	47.0586	33.252
Lengths to the door	27.5	6	12.4
Total length	53.6786	53.0586	45.652
Safety margin, 10 %	59.04646	58.36446	50.2172

Table E.0.8: The minimum cross section area (CSA) with the measured lengths, SunPower modules, SMA inverters. String 1 to string 5 ($\rho = 18.3\text{m}\Omega/\text{mm}^2/\text{m}$)

	String 1	String 2	String 3	String 4	String 5
Minimum CSA, mm2	1.688189	1.632713	1.445021	1.334422	1.104197
Closest CSA	2.5	2.5	1.5	1.5	1.5
Loss	1.01 %	0.98 %	1.45 %	1.33 %	1.10 %

Table E.0.9: The minimum cross section area (CSA) with the measured lengths, SunPower modules, SMA inverters. String 6 to string 8 ($\rho = 18.3\text{m}\Omega/\text{mm}^2/\text{m}$)

	String 6	String 7	String 8
Minimum CSA, mm2	1.211586	1.197592	1.030417
Closest CSA	1.5	1.5	1.5
Loss	1.21 %	1.20 %	1.03 %

Appendix F

Technical Data

Modules

Figure F.0.1 illustrates the technical data of the Peak Energy EU series by REC. Figure F.0.2 illustrates the technical data of the Eco Plus series by ITS while Figure F.0.3 illustrates the technical data of the E20 series by SunPower.

Inverters

Figure F.0.4 and Figure F.0.5 illustrate the technical data of the two Eltek inverters Theia TL String and Theia HE-t. Figure F.0.6 illustrates the technical data of the Danfoss inverter series TLX. Figure F.0.7 to Figure F.0.12 illustrate the technical data of the SMA Sunny Tripower series. Figure F.0.13 to Figure F.0.16 illustrate the technical data of the SMA Sunny Boy series without reactive power control. This Sunny Boy is the base inverter.

REC PEAK ENERGY EU SERIES

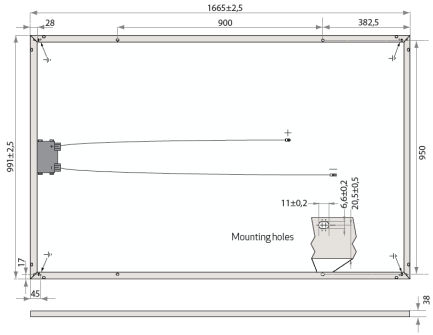

15.1% EFFICIENCY

10 YEAR PRODUCT WARRANTY

25 YEAR LINEAR POWER OUTPUT WARRANTY

ELECTRICAL DATA @ STC	REC225PE	REC230PE	REC235PE	REC240PE	REC245PE	REC250PE
Nominal Power - P_{MPP} (Wp)	225	230	235	240	245	250
Watt Class Sorting - (W)	0/+5	0/+5	0/+5	0/+5	0/+5	0/+5
Nominal Power Voltage - V_{MPP} (V)	28.9	29.2	29.6	29.9	30.2	30.5
Nominal Power Current - I_{MPP} (A)	7.8	7.9	8.0	8.0	8.1	8.2
Open Circuit Voltage - V_{OC} (V)	36.2	36.5	36.7	37.0	37.2	37.5
Short Circuit Current - I_{SC} (A)	8.3	8.4	8.5	8.6	8.7	8.8
Module Efficiency (%)	13.6	13.9	14.2	14.5	14.8	15.1

Values at standard test conditions STC (airmass AM 1.5, irradiance 1000 W/m², cell temperature 25°C).
At low irradiance of 200 W/m² (AM 1.5 and cell temperature 25°C) at least 97% of the STC module efficiency will be achieved.

ELECTRICAL DATA @ NOCT	REC225PE	REC230PE	REC235PE	REC240PE	REC245PE	REC250PE
Nominal Power - P_{MPP} (Wp)	167	170	173	176	179	182
Nominal Power Voltage - V_{MPP} (V)	26.6	26.8	27.1	27.3	27.6	27.9
Nominal Power Current - I_{MPP} (A)	6.3	6.3	6.4	6.4	6.5	6.6
Open Circuit Voltage - V_{OC} (V)	33.4	33.6	33.8	34.1	34.3	34.5
Short Circuit Current - I_{SC} (A)	6.8	6.8	6.9	7.0	7.0	7.1

Nominal cell operating temperature NOCT (800 W/m², AM 1.5, windspeed 1 m/s, ambient temperature 20°C).

TEMPERATURE RATINGS

Nominal Operating Cell Temperature (NOCT)	47.9°C (±2°C)
Temperature Coefficient of P_{MPP}	-0.43 %/°C
Temperature Coefficient of V_{OC}	-0.33 %/°C
Temperature Coefficient of I_{SC}	0.074 %/°C

GENERAL DATA

Cell Type	60 REC PE multi-crystalline cells 3 strings of 20 cells - 4 by-pass diodes
Glass	3.2 mm solar glass with antireflection surface treatment by Sunarc Technology
Back Sheet	Double layer highly resistant polyester
Frame	Anodized aluminium
Junction box	IP67
Cable	4mm² solar cable, 0.90m +1.20m
Connectors	Hosiden 4mm² (HSC 2009/2010) MC4 connectable

MAXIMUM RATINGS

Operational Temperature	-40 ... +80°C
Maximum System Voltage	1000V
Maximum Snow Load	550 kg/m² (5400 Pa)
Maximum Wind Load	244 kg/m² (2400 Pa)
Maximum Series Fuse Rating	25A
Maximum Reverse Current	25A

MECHANICAL DATA

Dimensions	1665 x 991 x 38 mm
Area	1.65 m²
Weight	18 kg

ORIGIN OF COMPONENTS

Wafers produced by REC Wafer, Herøya, Norway.

Note! Specifications subject to change without notice.

Rev D - 01.2012

CERTIFICATION

IEC 61215 & IEC 61730, IEC 62716 (ammonia resistance) & IEC 61701 (salt mist severity level 6)

Member of PV Cycle

WARRANTY

10 year product warranty.
25 year linear power output warranty
(max. degression in performance of 0.7% p.a.).

REC is a leading vertically integrated player in the solar energy industry. Ranked among the world's largest producers of polysilicon and wafers for solar applications, and a rapidly growing manufacturer of solar cells and modules, REC also engages in project development activities in selected PV segments. Founded in Norway in 1996, REC is an international solar company employing about 4,000 people worldwide with revenues close to NOK 14 billion (EUR 1.7 billion, USD 2.3 billion) in 2010.

REC

www.recgroup.com

Figure F.0.1: REC, Peak Energy EU Series [49]

EcoPlus – PolyUp

STC*

Pmax	Wp	210	220	230	240	250
Vmpp	V	28.6	29.1	29.6	30.2	31.0
Impp	A	7.53	7.73	7.95	8.11	8.22
Voc	V	36.2	36.4	36.7	37.1	37.6
Isc	A	8.19	8.31	8.50	8.66	8.79
IR****	A	20	20	20	20	20
η	%	12.7 – 13.3	13.3 – 13.9	13.9 – 14.5	14.6 – 15.2	15.2 – 15.8

NOCT**

Pmax	Wp	158	164	170	176	182
Vmpp	V	25.8	26.3	26.8	27.3	27.8
Voc	V	32.8	33.2	33.6	33.9	34.2
Isc	A	6.60	6.70	6.80	6.90	7.00

Temperature Coefficients

Pn	-0.43 %/K
Voc	-0.33 %/K
Isc	0.05 %/K

NOCT**	47.9°C (± 2°C)
Module efficiency reduction at 200 W/m²***	-0.6 (± 0.3)% abs.
Max. System Voltage	1000 V
IP protection level	IP 65
Module Technology	Glass-Foil-Laminate with anodized aluminium frame
Module Design	Cover material: Solar glass with anti-reflection surface treatment (Sunarc Technology), 3.2 mm; Encapsulation: EVA-Solar Cells -EVA; Back material
No. and Type of Solar Cells	60 crystalline solar cells, 156 x 156 mm, 180 µm ± 30 µm
Cables	Junction box with MC4 connectors, cable: 2 x 1 m / 4 mm²
Bypass-Diodes	3 pcs.
Dimensions (l x w x h)	1665 x 991 x 43 mm
Weight	22 kg
Operating Temperature Range	-40 ... +80°C
Ambient Temperature Range	-40 ... +45°C
Mechanical ratings	Suction pressure of 2400 Pa approved (Wind speed 130 km/h with safety factor 3), load of 5400 Pa approved
Certification	IEC 61215 : 2005 IEC 61730-1 / -2 : 2004 IEC 61701 : 1995 (salt mist resistant) MCS DLG Focus Test (ammonia resistant)
Positive sorting	-0 Wp / +10 Wp
Packing dimensions	1720 x 1045 x 180 mm, 30 modules per pallet
Product warranty	5 year standard warranty, expandable to 10 years after registration
Performance warranty	90% of output power for 10 years and 80% for 25 years, according to the Warranty Conditions of Innotech Solar

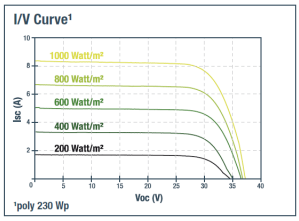

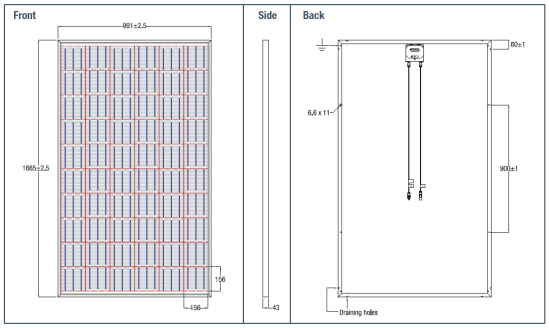

* STC – Standard Test Conditions, measurement conditions: intensity irradiation 1000 W/m², spectral distribution AM 1.5, temperature 25 ± 2°C, according to standard EN 60904-3
** NOCT – Normal Operation Cell Temperature, measurement conditions: irradiation intensity 800 W/m², AM 1.5, temperature 20°C, wind speed 1 m/s.
*** Reduced effiency with the decrease in the intensity of irradiation of 1000 W/m² and 200 W/m², temperature 25°C according EN 60904-1
**** Reverse current power rating: operation of the modules with an external power source is only permitted with a string fuse with a release current of < 2 x Isc @ STC*
Measuring tolerances of Pmax @ STC ± 5%, all other electric parameters ± 10%
This datasheet conforms to EN 50380. Innotech Solar reserves the right to change specifications without notice.

Revision 01-2012

Figure F.0.2: ITS, Eco Plus series [50]

MODEL: SPR-327NE-WHT-D

ELECTRICAL DATA

Measured at Standard Test Conditions (STC): irradiance of 1000W/m², AM 1.5, and cell temperature 25° C

Peak Power (+5/-3%)	P_{max}	327 W
Cell Efficiency	η	22.5 %
Panel Efficiency	η	20.1 %
Rated Voltage	V_{mpp}	54.7 V
Rated Current	I_{mpp}	5.98 A
Open-Circuit Voltage	V_{oc}	64.9 V
Short-Circuit Current	I_{sc}	6.46 A
Maximum System Voltage	UL	600 V
Temperature Coefficients	Power (P)	-0.38% / K
	Voltage (V_{oc})	-176.6mV / K
	Current (I_{sc})	3.5mA / K
NOCT		45° C +/-2° C
Series Fuse Rating		20 A
Grounding	Positive grounding not required	

I-V CURVE

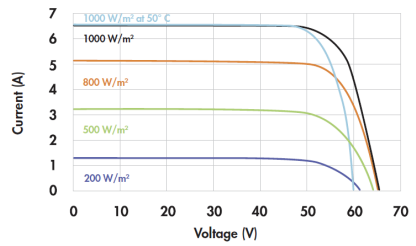

Current/voltage characteristics with dependence on irradiance and module temperature.

MECHANICAL DATA

Solar Cells	96 SunPower Maxeon™ cells
Front Glass	High transmission tempered glass with anti-reflective (AR) coating
Junction Box	IP-65 rated with 3 bypass diodes Dimensions: 32 x 155 x 128 mm
Output Cables	1000mm length cables / MultiContact (MC4) connectors
Frame	Anodized aluminum alloy type 6063 (black)
Weight	41.0 lbs (18.6 kg)

TESTED OPERATING CONDITIONS

Temperature	-40° F to +185° F (-40° C to + 85° C)
Max load	113psf 550 kg/m² (5400 Pa), front (e.g. snow) w / specified mounting configurations 50 psf 245 kg/m² (2400 Pa) front and back – e.g. wind
Impact Resistance	Hail: (25 mm) at 51mph (23 m/s)

WARRANTIES AND CERTIFICATIONS

Warranties	25-year limited power warranty
	10-year limited product warranty
Certifications	Tested to UL 1703. Class C Fire Rating

DIMENSIONS

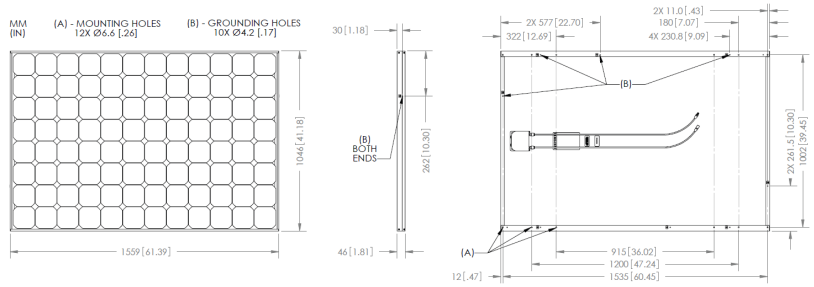

Please read safety and installation instructions before using this product, visit sunpowercorp.com for more details.

sunpowercorp.com

Document #001-65484 Rev*B / LTR_EN
CS 11_242

Figure F.0.3: SunPower, E20 series [51]

TECHNICAL SPECIFICATIONS

MODEL		4300TL	4800TL	5300TL	6300TL	7200TL
INPUT DATA						
Max. PV power	Wp	4800	5400	6000	7100	8100
Max. DC power	W	4300	4800	5300	6300	7200
Max. DC voltage	V_{dc}	880	880	880	880	880
Voltage range MPPT	V_{dc}	351 to 710	348 to 710	349 to 710	350 to 710	351 to 710
Max. input current	A_{dc}	13.0	14.5	16.0	18.5	21.0
Number of PV string inputs		2	2	2	3	3
Number of MPP trackers		1				
Input protection		Optional DC switch disconnector, integrated in the device Reverse voltage protection				
OUTPUT DATA						
Max. AC Power	W	4120	4600	5000	6000	6900
Nominal output power	W	3750	4200	4600	5500	6300
Mains output voltage range	V_{ac}	230V (+/-20 %) single phase *				
Mains frequency:	Hz	47.5 to 52.5 *				
Max. AC Current	A_{ac}	17.9	20.0	21.7	26.1	30.0
Nominal AC Current	A_{ac}	16.3	18.3	20.0	23.9	27.4
Output protection		Short circuit detection 1-phase or 3-phase grid monitoring				
PERFORMANCE DATA						
Maximum Efficiency:	%	>97,3	>97,4	>97,4	>97,7	>98,0
EU Efficiency:	%	>96,8	>96,9	>96,9	>97,3	>97,6
Power Feed Starts at	W	7	7	7	8	8
Night mode power	W	< 2				
MECHANICAL DATA						
Protection degree (EN 60529)		IP 66				
Dimensions	mm	H 720 x W 320 x D 250				
Weight	kg	27	28	28	29	29
Cable access		Bottom				
Input cable connection		MC4				
Output cable connection		Spring Clamp Technology				
DESIGN STANDARDS						
EM compatibility:		EN 61000-6-2, EN 61000-6-3				
CE marking:		Yes				
Other standards:		DIN VDE V 0126-1-1 EN 50438, AS 4777, ENEL Guidelines, RD 1663, RD 661, EN 61000-3-2, EN 61000-3-3, EN 61000-3-11, EN 61000-3-12				
ENVIRONMENTAL DATA						
Operating temperature:	°C	-20 to +60 (output power derating above +45°C)				
Storage temperature:	°C	-20 to +80				
Ventilation		Convection cooling (fan assist at high temperature)				
INTERFACE						
Front panel		Full graphic LCD: 170 x 76 pixels				
Embedded datalogger		Memory capacity for 30yrs operation				
Service		EIA 232, 9-pin D-sub female				
Remote connection option		EIA485, 2x RJ45 for network components				
Volt free contact option		1x Change over contact: 24V_{ac}/2A rated				

*– voltage and frequency range adjustable to specific grid settings

357101.DS3 rev6 - Specifications subject to change without notice

Figure F.0.4: Eltek, Theia TL String series [52]

TECHNICAL SPECIFICATIONS

Model	2.0HE-t [1]	2.9HE-t [1]	3.8HE-t	4.4HE-t
INPUT DATA				
Nominal DC power	2100 W	3000 W	4000 W	4600 W
Max. Recommended PV Power	2625 W	3750 W	5000 W	5750 W
Max. DC voltage	600 V_{dc}	600 V_{dc}	600 V_{dc}	600 V_{dc}
Voltage range MPPT	230 to 480 V_{dc}	230 to 480 V_{dc}	230 to 480 V_{dc}	230 to 480 V_{dc}
Max. input current	9.5 A	13.5 A	18.0 A	21.0 A
Number of PV string inputs	3			
Number of MPP trackers	1			
Input features	Reverse polarity protection, Ground fault monitoring, Integral DC switch disconnector (optional), Integral DC fuses for string inputs (optional) Field configurable for positive or negative grounding, or ungrounded			
OUTPUT DATA				
Nominal output power	2000 W	2900 W	3800 W	4400 W
Nominal AC current	9.0 A	13.0 A	17.0 A	20.0 A
Max. AC current	10.5 A	15.2 A	19.7 A	23.0 A
Mains output voltage	184Vac to 276Vac single or split phase [2]			
Mains frequency:	50Hz / 60Hz (+/- 5Hz) [2]			
Power factor (cos φ)	1			
PERFORMANCE DATA				
Maximum efficiency:	96.9 %	97.0 %	97.2 %	97.3 %
CEC efficiency:	96.1 %	96.4 %	96.9 %	97.0 %
EU efficiency:	96.0 %	96.2 %	96.6 %	96.9 %
Power feed starts at	< 7 W			
Night mode power	< 1 W			
MECHANICAL DATA				
Protection degree	IP 65 / NEMA 4X			
Dimensions	610H x 353W x 154D mm / 24.02H x 13.90W x 6.06D inches			
Weight	19kg / 42lbs	19kg / 42lbs	21kg / 46lbs	21kg / 46lbs
Cable access	Bottom and Sides			
Input cable connection	MC3, MC4, Tyco, Screw terminals, Cable clamp, Others on request			
Output cable connection	Screw terminals, Cable clamp			
DESIGN STANDARDS				
EM compatibility	EN 61000-6-2, EN 61000-6-3, FCC Level B			
CE / UL marking	Yes			
Other standards	UL 1741, DIN VDE V 0126-1-1, G83/1, EN 50438, AS 4777, ENEL Guidelines (DK 5940), EN 61000-3-2, EN 61000-3-3, EN 61000-3-11, EN 61000-3-12			
ENVIRONMENTAL DATA				
Operating temperature	-25 to +65 °C / -13 to +149 °F (possible power derating above +45°C / +113°F)			
Storage temperature	-30 to +80 °C / -22 to +176 °F			
Ventilation	Convection cooling			
ADDITIONAL FEATURES				
Topology	High frequency transformer, galvanic isolation			
Noise Emission	≤ 40 dB (A)			
Communication	Graphical, color display with touch sense buttons, Embedded web-server, Ethernet, CAN and RS485 bus interface, 3x LEDs for visual status indication			
Warranty	5 years, 10 years, 15 years, and 20 years options			

1) Preliminary data for THEIA models
2) Voltage and frequency range adjustable to specific grid settings

357115.DS3 rev7- Specifications subject to change without notice

Eltek ©2011 - Find your local office at: www.eltek.com

Figure F.0.5: Eltek, Theia HE-t series [52]

Nomenclature[1]	Parameter	TLX Pro 6 k[6]	TLX Pro 8 k	TLX Pro 10 k	TLX Pro 12.5 k	TLX Pro 15 k
	AC					
$P_{ac,r}$	Max./Nom. power AC	6000 W	8000 W	10000 W	12500 W	15000 W
	Reactive power range	0-3.6 kVAr	0-4.8 kVAr	0-6.0 kVAr	0-7.5 kVAr	0-9.0 kVAr
$V_{ac,r}$	Rated output voltage	3x 230 V				
$V_{ac,min}$; $V_{ac,max}$	AC voltage range (P-N)	3x 230 V ± 20 %				
	Nominal current AC	3 x 9 A	3 x 12 A	3 x 15 A	3 x 19 A	3 x 22 A
I_{acmax}	Max. current AC	3 x 9 A	3 x 12 A	3 x 15 A	3 x 19 A	3 x 22 A
	AC current distortion (THD %)	< 4 %	< 4 %	< 5 %	< 5 %	< 5 %
$cosphi_{ac,r}$	Power factor at 100 % load	> 0.99				
	Controlled power factor range	0.8 over-excited 0.8 under-excited				
	"Connecting" power loss	10 W				
	Night-time power loss (off grid)	< 5 W				
f_r	Rated grid frequency	50 Hz				
f_{min}, f_{max}	Grid frequency range	50 ± 5 Hz				
	DC					
	Nominal power DC	6200 W	8250 W	10300 W	12900 W	15500 W
	Max. recommended PV power at STC[2]	7100 Wp	9500 Wp	11800 Wp	14700 Wp	17700 Wp
$V_{dc,r}$	Nominal voltage DC	700 V				
V_{mppmin} V_{mppmax}	MPP voltage-nominal power[3]	260 - 800 V	345-800 V	430-800 V	358-800 V	430-800 V
	MPP efficiency	99.9 %				
V_{dcmax}	Max. DC voltage	1000 V				
$V_{dcstart}$	Turn on voltage	250 V				
V_{dcmin}	Turn off voltage	250 V				
I_{dcmax}	Max. current DC	2 x 12 A			3 x 12 A	
	Max. short circuit current DC at STC	2 x 12 A			3 x 12 A	
	Min. on grid power	20 W				
	Efficiency					
	Max. efficiency	97.8 %	97.9 %	98 %		
	Euro efficiency	96.5 %	97.0 %	97.0 %	97.3 %	97.4 %
	Other					
	Dimensions (H, W, D)	700 x 525 x 250 mm				
	Mounting recommendation	Wall bracket				
	Weight	35 kg				
	Acoustic noise level[4]	56 db(A)				
	MPP tracker	2			3	
	Operation temperature range	-25..60 °C				
	Nom. temperature range	-25..45 °C				
	Storage temperature	-25..60 °C				
	Overload operation	Change of operating point				
	Overvoltage category AC	Class III				
	Overvoltage category DC	Class II				
	PLA[5]	Included				
	Reactive power	TLX+ and TLX Pro+				
	Relative humidity	95 % (non-condensing)				
	Functional Safety					
	Safety (protective class)	Class I				
	PELV on the communication and control card	Class II				
	Islanding detection-loss of mains	Three-phase monitoring, ROCOF				
	Voltage magnitude	Included				
	Frequency	Included				
	DC content of AC current	Included				
	Insulation resistance	Included				
	RCMU-Type B	Included				
	Indirect contact protection	Yes (class I, grounded)				
	Short circuit protection	Yes				

[1] According to EN 50524: 2009
[2] For fixed systems with semi-optimal conditions
[3] At identical input voltages. At unequal input voltages V_{mppmin} can be as low as 250 V depending on total input power.
[4] SPL (Sound Pressure Level) at 1.5 m.
[5] Grid Management Box (TLX Pro, TLX Pro+) or 3rd party product
[6] Only TLX + and TLX Pro + variants

Danfoss Solar Inverters A/S

Ulsnaes 1
DK-6300 Graasten
Denmark
Tel: +45 7488 1300
Fax: +45 7488 1301
E-mail: solar-inverters@danfoss.com
www.danfoss.com/solar

DKSI.PK.22.A4.02 December 2011© Produced by Danfoss A/S ©

Figure F.0.6: Danfoss, TLX series [53]

Show All / Hide All	SUNNY TRIPOWER 8000TL	SUNNY TRIPOWER 10000TL	SUNNY TRIPOWER 12000TL	SUNNY TRIPOWER 15000TL	SUNNY TRIPOWER 17000TL
- Input (DC)					
Max. DC power (@ cos φ=1)	8200 W	10200 W	12250 W	15340 W	17410 W
Max. input voltage	1000 V	1000 V	1000 V	1000 V	1000 V
MPP voltage range / rated input voltage	320 V – 800 V / 600 V	320 V – 800 V / 600 V	380 V – 800 V / 600 V	360 V – 800 V / 600 V	400 V – 800 V / 600 V
Min. input voltage / initial input voltage	150 V / 188 V	150 V / 188 V	150 V / 188 V	150 V / 188 V	150 V / 188 V
Max. input current input A / input B	22 A / 11 A	22 A / 11 A	22 A / 11 A	33 A / 11 A	33 A / 11 A
Max. input current per string input A** / input B**	33 A / 12.5 A	33 A / 12.5 A	33 A / 12.5 A	33 A / 12.5 A	33 A / 12.5 A
Number of independent MPP inputs / strings per MPP input	2 / A:4; B:1	2 / A:4; B:1	2 / A:4; B:1	2 / A:5; B:1	2 / A:5; B:1

Figure F.0.7: SMA, Tripower input specifications [54]

- Output (AC)					
Rated power (@ 230 V, 50 Hz)	8000 W	10000 W	12000 W	15000 W	17000 W
Max. apparent AC power	8000 VA	10000 VA	12000 VA	15000 VA	17000 VA
Nominal AC voltage	3 / N / PE; 220 / 380 V 3 / N / PE; 230 / 400 V 3 / N / PE; 240 / 415 V	3 / N / PE; 220 / 380 V 3 / N / PE; 230 / 400 V 3 / N / PE; 240 / 415 V	3 / N / PE; 220 / 380 V 3 / N / PE; 230 / 400 V 3 / N / PE; 240 / 415 V	3 / N / PE; 220 / 380 V 3 / N / PE; 230 / 400 V 3 / N / PE; 240 / 415 V	3 / N / PE; 220 / 380 V 3 / N / PE; 230 / 400 V 3 / N / PE; 240 / 415 V
Nominal AC voltage range	160 V – 280 V	160 V – 280 V	160 V – 280 V	160 V – 280 V	160 V – 280 V
AC power frequency / range	50 Hz, 60Hz / -6 Hz ... +5 Hz	50 Hz, 60Hz / -6 Hz ... +5 Hz	50 Hz, 60Hz / -6 Hz ... +5 Hz	50 Hz, 60Hz / -6 Hz ... +5 Hz	50 Hz, 60Hz / -6 Hz ... +5 Hz
Rated grid frequency / rated grid voltage	50 Hz / 230 V	50 Hz / 230 V	50 Hz / 230 V	50 Hz / 230 V	50 Hz / 230 V
Max. output current	16 A	16 A	19.2 A	24 A	24.6 A
Power factor at rated power	1	1	1	1	1
Adjustable displacement factor	0.8 overexited ... 0.8 underexited	0.8 overexited ... 0.8 underexited	0.8 overexited ... 0.8 underexited	0.8 overexited ... 0.8 underexited	0.8 overexited ... 0.8 underexited
Phase conductors / connection phases	3 / 3	3 / 3	3 / 3	3 / 3	3 / 3

Figure F.0.8: SMA, Tripower output specifications [54]

- Efficiency

Max. efficiency / European efficiency	98.1 % / 97.5 %	98.1 % / 97.7 %	98.1 % / 97.7 %	98.2 % / 97.8 %	98.2 % / 97.8 %

- Protective devices

Input-side disconnection device	yes	yes	yes	yes	yes
Ground-fault monitoring / grid monitoring	yes / yes	yes / yes	yes / yes	yes / yes	yes / yes
DC surge arrester Type II, can be integrated	opt.	opt.	opt.	opt.	opt.
DC reverse-polarity protection / AC short-circuit current capability / galvanically isolated	yes / yes / —	yes / yes / —	yes / yes / —	yes / yes / —	yes / yes / —
All-pole sensitive residual current monitoring unit	yes	yes	yes	yes	yes
Protection class (according to IEC 62103) / overvoltage category (according to IEC 60664-1)	I / III	I / III	I / III	I / III	I / III

Figure F.0.9: SMA, Tripower efficiency and protection specifications [54]

- General data

Dimensions (W / H / D)	665 / 690 / 265 mm (26.2 / 27.2 / 10.4 inch)	665 / 690 / 265 mm (26.2 / 27.2 / 10.4 inch)	665 / 690 / 265 mm (26.2 / 27.2 / 10.4 inch)	665 / 690 / 265 mm (26.2 / 27.2 / 10.4 inch)	665 / 690 / 265 mm (26.2 / 27.2 / 10.4 inch)
Weight	64 kg / 141.1 lb	64 kg / 141.1 lb	64 kg / 141.1 lb	64 kg / 141.1 lb	64 kg / 141.1 lb
Operating temperature range	-25 °C ... +60 °C / -13 °F ... +140 °F	-25 °C ... +60 °C / -13 °F ... +140 °F	-25 °C ... +60 °C / -13 °F ... +140 °F	25 °C ... +60 °C / -13 °F ... +140 °F	-25 °C ... +60 °C / -13 °F ... +140 °F
Noise emission (typical)	51 dB(A)	51 dB(A)	51 dB(A)	51 dB(A)	51 dB(A)
Self-consumption at night	1 W	1 W	1 W	1 W	1 W
Topology / cooling concept	Transformerless / OptiCool	Transformerless / OptiCool	Transformerless / OptiCool	Transformerless / OptiCool	Transformerless / OptiCool
Degree of protection / degree of protection of connection area (according to IEC 60529)	IP65 / IP54	IP65 / IP54	IP65 / IP54	IP65 / IP54	IP65 / IP54
Climatic category (according to IEC 60721-3-4)	4K4H	4K4H	4K4H	4K4H	4K4H
Maximum permissible value for relative humidity (non-condensing)	100 %	100 %	100 %	100 %	100 %

Figure F.0.10: SMA, Tripower, general data [54]

- Features

DC terminal	SUNCLIX	SUNCLIX	SUNCLIX	SUNCLIX	SUNCLIX
AC terminal	Spring-type terminal	Spring-type terminal	Spring-type terminal	Spring-type terminal	Spring-type terminal
Display	Graphic	Graphic	Graphic	Graphic	Graphic
Interface: RS485 / *Bluetooth*	opt. / yes	opt. / yes	opt. / yes	opt. / yes	opt. / yes
Warranty: 5 / 10 / 15 / 20 / 25 years	yes / opt. / opt. / opt. / opt.	yes / opt. / opt. / opt. / opt.	yes / opt. / opt. / opt. / opt.	yes / opt. / opt. / opt. / opt.	yes / opt. / opt. / opt. / opt.
Multi-function relay	yes	yes	yes	yes	yes
Certificates and approvals (more available on request)	CE, VDE-AR-N 4105, VDE0126-1-1, G83/1-1, RD 1663/2000, RD 661/2007, G59/2, PPC, AS4777, EN 50438*, C10/11, PPDS, IEC 61727, ENEL-Guida, UTE C15-712-1	CE, VDE0126-1-1, G83/1-1, RD 1663/2000, RD 661/2007, G59/2, PPC, AS4777, EN 50438*, C10/11, PPDS, IEC 61727, ENEL-Guida, UTE C15-712-1	CE, VDE0126-1-1, G83/1-1, RD 1663/2000, RD 661/2007, G59/2, PPC, AS4777, EN 50438*, C10/11, PPDS, IEC 61727, ENEL-Guida, UTE C15-712-1	CE, VDE0126-1-1, G83/1-1, RD 1663/2000, RD 661/2007, G59/2, PPC, AS4777, EN 50438*, C10/11, PPDS, IEC 61727, ENEL-Guida, UTE C15-712-1	CE, VDE0126-1-1, G83/1-1, RD 1663/2000, RD 661/2007, G59/2, PPC, AS4777, EN 50438*, C10/11, PPDS, IEC 61727, ENEL-Guida, UTE C15-712-1

Figure F.0.11: SMA, Tripower, features [54]

- Footnotes

* Does not apply to all national deviations of EN 50438 ** To be observed in case of a short circuit in the electronic string fuse					
Data at nominal conditions					
Type designation	STP 8000TL-10	STP 10000TL-10	STP 12000TL-10	STP 15000TL-10	STP 17000TL-10

Figure F.0.12: SMA, Tripower, footnotes [54]

Show All / Hide All	SUNNY BOY 3000TL	SUNNY BOY 4000TL	SUNNY BOY 5000TL
- Input (DC)			
Max. DC power (@ cos φ=1)	3200 W	4200 W	5300 W
Max. input voltage	550 V	550 V	550 V
MPP voltage range / rated input voltage	188 V – 440 V / 400 V	175 V – 440 V / 400 V	175 V – 440 V / 400 V
Min. input voltage / initial input voltage	125 V / 150 V	125 V / 150 V	125 V / 150 V
Max. input current input A / input B	17 A / —	15 A / 15 A	15 A / 15 A
Max. input current per string input A / input B	17 A / —	15 A / 15 A	15 A / 15 A
Number of independent MPP inputs / strings per MPP input	1 / 2	2 / A:2; B:2	2 / A:2; B:2
- Output (AC)			
Rated output power (@ 230 V, 50 Hz)	3000 W	4000 W	4600 W
Max. apparent AC power	3000 VA	4000 VA	5000 VA
Nominal AC voltage / range	220 V, 230 V, 240 V / 180 V – 280 V	220 V, 230 V, 240 V / 180 V – 280 V	220 V, 230 V, 240 V / 180 V – 280 V
AC power frequency / range	50 Hz, 60 Hz / -5 Hz ... +5 Hz	50 Hz, 60 Hz / -5 Hz ... +5 Hz	50 Hz, 60 Hz / -5 Hz ... +5 Hz
Rated power frequency / rated power voltage	50 Hz / 230 V	50 Hz / 230 V	50 Hz / 230 V
Max. output current	16 A	22 A	22 A
Power factor at rated power	1	1	1
Adjustable displacement factor	—	—	—
Feed-in phases / connection phases	1 / 1	1 / 1	1 / 1

Figure F.0.13: SMA, Sunny Boy input and output specifications [55]

- Efficiency

Max. efficiency / European efficiency	97 % / 96.3 %	97 % / 96.4 %	97 % / 96.5 %

- Protective devices

Input-side disconnection device	yes	yes	yes
Ground-fault monitoring / grid monitoring	yes / yes	yes / yes	yes / yes
DC surge arrester Type II, can be integrated	—	—	—
DC reverse-polarity protection / AC short-circuit current capability / galvanically isolated	yes / yes / —	yes / yes / —	yes / yes / —
All-pole sensitive residual current monitoring unit	yes	yes	yes
Protection class (according to IEC 62103) / overvoltage category (according to IEC 60664-1)	I / III	I / III	I / III

Figure F.0.14: SMA, Sunny Boy efficiency and protection specifications [55]

- General data

Dimensions (W / H / D)	470 / 445 / 180 mm (18.5 / 17.5 / 7.1 inch)	470 / 445 / 180 mm (18.5 / 17.5 / 7.1 inch)	470 / 445 / 180 mm (18.5 / 17.5 / 7.1 inch)
Weight	22 kg / 48.5 lb	25 kg / 55.12 lb	25 kg / 55.12 lb
Operating temperature range	-25 °C ... +60 °C / -13 °F ... +140 °F	-25 °C ... +60 °C / -13 °F ... +140 °F	-25 °C ... +60 °C / -13 °F ... +140 °F
Noise emission (typical)	25 dB(A)	29 dB(A)	29 dB(A)
Self-consumption (night)	0.5 W	0.5 W	0.5 W
Topology	Transformerless	Transformerless	Transformerless
Cooling concept	Convection	Convection	OptiCool
Degree of protection (according to IEC 60529)	IP65	IP65	IP65
Degree of protection of connection area (according to IEC 60529)	IP54	IP54	IP54
Climatic category (according to IEC 60721-3-4)	4K4H	4K4H	4K4H
Maximum permissible value for relative humidity (non-condensing)	100 %	100 %	100 %

Figure F.0.15: SMA, Sunny Boy general specifications [55]

- Features

DC terminal	SUNCLIX	SUNCLIX	SUNCLIX
AC terminal	Spring-type terminal	Spring-type terminal	Spring-type terminal
Display	Graphic	Graphic	Graphic
Interface: RS485 / *Bluetooth*	opt. / yes	opt. / yes	opt. / yes
Warranty: 5 / 10 / 15 / 20 / 25 years	yes / opt. / opt. / opt. / opt.	yes / opt. / opt. / opt. / opt.	yes / opt. / opt. / opt. / opt.
Multi-function relay	yes	yes	yes
Certificates and approvals (more available on request)	CE, VDE0126-1-1, DK 5940 ED2.2, G83/1-1, G59/2 RD 1663/2000, RD 661/2007, PPC, AS4777, EN 50438*, PPDS, KEMCO**, C10/11, UTE C15-712-1	CE, VDE0126-1-1, DK 5940 ED2.2, G83/1-1, G59/2 RD 1663/2000, RD 661/2007, PPC, AS4777, EN 50438*, PPDS, KEMCO**, C10/11, UTE C15-712-1	CE, VDE0126-1-1, DK 5940 ED2.2, G83/1-1 G59/2, C10/11, UTE C15-712-1, RD 1663/2000, RD 661/2007, PPC, AS4777, EN 50438*, PPDS

- Footnotes

* Does not apply to all national deviations of EN 50438 ** Only for SB 3000TL-20

Data at nominal conditions			
Type designation	SB 3000TL-20	SB 4000TL-20	SB 5000TL-20

Figure F.0.16: SMA, Sunny Boy features and footnotes [55]

Appendix G

Simulation Results

A number of simulations were performed when varying the fraction of electrical effect, the module tilt angles and simulating with several inverters. Attachments of the complete result reports would be to extensive in this appendix. The result reports are, therefore, found in an attached CD.

Two meteorological datasets

Comparing the two data sets

Figure G.0.1 illustrates the global horizontal irradiation of the default and the new meteorological data set performed on the same system with a module tilt of 20° and an electrical effect of 60 %. Table G.0.1 and Table G.0.2 shows the horizontal global irradiation and incident global irradiation in the tilted plane and the difference between these two factors for the default and the new meteorological data sets respectively.

Table G.0.1: The horizontal and incident global irradiation of the default meteorological data set

DEFAULT	Horizontal kWh/m^2	Incident kWh/m^2	Difference kWh/m^2
January	11	19.2	8.2
February	28	43.0	15.0
March	66	83.7	17.7
April	106	122.1	16.1
May	172	186.3	14.3
June	166	172.0	6.0
July	169	178.8	9.8
August	131	145.2	14.2
September	78	96.0	18.0
October	37	50.3	13.3
November	15	27.2	12.2
December	8	19.2	11.2
Yearly	987	1143	156

Table G.0.2: The horizontal and incident global irradiation of the new meteorological data set

METEO2	Horizontal kWh/m^2	Incident kWh/m^2	Difference kWh/m^2
January	11.1	20.8	9.7
February	27.4	42.9	15.5
March	67.5	88.8	21.3
April	111.8	131.3	19.5
May	157.9	169.6	11.7
June	166.6	172.6	6.0
July	149.4	157.8	8.4
August	119.7	132.8	13.1
September	77.6	95.3	17.7
October	39.1	56.3	17.2
November	14.8	27.2	12.4
December	7.2	16.5	9.3
Yearly	950.1	1111.9	161.8

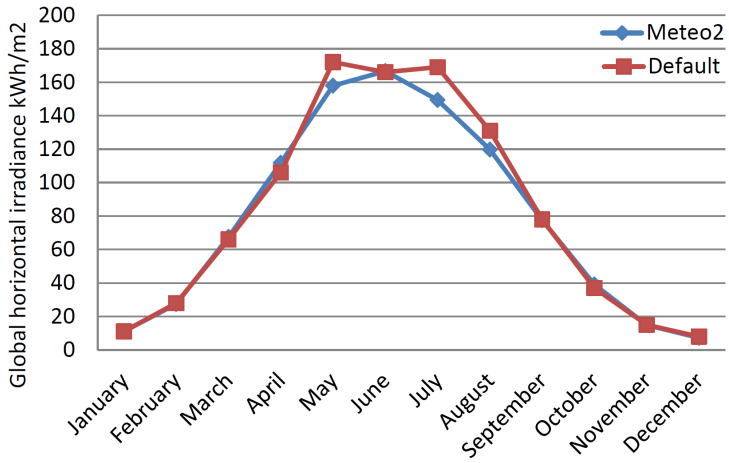

Figure G.0.1: The horizontal global irradiation for the default and new meteorological data set

Appendix H

Production and Demand

Energy Production

Table H.0.1 presents the produced energy of all three alternatives for each month of the year.

Table H.0.1: The monthly and yearly energy production for all three alternatives in kWh

	REC Eltek	REC SMA	SunPower SMA
January	127.62	122.07	175.73
February	508.04	512.73	683.57
March	1 961.94	2 008.37	2 685.34
April	2 883.48	2 956.53	3 999.27
May	3 627.53	3 720.74	5 050.32
June	3 596.34	3 687.90	5 021.18
July	3 273.12	3 353.64	4 568.55
August	2 779.12	2 847.56	3 871.60
September	2 031.46	2 080.11	2 811.11
October	1 099.82	1 121.53	1 489.71
November	391.26	392.93	537.25
December	117.28	113.91	162.90
Yearly	22.40	22 918.01	31 056.54

Consumption

Figure H.0.1 illustrates the consumption in the building from the main meter, where the consumptions from Figure H.0.2 are withdrawn.

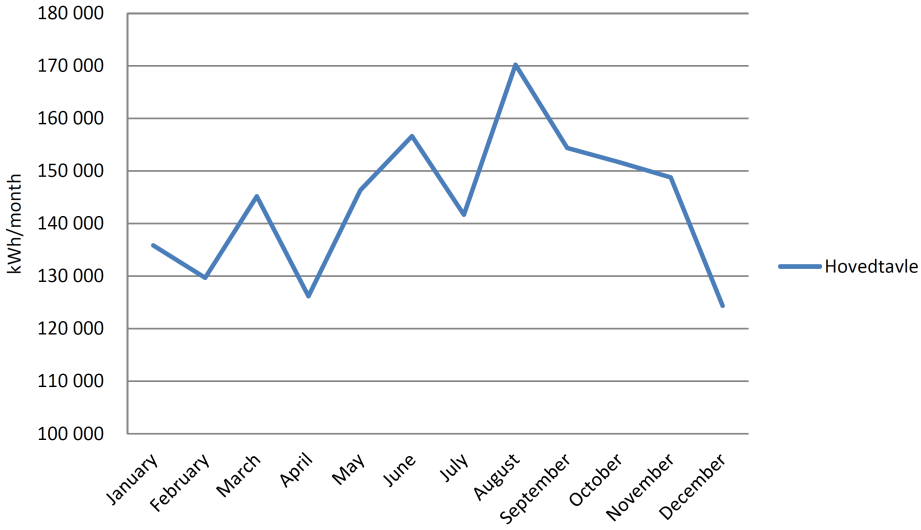

Figure H.0.1: Consumption of the main meter, 2011

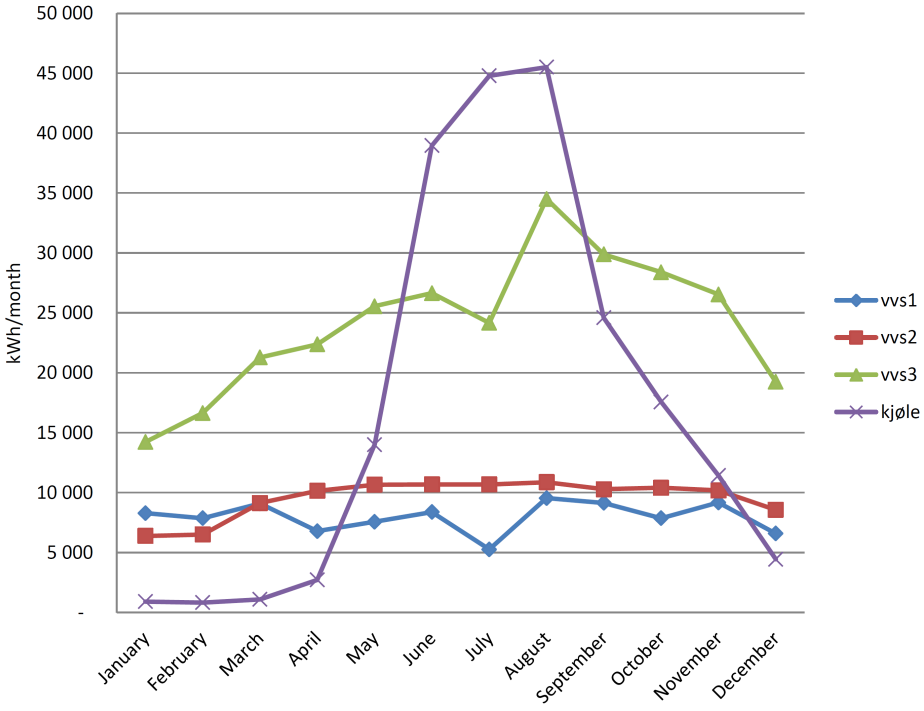

Figure H.0.2: Consumption for four part-meters in the building, 2011

Table H.0.2: The average time of occurring power peaks and the average maximum load peak value of the 15 highest power peaks occurring in each month, 2011

	Average time of occurrence	Average max peak
January	11.93	329.50
February	11.27	340.50
March	12.27	343.00
April	12.87	350.75
May	14.80	406.50
June	14.67	460.25
July	14.20	439.50
August	14.47	488.00
September	14.33	401.75
October	12.80	380.50
November	11.87	370.50
December	12.20	362.25

Appendix I

Economics

Investment costs

Table I.0.1 illustrates the investment cost for the three final alternatives. The figures marked with [1] are from Photon Magazine [45]. The figures marked with [2] are experience based on previous calculations from Multiconsult. The figures marked with [3] are figures based on calculations from a German roof installation of installed capacity of 60 kWp (from Multiconsult).

Income

Figure I.0.2 presents the Hafslund tariff agreement which is in effect today (2012). It is from these numbers the income from the savings when producing energy is calculated. Table I.0.3 presents the simulated energy production form the three alternatives, while Table I.0.4 presents two power generating situations for the three alternatives. Table I.0.5 presents the calculated income when considering both power situations and the energy variable. Table I.0.6 presents the income if all of the energy was sold on the spot market.

Table I.0.1: Investment cost for the three alternatives. Rate per May 11th, 2012: 7.622 EUR/NOK

	REC Eltek	REC SMA	SunPower SMA	Unit
Module price	750	750	1140[1]	€/kWp
Length	1.665	1.665	1.559	m
Width	0.991	0.991	1.046	m
Power	250	250	327	Wp
Efficiency	15.15	15.15	20.05	%
Inverter	297.14	210.00[1]	210.00[1]	€/kWp
Mounting system	250.00[2]	250.00[2]	188.90	€/kWp
Montage	200.00[2]	200.00[2]	151.12	€/kWp
DC cables	214.00[3]	214.00[3]	161.69	€/kWp
AC cables	131.20[2]	131.20[2]	99.13	€/kWp
Communication	40.00[2]	40.00[2]	30.22	€/kWp
Total BoS cost	1 132.34	1 045.20	841.06	€/kWp
Module + BoS cost	1 882.34	1 795.20	1 981.06	€/kWp
	14 347.12	13 682.93	15 099.56	NOK/kWp

Discounted Costs and Income

Figure I.0.1 shows the discounted module maintenance and repair costs of the three alternatives. Module maintenance is in this case considered necessary once a year, while the inverter repair is considered necessary every five years. The period of analysis is 20 years, the discount rate is 6 % and the inflation rate is 2.5 %. Figure I.0.2 presents the calculated discounted income in a best case and worst case scenario and the discounted yield in kWh for the three alternatives with 0.75 % degradation in production per year. A 0.75 % degradation per year results in a total degradation of the modules to be 13.3 % during the analysis period of 20 years.

Table I.0.2: The tariff in 2012 for low voltage connections (230 V and 400 V) to Hafslunds grid [41]. Summer = April - October, winter = November - March.

Set price	Power variable		Energy variable	
NOK/mth	NOK/kW/mth		NOKcent/kWh	
	Summer	Winter	Summer	Winter
415	25	74	5.25	7.4

Table I.0.3: The simulated energy production from the three alternatives

	Eltek	SMA	SunPower
Energy	kWh/mth	kWh/mth	kWh/mth
January	128	122	176
February	508	513	684
March	1 962	2 008	2 685
April	2 883	2 957	3 999
May	3 628	3 721	5 050
June	3 596	3 688	5 021
July	3 273	3 354	4 569
August	2 779	2 848	3 872
September	2 031	2 080	2 811
October	1 100	1 122	1 490
November	391	393	537
December	117	114	163
Yearly	22 397	22 918	31 057

Table I.0.4: The power production in an average situation and maximum situation for the three alternatives

	Eltek		SMA		SunPower	
	Min.	Max.	Min.	Max.	Min.	Max.
Power	kW	kW	kW	kW	kW	kW
January	0.67	3.15	0.68	3.21	0.96	3.81
February	2.20	9.38	2.28	9.63	2.98	12.57
March	5.58	17.66	5.78	18.19	7.64	24.19
April	7.00	18.88	7.39	19.43	9.86	26.41
May	7.24	19.73	7.53	20.31	10.13	27.80
June	6.82	19.68	7.27	20.26	9.72	28.00
July	6.25	20.21	6.52	20.81	8.85	28.72
August	6.20	19.95	6.48	20.54	8.69	28.41
September	5.52	17.24	5.75	17.75	7.72	24.22
October	3.88	16.88	4.03	17.38	5.28	23.07
November	1.99	9.27	2.11	9.52	2.75	12.33
December	0.79	3.12	0.78	3.18	1.11	4.41

Table I.0.5: The calculated income in an worst and a best case scenario when the PV installation is not producing more than the building consumes

	Energy	Power		Total	
		Min.	Max.	Min.	Max.
Eltek	1 243	1 904	6 465	3 147	7 708
SMA	1 271	1 985	6 647	3 256	7 918
SunPower	1 722	2 649	8 906	4 370	10 627

Table I.0.6: The theoretical income if the total amount of energy was sold at spot price

	Spot Price
Eltek	7 647.76
SMA	7 825.66
SunPower	10 604.67

	Eltek	SMA	SunPower		
Module maintenance	1 592.99	1 457.70	2 954.96	NOK	Once a year
Inverter repair	2 157.66	2 031.45	2 180.10	NOK	Every five years

Period of analysis	20	years
Discount	6	%
Inflation	2.5	%

Discounted costs (NOK)

			Year									
		Sum	0	1	2	3	4	5	6	7	8	9
Sunpower	Maintenance	43 769	2 955	2 857	2 763	2 672	2 584	2 498	2 416	2 336	2 259	2 184
	Repair cost, inv	6 032	2 180	2 108	2 039	1 971	1 906	1 843	1 782	1 723	1 667	1 612
SMA	Maintenance	21 591	1 458	1 410	1 363	1 318	1 274	1 232	1 192	1 152	1 114	1 078
	Repair cost, inv	5 621	2 031	1 964	1 900	1 837	1 776	1 717	1 661	1 606	1 553	1 502
Eltek	Maintenance	23 595	1 593	1 540	1 490	1 440	1 393	1 347	1 302	1 259	1 218	1 178
	Repair cost, inv	5 970	2 158	2 086	2 018	1 951	1 886	1 824	1 764	1 706	1 649	1 595

										Year	
										10	11	12	13	14	15	16	17	18	19
										2 112	2 042	1 975	1 910	1 847	1 786	1 727	1 670	1 615	1 561
										1 558	1 507	1 457	1 409	1 362	1 317	1 274	1 232	1 191	1 152
										1 042	1 008	974	942	911	881	852	824	797	770
										1 452	1 404	1 358	1 313	1 270	1 228	1 187	1 148	1 110	1 073
										1 139	1 101	1 065	1 030	996	963	931	900	870	842
										1 542	1 491	1 442	1 394	1 348	1 304	1 261	1 219	1 179	1 140

Figure I.0.1

Discounted income (NOK)

		Sum	Year 0	1	2	3	4	5	6	7	8	9
SunPower	Income worst	64 733	4 370	4 226	4 087	3 952	3 821	3 695	3 573	3 455	3 341	3 231
	Income best	157 411	10 627	10 276	9 937	9 609	9 292	8 985	8 688	8 401	8 124	7 856
SMA	Income worst	48 227	3 256	3 148	3 045	2 944	2 847	2 753	2 662	2 574	2 489	2 407
	Income best	117 284	7 918	7 657	7 404	7 160	6 923	6 695	6 473	6 260	6 053	5 853
Eltek	Income worst	46 607	3 147	3 043	2 942	2 845	2 751	2 660	2 572	2 488	2 405	2 326
	Income best	114 163	7 708	7 453	7 207	6 969	6 739	6 516	6 301	6 093	5 892	5 697

		Year 10	11	12	13	14	15	16	17	18	19
SunPower	Income worst	3 124	3 021	2 921	2 825	2 731	2 641	2 554	2 470	2 388	2 309
	Income best	7 596	7 346	7 103	6 868	6 642	6 422	6 210	6 005	5 807	5 615
SMA	Income worst	2 327	2 251	2 176	2 104	2 035	1 968	1 903	1 840	1 779	1 720
	Income best	5 660	5 473	5 292	5 118	4 949	4 785	4 627	4 474	4 327	4 184
Eltek	Income worst	2 249	2 175	2 103	2 034	1 966	1 902	1 839	1 778	1 719	1 663
	Income best	5 509	5 327	5 151	4 981	4 817	4 658	4 504	4 355	4 212	4 072

0.75 % degradation per year

Yield (kWh)

	Sum	Year 0	1	2	3	4	5	6	7	8	9
Eltek	417 416	22 397	22 229	22 062	21 897	21 733	21 570	21 408	21 247	21 088	20 930
SMA	427 126	22 918	22 746	22 576	22 406	22 238	22 071	21 906	21 742	21 578	21 417
SunPower	578 813	31 057	30 824	30 593	30 363	30 136	29 910	29 685	29 463	29 242	29 022

	Year 10	11	12	13	14	15	16	17	18	19
Eltek	20 773	20 617	20 462	20 309	20 157	20 005	19 855	19 706	19 559	19 412
SMA	21 256	21 097	20 938	20 781	20 625	20 471	20 317	20 165	20 014	19 864
SunPower	28 805	28 589	28 374	28 162	27 950	27 741	27 533	27 326	27 121	26 918

Figure I.0.2